Factors Governing Flexure and Shear Behavior of Reinforced Concrete Wide Beams

by

Hazoor Bakhsh

2011-NUST-MS Ph.D-Str-13

NUST Institute of Civil Engineering

School of Civil and Environmental Engineering

National University of Sciences and Technology

Islamabad, Pakistan

2015

This is to certify that thesis entitled

Factors Governing Flexure and Shear Behavior of Reinforced Concrete Wide Beams

submitted by

Hazoor Bakhsh

Has been accepted towards the partial fulfillment

of the requirements for

Master of Science

In

Civil Engineering

_____

Dr. Wasim Khaliq

NUST Institute of Civil Engineering
School of Civil and Environmental Engineering
National University of Sciences and Technology
Islamabad, Pakistan

Dedicated

to

My Parents

Acknowledgements

All praises and thanks to Almighty Allah, who gave me strength and patience to complete my Masters in Structural Engineering. I heartily thank to my supervisor Dr. Wasim Khaliq, Associate Professor of Civil Engineering at National University of Sciences and Technology Islamabad, whose guidance, support and patience throughout the course of my research work made it possible for me to complete this thesis. Without his technical and moral support the completion of this work was impossible.

I would also like to thank my family and friends for their support and encouragement to complete my research work.

Abstract

Reinforced concrete (RC) has become one of the most main building materials and is being broadly used in many types of engineering structures. High-rise buildings and many other structures due to architectural constraints often employ thick slabs and wide beams of varying width as transfer girder, to reduce the floor height and to facilitate utility services under the floor. In the design of such important members, the engineers must balance economy and safety while satisfying the architectural constraints and design such wide beams within strength and serviceability limits allowed by codes and standards.

Many researchers have experimentally demonstrated that shear design provisions for large wide beams and thick slabs in ACI Standards can be unsafe and may result inadequate level of safety. Various response parameters of wide beams such as shear and flexure capacity demand, effect of longitudinal, web steel reinforcement and beam size effect on shear and flexure strength of RC wide beams are required to be investigated. To study these parameters commercial software ANSYS multi-function finite element package was used for numerical simulation and nonlinear analysis of wide beams.

Results obtained from the analytical study were compared to published data on wide beams with similar design parameters available in literature. ANSYS simulation results on predicting the behavior of wide beams in this study were found in good agreement with available experimental data. It was also observed that shear and flexure response parameters obtained from analyses were also in good agreement with those obtained from theoretical elastic analysis of similar wide beams.

List of Figures

List of Tables

Table of Contents

CHAPTER 1

INTRODUCTION

General: In beam resist loads are resisted by means of primarily two internal actions moment M, and shear V, while designing a reinforced concrete member, usually flexure is considered first, and then the size of the section and the organization of reinforcement to provide the necessary moment resistance. Generally flexure reinforcement amount and its placing are subject to limits, which can be used to ensure that if failure was ever to occur; it would develop gradually, giving warning to the occupants. After the flexure design beam then same is proportioned for shear. It is very common that shear failure is often sudden and brittle, so it is necessary to design beam in a way that design for shear must ensure that at least shear strength equals or exceeds the flexural strength at all points in the beam.

The shear failures can occur in many ways and varies widely with the dimensions, geometry, loading and properties of the members. For this reason, there is no unique way to design for shear

Extensive experimental research has been carried out to study flexure and specially shear strength controlling factors of concrete beams that includes function of flexure and shear reinforcement, concrete tension and compression zone at cracked and un-cracked regions, beam size, shear span to depth (a/d) ratio, aggregate size effect, dowel and arch action effect etc. Most popularly adopted structure design codes like ACI, AASHTO and Eurocode lack consistency in their shear strength formulas for concrete beams, while there is an almost uniformity and consensus for flexure strength formulas. That is why keeping in view the more uncertainty in shear strength prediction of concrete beams; design standard usually put higher value of shear strength reduction factor than for flexure. Shear failure of RC structures means rapid strength degradation and significant loss of energy dissipation capacity. So it become necessary to avoid such failure modes by assuring that the shear capacity exceeds the corresponding to the maximum flexural strength at each and every sections of beam.

When we examined of ACI 318 building design code provisions for flexure and shear strength, it is observed that all basic flexure strength provisions are uniform and consistent

only with some text modification as in ACI-318-14, while ACI and others mostly adopted design standard like Eurocode and AASHTOO, there exist different formulas of shear strength prediction. Perhaps the most significant changes for concrete design in AASHTO Bridge Design Specifications is the shear design methodology. ACI conditions for minimum shear reinforcement provisions in narrow and wide beams (b/h<0.5) are not same and various versions of ACI Codes are inconsistent in description and exemption of certain structure members for provision of such minimum shear reinforcement i.e. in footings, slabs and wide beams etc.

Although ACI 318-8 and in its proceedings versions has imposes condition that wide beams not equipped with shear reinforcement should be integrally built with slab. To some extent it will be beneficial for redistribution of loads and resultantly stresses. But even for certain cases where chances of such possibilities are limited or even absent and beams are lightly reinforced with more longitudinal bars spacing and when relatively finer coarse aggregate are used in mix design for wide beams and thick slabs, there may be chances of sudden shear failure without warning, which is highly undesirable phenomena.
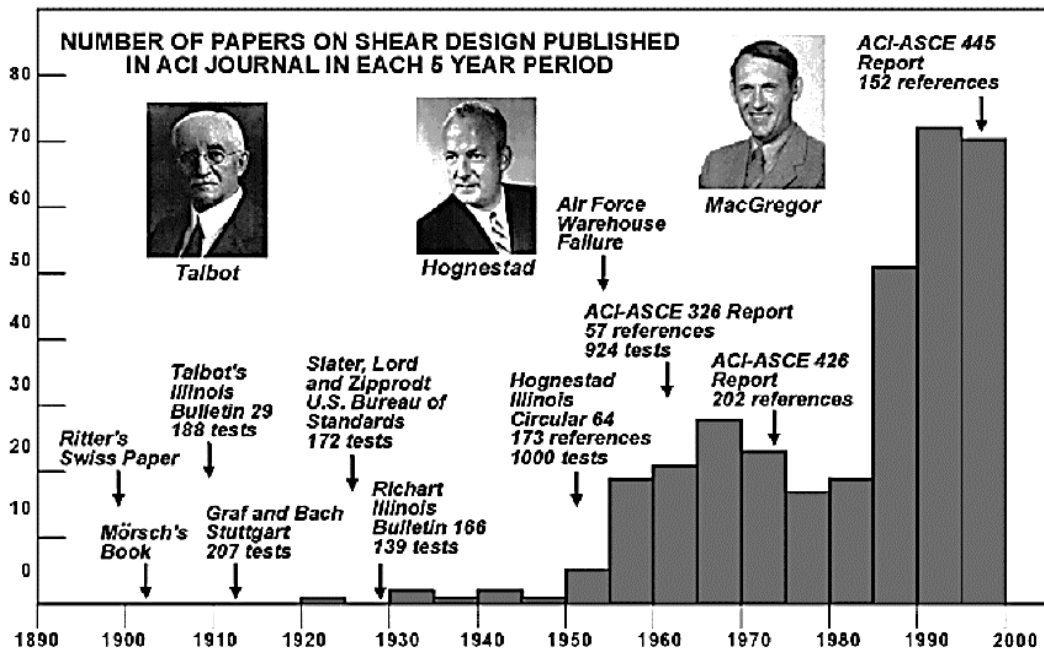
Figure 1.1: Overview of number of papers published in ACI Journal in last century (Shehzad 2014).

Since last three decades, reasonable number of tests has shown that the ACI equations for the shear strength of large lightly reinforced narrow beams not equipped with shear reinforcement can be seriously unconservative. These tests include members subjected to

15

both uniformly-distributed loading and the concentrated loading that is more typical of large transfer elements. The researchers have shown that one-way shear behavior in wide beams and slabs is similar to that in narrow beams, with no significant influence on the shear capacity from member width or from shrinkage and temperature reinforcement. This implies that it is appropriate to use similar design procedures in checking the one-way shear capacity of narrow beams, of wide beams, and of slabs (Angelakos et al. 2001; Bentz 2005; Collins and Kuchma 1999; Lubell et al. 2004; Shioya 1989).

1.1 Background to ACI 318 Shears Design Provisions

In many respect ACI 318-14 shear design provisions are similar to those first published in ACI 318-71.These 1971 procedures were developed in the years immediately following the August 1955 partial collapse of a large warehouse at Wilkins Air Force Base in Shelby, (Figure 1.2). Prior to this collapse, the ACI standard permitted stirrups to be omitted at locations where the shear stress under service loads was calculated to be less than $0.03\,f_c^{'}$.

Figure 1.2: Shear failure of 36-in deep beams in air force warehouse, Shelby, Ohio USA
(Lubell et al. 2004).

Thus, in the warehouse beams, the stirrups had been stopped when the calculated shear stress due to the 80 lb/ft^2 dead load plus the 20 lb/ft^2 live load was less than 0.03×3000 = 90 psi. The 36 in deep beams failed, under dead load only, at a shear stress less than 70 psi.

16

Experiments conducted by the Portland Cement Association (PCA) on 1/3 scale models of the warehouse beams indicated that, without axial tension, the beams could resist a shear stress of about 150 psi prior to failure. The application of a tensile stress of about 200 psi, however, reduced the shear capacity by about 50%. PCA concluded that the tensile stresses caused by the restraint of shrinkage and thermal movements were the reason why the warehouse beams failed at such low shear stresses. The shear stress at which stirrups could be omitted was reduced substantially in the 1963 ACI Code, and then, in 1971, the current provisions, which require at least minimum stirrups in nearly all beams, were introduced. Note the reference to "unexpected tensile force" as the reason for providing minimum shear reinforcement. Also note that the commentary describes the only beams that are excluded from the requirement (to provide minimum shear reinforcement whenever V_u exceeds 1/2 of ϕV_c) as "wide, shallow beams." While the commentary clearly indicates that the 1971 Committee had wide, shallow beams in mind when formulating the exclusion of 11.1.1(c), ACI 318 wording does not make this clear. In ACI 318-89, this apparent conflict between the code and the commentary was resolved by removing the reference to "wide, shallow beams" from the commentary. Essentially, the decision of ACI Committee 318 at that time was that if the web width of a beam is at least twice its total depth, the beam could be treated as a slab, irrespective of the depth of the beam. The ACI 318-14 basic expression for V c, Eq. 22.5.5.1, is:

$$V_c = 2\lambda \sqrt{f_c^{'}} b_w d$$

and it is intended to conservatively estimate the shear failure load of sections not containing shear reinforcement. This expression was formulated in 1962 and, at that time, it was not appreciated that for members without stirrups, the shear stress at failure decreases as the members become size increases. This decrease in failure shear stress as member size increases is called the "size effect" in shear. Obviously, the 71 in deep Bahen Center design will be influenced by this size effect as described in chapter 2 of literature review of this research.

1.2   Objective and Scope

The objective and aim of this research is to investigate the flexure and shear response influencing parameters of RC wide beams, such as;

- Shear capacity demand.
- Effect of beam width on shear and flexure.
- Effect of longitudinal and web reinforcement on flexure and shear capacity of wide beams.
- Suggest measures/methods for better prediction of shear strength of RC wide beams.

Following the introduction and brief review of literature and previous studies in Chapter 1 and chapter 2, chapter 3 deals with flexure and shear characteristics of concrete beam. Chapter 4 pertains to modeling and analysis details of eight numbers RC wide beams considered in this research. Finally Chapter 5 includes with results, discussions, interpretation and recommendations for future work.

1.3   Methodology

The present study has been primarily designed to examine the relationship between one-way shear capacities and shear reinforcement for wide beams, and similar members like design strips taken from one-way slabs or large shell structures. For this purpose, nonlinear finite element analysis will be carried out for total eight wide reinforced concrete beams of sized four of BX series, 120 x 20 x 10 in, and sized four of BZ series, 120 x 40 x 10 in. Two point loading will be applied on all specimens have same span to depth ratio of 3.75 (a/d=3.75). Above mentioned series of beams have different longitudinal reinforcement ratios of 0.5% and 1.98%, with and without web reinforcement and the same will be analyzed in ANSYS to examine the shear and flexure response at different load stages and the results will be compare to those experimentally tested beams. A summary detail of these eight number beams is presented in fallowing Table 1.1.

Table 1.1: Summary of beams consider for FE-analysis.

S.N0	Series	Beam Type	Size (bxh)	Flexure Rebar	ρ (Long)	depth-d	Conc $f_c^{'}$ (psi)	Shear Rebar
1		BXL1	40"x10"	10#4	0.50%	8"	4,000	-----
2	X	BXL2	40"x10"	10#8	1.98%	8"	4,000	-----
3		BXL1W	40"x10"	10#4	0.5%	8"	4,000	# 3 @ 4"
4		BXL2W	40"x10"	10#8	1.98%	8"	4,000	# 3 @ 4"
5		BZL1	20"x10"	5#4	0.50%	8"	4,000	-----
6	Z	BZL2	20"x10"	5#8	1.98%	8"	4,000	-----
7		BZL1W	20"x10"	5#4	0.50%	8"	4,000	# 3 @ 4"
8		BZL2W	20"x10"	5#8	1.98%	8"	4,000	# 3 @ 4"

Linear-elastic methods which are usually used for the analysis and design of concrete structures, predict the response of the structure when the material response is within linear elastic limits. On the other hand, concrete distinctly exhibits nonlinear behavior even under low level of loading because of several factors such as non-linear material response due to crack formation, growth and stress strain relation. On the other hand post yield strain hardening of steel also is usually obtained near failure conditions. Consequently, linear elastic finite element analysis generally leads to conservative results. As a whole therefore the behavior of wide beam must be checked at failure. Nonlinear analysis was used to capture response of concrete beams referred in obove table 1.1.

LITERATURE REVIEW

2.1 General

Since from twenty century and onward lot of experimental as well as analytical work has been done to understand the phenomenon of shear and yet it is not still completely understood. Consensus to develop single shear theory that predicts shear response of the member does not exist even after extensive research and the same is obvious from the dissimilarities found in the formulas of shear strength of various standard and structure design codes. Researchers have identified many factors which influence the shear response of the concrete beams. However, it seems that ACI-318 shear design provision have not been fully incorporated with major shear response influencing factors. Current ACI-318 shear design provisions are based empirical findings.

Many investigators (Bazant and Kazemi 1991; Collins and Kuchma 1999; Kani 1967; Shioya 1989; Shioya et al. 1990) have experimentally established the fact that, for members without stirrups, shear stress at failure decreases as the member becomes larger and as the percentage of longitudinal reinforcement becomes lower. Unluckily, about more than fifty years ago, when the basic ACI shear design provisions were being framed, the sensitivity of size effect and longitudinal steel reinforcement towards shear stress at failure was not recognized.

Substantial numbers of test on large, wide beams as reported in this article in table 2.1 confirms Kani and others (Kani 1966; Kani 1979; Kani 1967; Lubell et al. 2004), conclusion that the shear strength of wide beams is about directly proportional to the width of the beam. Because of this, it is possible to use experimental results from narrow beams to investigate the safety of wide beams. The experimental results, shown in Fig. 2.1, demonstrate that there is a significant size (depth) effect in shear.

About fifty years ago, ACI 318 required stirrups to be provided in reinforced concrete beams only at those locations where the calculated shear stress under service loads exceeded $0.03 fc'$. Air force warehouse beams at Ohio U.S.A, which were designed fallowing procedure valid than at time failed at about 80% of service loads. The experiment on the

large, wide, high-strength concrete beam reported in this article shows that it is still possible for a beam designed by ACI 318-05 to fail under service loading.

The ACI 318-02 basic expression for V_c, is

$$V_c = 2\sqrt{f_c'}\, b_w d \qquad (2.1)$$

and it is intended to conservatively estimate the shear failure load of sections not containing shear reinforcement. This expression was formulated in 1962 and, at that time, it was not appreciated that for members not equipped with stirrups, the shear stress at failure decreases as the members become larger. This decrease in failure shear stress as member size increases is called the "size effect" in shear.
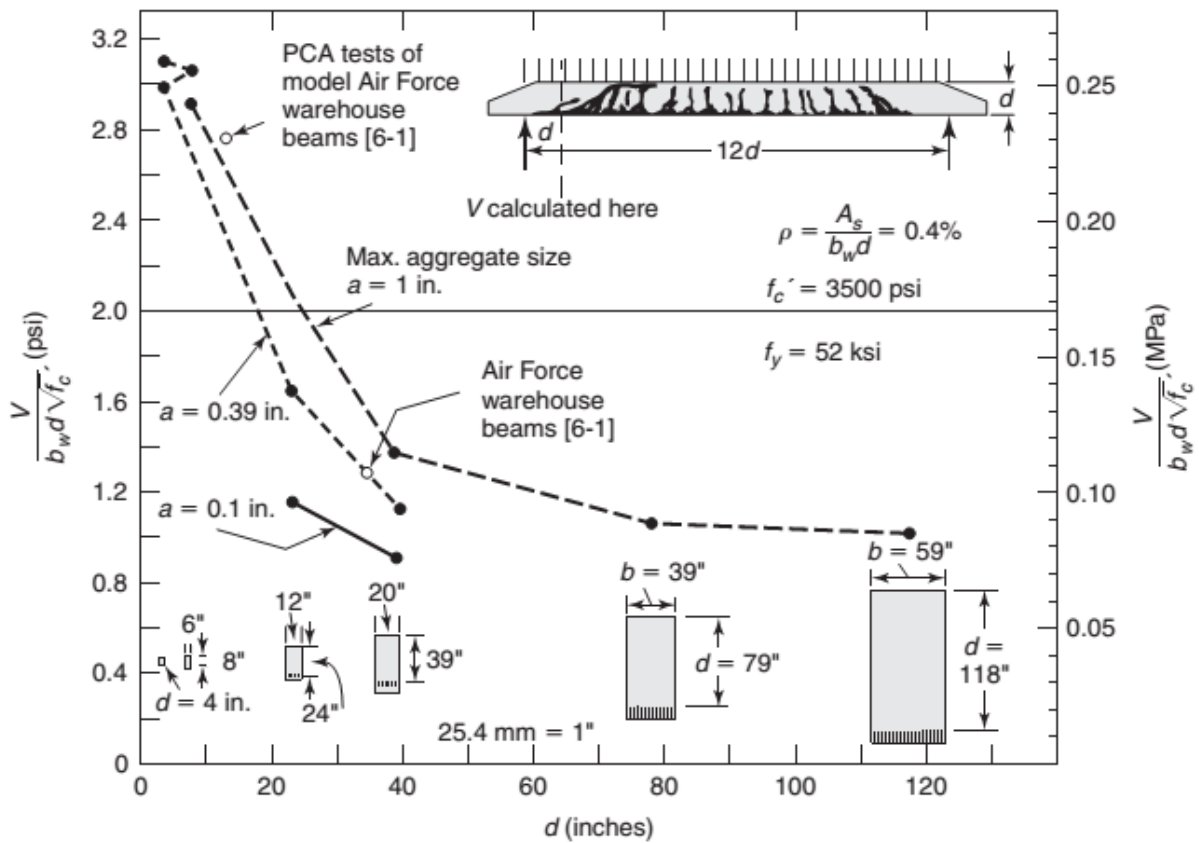
Figure 2.1: Influence of member depth and maximum aggregate size on shear stress at failure (James K. Wight and Macgregor 2012).

Table 2.1: Experimental result from different size effect series involving large beams (Lubell et al. 2004).

No.	Series	Specimen	A_{gg} (inch)	d (inch)	b_w (Inch)	f'_c (psi)	ρ (%)	f_s (psi)	a/d	V_{exp} (Kips)	V_{exp}/V_{aci}
Series-1											
1	Kawano	A-4A	1.6	78.7	23.6	3220	1.2	60	3	137.2	0.65
2	Kawano	A-4B	1.6	78.7	23.6	3350	1.2	60	3	125.9	0.58
3	Tayler	A1	1.5	36.6	15.7	4170	1.35	62.5	3	80.6	1.08
4	Tayler	B1	1.5	18.3	7.9	3890	1.35	62.5	3	23.4	1.3
Series-2											
6	Bhal	B1	1.2	11.7	9.4	3360	1.29	62.9	3	16	1.25
7	Bhal	B2	1.2	23.6	9.4	4300	1.28	62.9	3	27.4	0.94
8	Bhal	B3	1.2	35.4	9.4	3990	1.28	62.9	3	38.6	0.91
9	Bhal	B4	1.2	47.2	9.4	3660	1.28	62.9	3	43.6	0.81
10	Bhal	B5	1.2	23.6	9.4	3880	0.64	62.9	3	24.4	0.88
11	Bhal	B6	1.2	23.6	9.4	3590	0.6	62.4	3	26.2	0.98
12	Bhal	B7	1.2	35.4	9.4	3950	0.64	62.9	3	32.5	0.77
13	Bhal	B8	1.2	36	9.4	4020	0.59	62.4	3	29.8	0.69
Series-3											
1	Cao	SB20003/0	0.75	75.8	11.8	4470	0.36	62.8	2.8	56.3	0.47
2	Yoshida	YB2000/0	0.75	74.4	11.8	4870	0.74	68.2	2.9	63.2	0.52
3	Stanik	BN100	0.75	36.4	11.8	5370	0.76	79.8	2.9	45	0.73
4	Stanik	BN50	0.75	17.7	11.8	5370	0.81	69.6	3	30	0.98
5	Stanik	BN25	0.75	8.9	11.8	5370	0.89	70	3	16.6	1.08
6	Stanik	BN12	0.75	4.3	11.8	5370	0.91	75.7	3.1	9	1.21
7	Kuchma	SE100A-45	0.75	36.2	11.6	7250	1.03	70	5	45	0.63
8	Shioya	1-4	0.75	39.4	19.7	3950	0.4	53.7	UDL	44.4	0.46
9	Shioya	1-3	0.75	23.6	11.8	3060	0.4	63.8	UDL	20.8	0.68
10	Kuzmanovic	----	0.75	24.2	37.8	6520	0.71	70.2	UDL	109.8	0.74
11	Tayler	B3	0.75	18.3	7.9	4130	1.35	62.5	3	19.2	1.03
12	Tayler	C2	0.75	9.2	3.9	3670	1.35	62.5	3	5.4	1.23
Series-4											
1	Lube	AT-1	0.17	36	79.1	9300	0.76	66.7	3	294	0.54
2	Angelakes	DB165	0.14	36.4	11.8	9430	1.01	79.8	2.9	42.9	0.51
3	Kuchma	BRL100	0	36.4	11.8	13600	0.5	79.8	2.9	38.1	0.44
4	Stanic	BH100	0	36.4	11.8	14300	0.76	79.8	2.9	44.7	0.52
5	Stanic	BH50	0	17.7	11.8	14300	0.81	69.6	3	29.9	0.71
6	Stanic	BH25	0	8.9	11.8	14300	0.89	70	3	19.2	0.92
7	Grimm	S3.1	0	29.5	11.8	13200	0.42	68.2	3.5	33.3	0.48
8	Grimm	S3.3	0	29.4	11.8	13700	0.83	70.6	3.5	45.8	0.66
9	Shioya	2-6	0.2	39.4	19.7	4090	0.4	53.7	UDL	37.1	0.37
10	Shioya	2-4	0.1	23.6	11.8	3960	0.4	63.8	UDL	17.2	0.49
11	Shioya	2-2	0.04	7.9	6.2	4130	0.4	63.8	UDL	6.4	1.01

Figure 2.2: Failure of large beam at 47% of ACI shear failure loads (Lubell et al. 2004).

Considerable number of experiment (Kani 1966; Lai et al. 1978; Tompos and Frosch 2002) have been performed to examine the relation of longitudinal steel reinforcement and shear strength of concrete beams, and now it has been established that amount of longitudinal steel reinforcement has significant effect on strength of beam particularly without web reinforcement. For beams having about longitudinal reinforcement less than 1% may fail before the ACI-318 predicted shear strength of beams, further as amount of longitudinal steel reinforcement increases beam strength also increases as shown in figure 2.3.
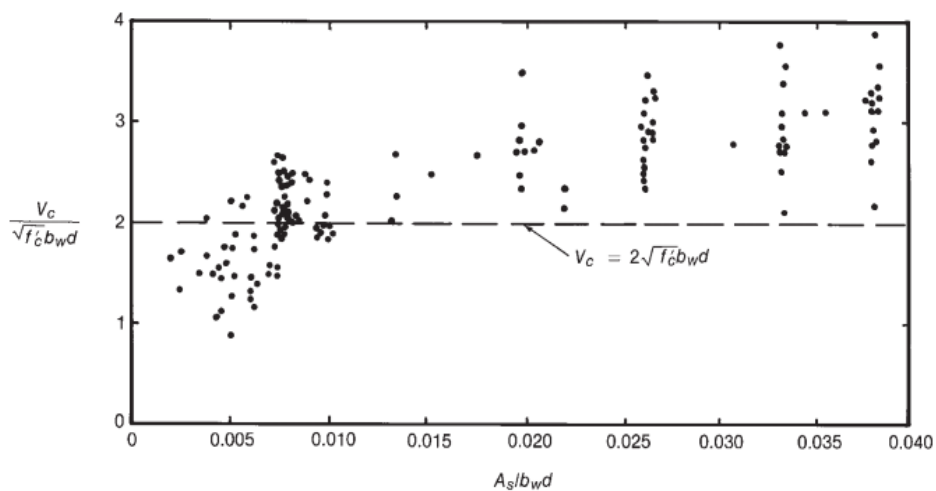
Figure 2.3: Effect of longitudinal steel reinforcement of shear strength of concrete beam (Lai et al. 1978).

23

2.2   Size Effect in Shear

A significant number of tests have shown that the ACI equations for the shear strength of large, lightly reinforced narrow beams not containing shear reinforcement can be seriously unconservative (Angelakos et al. 2001; Bentz 2005; Collins and Kuchma 1999; Kani 1967; Lubell et al. 2004; Shioya 1989), these tests include members subjected to both uniformly-distributed loading and the concentrated loading that is more typical of large transfer elements. The research presented in these papers indicates that one-way shear behavior in wide beams and slabs is similar to that in narrow beams, with no significant influence on the shear capacity from member width. This implies that it is appropriate to use similar design procedures in checking the one-way shear capacity of narrow beams, of wide beams, and of slabs.

Kani (Kani 1967) from department of civil engineering, university of Toronto, were among the first to study size effect of both depth and width in shear. He tested the series of beams with depth ranging from 6 inch to 48 in. He found that there is a considerable influence of beam depth on shear strength of beams and even for beams of larger depth factor of safety may drop up to 40 % of smaller one. The typical loading arrangements and cross section of Kani tested beams are shown in figure 2.4 and results showing the effect beam depth versus relative shear strength of beams are plotted in figure 2.5.
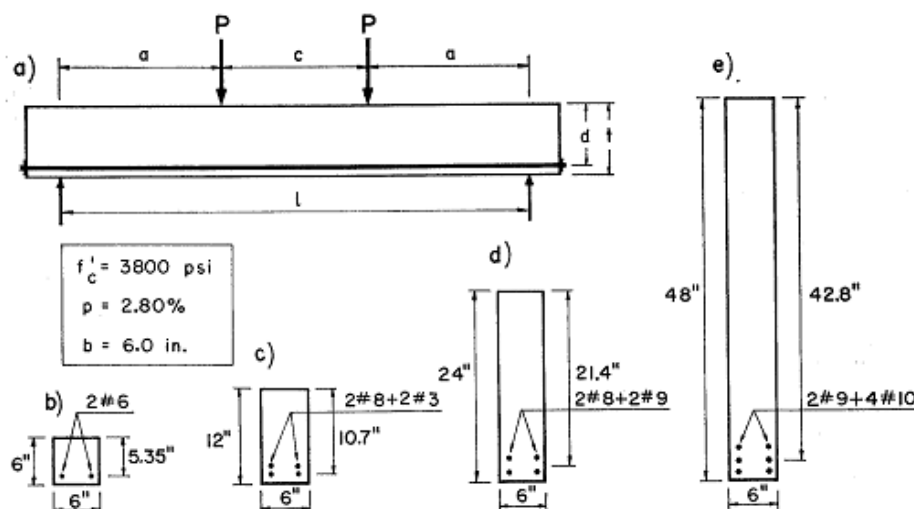
Figure 2.4: Typical loading arrangement and cross section of beams (Kani 1967).

24
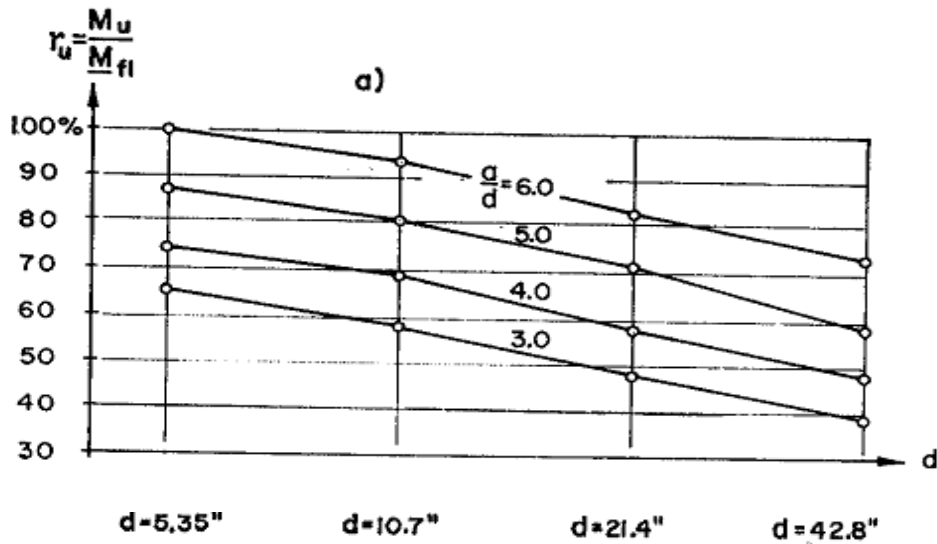
Figure 2.5: Variation of relative beam strength versus depth (Kani 1967).

In their research Kani and Collins (Collins and Kuchma 1999; Kani 1966) also experimentally showed that influence of beam width on shear failure strength is negligible. Kani tested the beams under two points loading with two different width of 6 inch and 24. The results of these tests are shown in figure 2.6. Kani also reported that relative shear failure strength of wider beams of 24 inch was greater (Max. 10%) than the smaller one of 6 inch width.
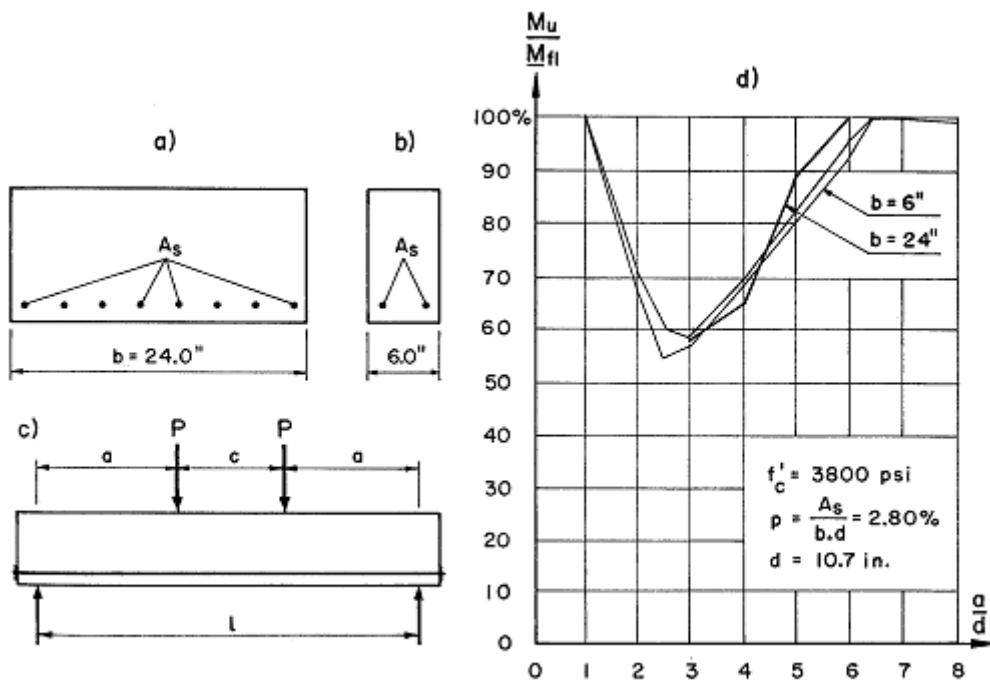
Fig. 10—Comparison of tested beams of different width

Figure 2.6: Variation of relative beam strength versus width (Kani 1967).

Other researchers Shioya and Shioya et al (Shioya 1989; Shioya et al. 1990) in Japan conducted most extensive experimental research to investigate the beam size effect in shear. Five series of beams were tested with depth ranging from 8 inch to 118 inch. The main results of their research work are summarized in figure 2.1. The results are very clear in depicting the depth effect of beams. It can be seen that at failure shear stress decreases, both as the member depth increases and as the maximum aggregate size decreases.

The simplest explanation of the size effect in shear is that the larger crack widths that occur in larger members reduce aggregate interlock. Crack widths increase nearly linearly both with the tensile strain in the reinforcement and with the spacing between cracks.

Although considerable numbers of experiment conducted till to date have established the size effect in shear. Many of these tests were on beams with depth ranging from 9 inch to 15 inch (Kani 1967). But none of these tests have been on large, wide beams that satisfy the ACI 318 requirement of having a width at least twice as great as the overall depth of the beam. Toronto university Bahen center beam AT-1 was designed in accordance with ACI 318-02 to resist an un-factored point load of 600 k (2700 kN) applied at mid span (Lubell et al. 2004).

Figure 2.7: Construction and loading of Bahen Centre large wide beam AT-1 under testing machine at the University of Toronto (Lubell et al. 2004).

Beam AT-1 showed a brittle shear failure, typical for large high-strength concrete beams as the central load reached 549 k. This failure load is only 52% of the failure load predicted by the current ACI shear provisions and means that the beam would fail under the actual service loads.

Figure 2.8: Failure surface of beam AT-1 (Lubell et al. 2004).

Prodromos D. Zararis (Zararis 2003) in his research argued that problem of diagonal shear failure of RC slender beams without Web reinforcement can be reduced to the problem of size effect on split tensile failure. Many researchers (Bazant and Kazemi 1991; Hasegawa et al. 1985) have conducted test on cylindrical disks of constant thickness. The results confirm the existence of size effect on split-tensile failure, and show that up to a certain critical diameter the split cylinder strength decreases as the diameter increases.

2.3 Application of Finite Element Method for Structural Analysis

The history of finite element analysis can be found back to the work by Alexander Hrennikoff (Hrennikoff 1941). He presented the framework method, in which collection of bars and beams were presented by a plane elastic medium. He was the pioneer of one important characteristic of finite element analysis, the mesh discretization of continuous domain into discrete subdomain called finite element.

▪ The term finite element method was first used by Clough in his research paper published in 1965 (Clough and Tocher 1965).

▪ A Dayton conference on finite elements (at the Air Force Flight Dynamics Laboratory in Dayton, Ohio, U.S.A.) was held in 1965.

- First book on the "Finite Element Method" was published by Zienkiewicz and Chung in 1967.
- FEM was applied to a wide variety of engineering problems in the late 1960s and early 1970s.
- Most commercial FEM software packages (ABAQUS, NASTRAN, ANSYS, etc.) originated in the 1970s.

Ngo and Scordelis (Ngo and Scordelis 1967) presented their earliest publication on analysis of RC structures. They studied simple beam for analysis and material of the same i.e. concrete and steel was represented by constant strain triangle. Special bond slip element was used to define the bond slippage effect. They performed linear elastic analysis by already defined cracks patterns for the determination of principle stresses in concrete, steel reinforcement.

Scordelis et al (Scordelis et al. 1974) used same concept to investigate the influence of shear in beams with diagonal tension crack, he also accounted for the effect stirrups, dowel shear, aggregate interlocking and horizontal splitting along the main reinforcing bar near supports. Nilson (Nilson 1972) used incremental load for nonlinear analysis and bring together nonlinear material properties for concrete and steel and non-linear relation of bond slip. Nayak and Zienkiewicz (Nayak and Zienkiewicz 1972) performed two dimensional stress studies that include the tensile cracking of concrete using initial stress approach.

Because of lack of sufficient knowledge of concrete material behaviour under tri-axial stress state and the computational effort involved, little work has been done on three-dimensional behavior of reinforced concrete systems using solid finite element analysis. Suidan and Schnobrich (Suidan and Schnobrich 1973) first studied the behavior of beams with 20-node three-dimensional element by using isoperimetric finite elements. Based on the von-Mises yield criterion, concrete behavior in compression was assumed elastic-plastic. Much of conclusions of general applicability of finite element analysis have been arrived for reinforced concrete structures.

FLEXURE AND SHEAR RESISTANCE OF CONCRETE BEAM

3.1   Flexure Theory

A structure member called beam supports applied loads and its own weight primarily by two internal actions moment M and shear V. A simple beam supporting uniformly distributed load per unit length, plus a concentrated load as shown in figure 3.1a.
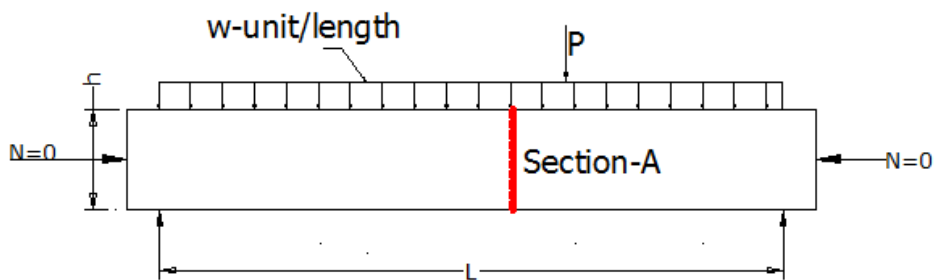
a): Beam L-Section
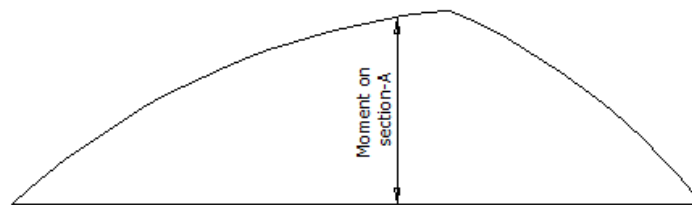
b): Bending moment diagram

Figure 3.1: L-section and bending moment diagram for beam.

Due to loads, bending moment distribution along beam length is shown in Fig. 3.1b. The bending moment is calculated from the loads by using the laws of statics. The moments are independent of the composition and size of beam for a given span length L and a given set of loads ω and P.

For an uncracked, homogeneous rectangular beam without reinforcement, conventional elastic beam theory results in the equation which gives the distribution of stresses shown in Fig. 3-2.
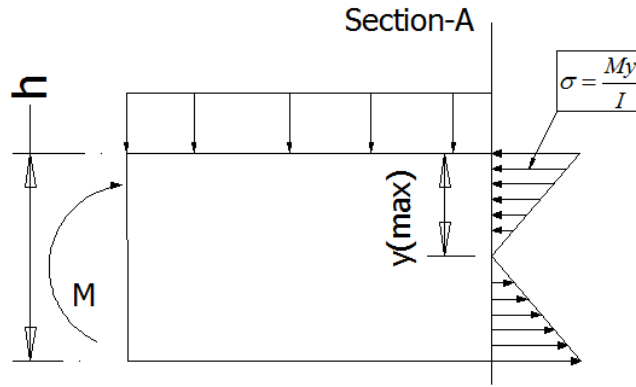
Figure 3.2: Elastic beam stress and stress distribution in homogeneous beam.

The resultant compressive force C and tensile force T, which is equal to the volume of the compressive or tensile stress block that is formed along width of beam of Fig. 3.2, is given by

$$C = T = \frac{\sigma \, y_{(max)}}{2} (b \frac{h}{2}) \qquad (3.1)$$

Where b is width of beam. The forces C (upper triangle of stress distribution diagram in figure 3.2) and T (lower triangle of stress distribution diagram in figure 3.2) act through the centroids of the volumes of the respective stress blocks. When distribution of stress variation along beam depth are considered to vary linearly as in the elastic case, these forces act at h/3 above or below the neutral axis, so that external moment M can be written as:

Moment M= Force * lever arm

$$M = \sigma \, y_{(max)} \frac{bh}{2} (\frac{2h}{3}) \qquad (3.2)$$

$$M = \sigma \, y_{(max)} \frac{bh^3 / 12}{h / 2} \qquad (3.3)$$

Moment of inertia "I" for rectangular section can be written as:

$$I = \frac{bh^3}{12} \quad \text{and} \quad y_{(max)} = \frac{h}{2}$$

It fallows that $$\sigma = \frac{My}{I} \qquad (3.4)$$

30

The elastic beam theory of Eq. (3.4) cannot be used in the design of reinforced concrete beams, because the compressive stress–strain relationship for concrete becomes nonlinear at higher strain values.

What is even more important is that concrete cracks at low tensile stresses, making it necessary to provide steel reinforcement to carry the tensile force T.

3.1.1   Basic Assumptions in Flexure Theory for Concrete

The flexure theory when applied to reinforced concrete is based on three fundamental assumptions that are considered sufficient to calculate the moment resistance of a concrete beam, which are given below:

- Section that is perpendicular to the beam axis, remains plane before and after bending.
- To ensure perfect bond between concrete and steel, strain in the reinforcement is supposed to be equal to the strain in the concrete at the same level.
- The concrete and steel reinforcement stresses can be computed from the strains by using stress–strain curves for both materials i.e. concrete and steel.

The first of these is the traditional "plane sections remain plane" assumption made in the development of flexural theory for beams constructed with any material. The second assumption is necessary, because the concrete and the reinforcement must act together to carry load. This assumption implies a perfect bond between the concrete and the steel. The third assumption will be demonstrated in the following development of moment–curvature relationships for beam sections.

3.1.2   Simplifications in Flexure Theory for Design

The three assumptions already made are sufficient to allow calculation of the strength and behavior of reinforced concrete elements. For design purposes, however, the following additional assumptions are introduced to simplify the problem with little loss of accuracy.

1. The tensile strength of concrete is neglected in flexural-strength calculations (ACI-318-14, Section 22.2.2.2). The strength of concrete in tension is roughly one-tenth of the compressive strength, and the tensile force in the concrete below the zero strain axes, is small compared with the tensile force in the steel. Hence, the contribution of

the tensile stresses in the concrete to the flexural capacity of the beam is small and can be neglected. It should be noted that this assumption is made primarily to simplify flexural calculations. In some instances, particularly shear, bond, deflection, and service-load calculations for prestressed concrete, the tensile resistance of concrete is not neglected.

2. When the strain in extreme concrete compression fibers reached to value of 0.003, the section is assumed to have its nominal flexural, this is an artificial limit developed by code committees to define at what point on the general moment–curvature relationship the nominal strength of the section is to be calculated. Thus, design calculations are simplified when a limiting strain is assumed. ACI 318-14 Code Section 22.2.2.1 specifies a limiting compressive strain, equal to 0.003.
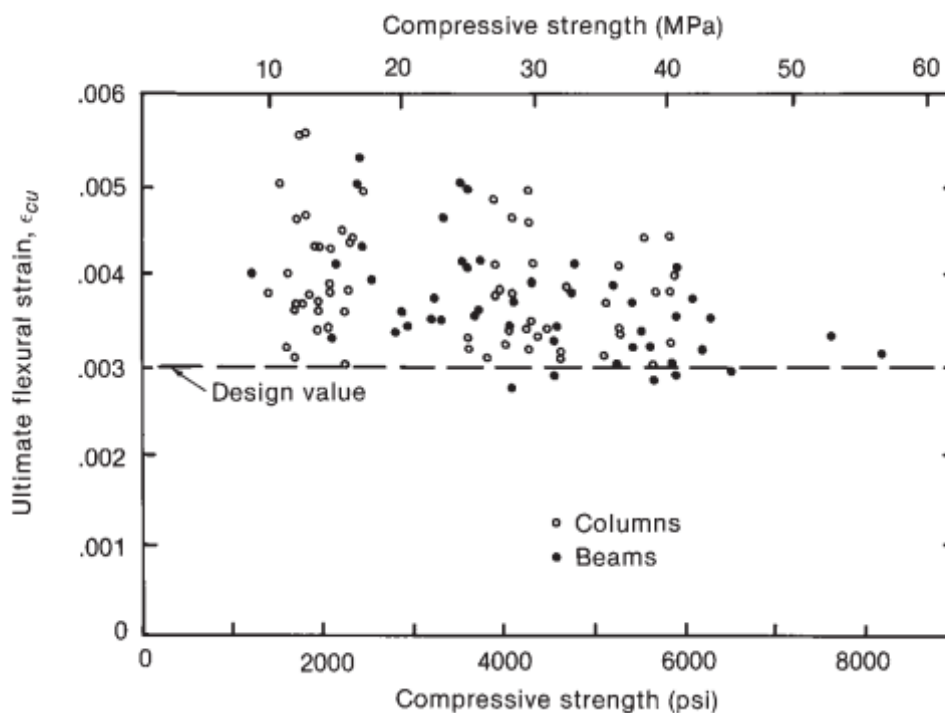
Figure 3.3: Ultimate strain from tests of reinforced concrete member (James K. Wight and Macgregor 2012).

3. The compressive stress–strain relationship for concrete may be based on measured stress–strain curves or may be assumed to be rectangular, parabolic, trapezoidal, or any other shape that results in prediction of flexural strength in substantial agreement with the results of comprehensive tests (ACI Code Section 22.2.2.3)

As a further simplification, ACI Code Section 10.2.7 permits the use of an equivalent rectangular concrete stress distribution shown in Fig. 3.4 for nominal flexural strength calculations. This rectangular stress block, originally proposed by Whitney (Whitney 1937), is defined by the following:

A uniform compressive stress of 0.85 shall be considered distributed over an equivalent compression zone bounded by the edges of the cross section and a straight line located parallel to the neutral axis at a distance "a" from the concrete fiber with the maximum compressive strain. Thus, as shown in Fig. 3.4.
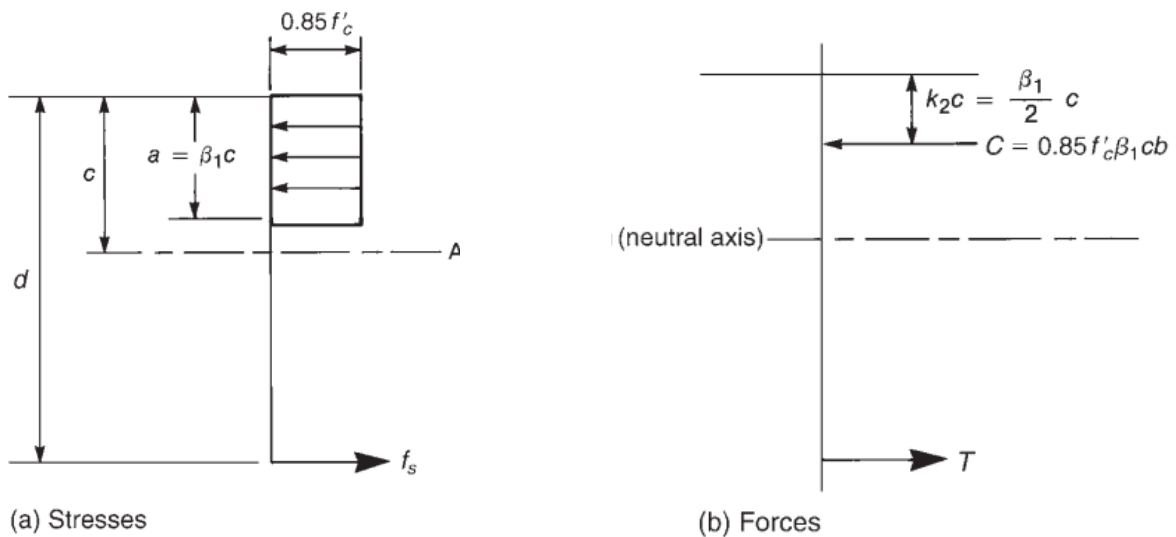
Figure 3.4: Equivalent rectangular stress block (James K. Wight and Macgregor 2012).

The distance c from the fiber of maximum compressive strain to the neutral axis is measured perpendicular to that axis.

The factor β1 shall be taken as fallows

For concrete strength, f_c' up to and including 4,000 psi

$$\beta_1 = 0.85$$

For 4,000 psi $< f_c' <$ 8,000 psi

$$\beta_1 = 0.85\text{-}0.05(f_c'\text{-}4000)/1000$$

For f_c' greater than 8,000 psi

$$\beta_1 = 0.65$$

For a rectangular compression zone of constant width b and depth to the neutral axis c, the resultant compressive force is

$$C = 0.85\, f_c'\, b\, \beta_1 c = 0.85\beta_1\, f_c'\, bc$$

3.2   Shear in Concrete Beams

A beam resists loads primarily by means of two internal actions moment M, and shear, V. While designing reinforced concrete member usually flexure is considered first, leading to the size of the section and the arrangement of reinforcement to provide the necessary moment resistance. Limits are placed on the amounts of flexural reinforcement which can be used to ensure that if failure was ever to occur; it would develop gradually, giving warning to the occupants. The beam is then proportioned for shear. The manner in which shear failures can occur varies widely with the dimensions, geometry, loading, and properties of the members. For this reason, there is no unique way to design for shear.

3.3   Behavior of Beams Failing in Shear

When determining the flexural strength of concrete beams, a theory based on Hooke's Law is used, where stress is proportional to strain and the section remains plane before and after bending. When determining the shear strength of concrete beams or shear resistance, we have the two following

3.4   Behavior of Beams without Web Reinforcement

The moments and shears at inclined cracking and failure of rectangular beams without web reinforcement are plotted in Fig. 3.5b and c as a function of the ratio of the shear span a to the depth d. (See Fig. 3.5a.) The beam cross section remains constant as the span is varied. The maximum moment and also shear that can be developed corresponds to the nominal moment capacity, of the cross section plotted as a horizontal line in Fig. 3.5b. The shaded areas in this

figure show the reduction in strength due to shear. Web reinforcement is normally provided to ensure that the beam reaches the full flexural capacity.

Figure 3.5b suggests that the shear spans can be divided into three types: short, slender, and very slender shear spans. The term deep beam is also used to describe beams with short shear spans. Very short shear spans, with a/d from 0 to 1, develop inclined cracks joining the load and the support. Here, the reinforcement serves as the tension ties of a tied arch and has a uniform tensile force from support to support. The most common mode of failure in such a beam is an anchorage failure at the ends of the tension tie.

Short shear spans with a/d from 1 to 2.5 develop inclined cracks and, after a redistribution of internal forces, are able to carry additional load, in part by arch action. The final failure of such beams will be caused by a bond failure, a splitting failure, or a dowel failure along the tension reinforcement, or by crushing of the compression zone over the top of the crack. The latter is referred to as a shear compression failure. Because the inclined crack generally extends higher into the beam than does a flexural crack, failure occurs at less than the flexural moment capacity.
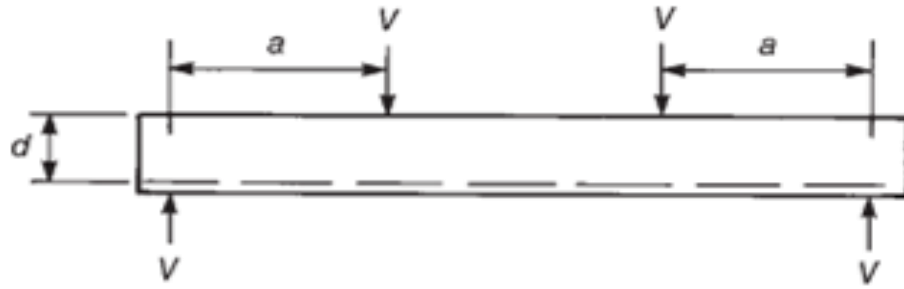
(a) Beam.
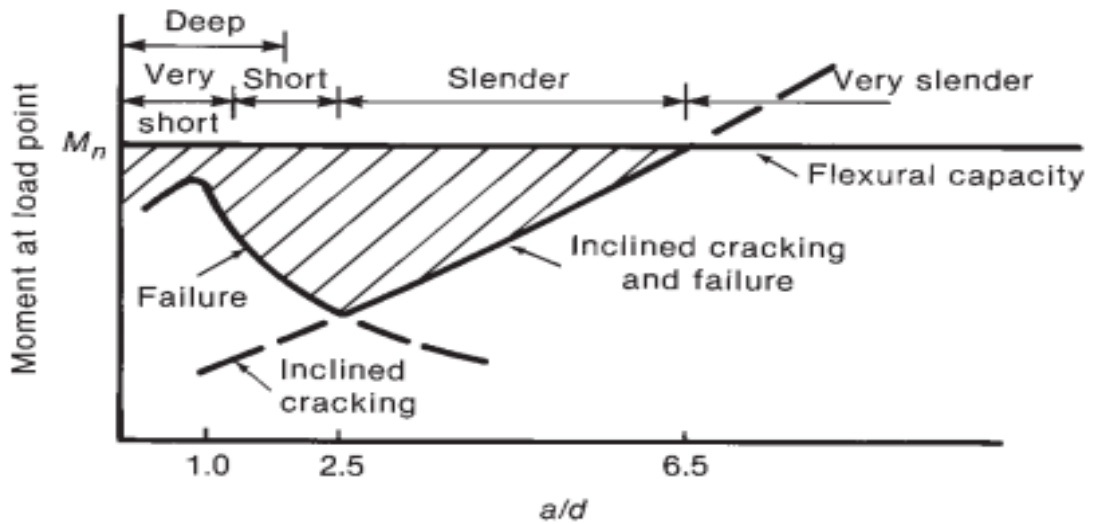
(b) Moments at cracking and failure.
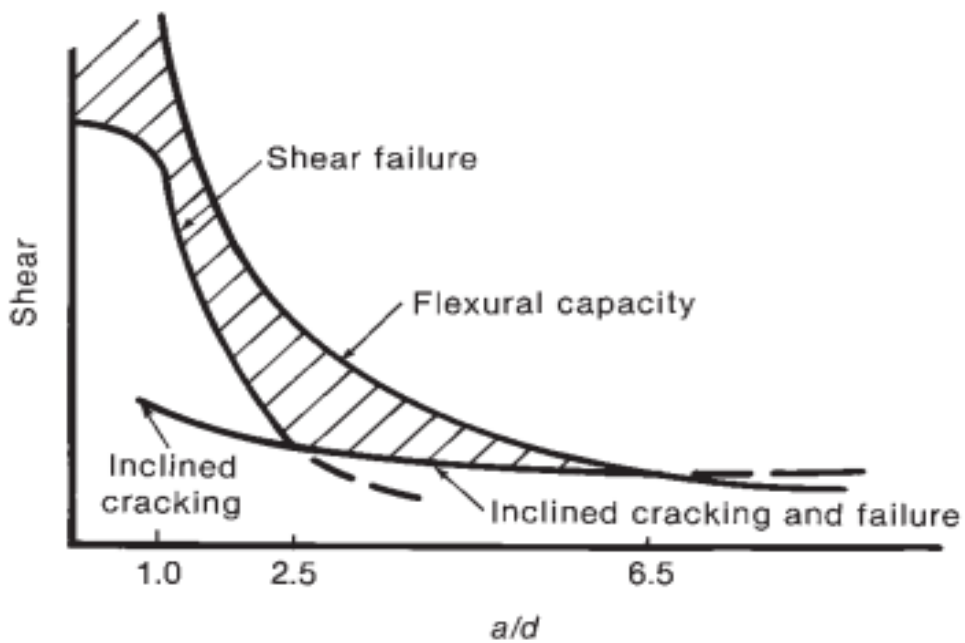
(c) Shear at cracking and failure.

Figure 3.5: Effect of a/d ratio on shear strength of beams without stirrups.

In slender shear spans, those having a/d from about 2.5 to about 6, the inclined cracks disrupt equilibrium to such an extent that the beam fails at the inclined cracking load, as shown in Fig. 3.5b. Very slender beams, with a/d greater than about 6, will fail in flexure prior to the formation of inclined cracks

Figures 3.6 and 3.7 presents discussion of the behavior of beams failing in shear and the factors affecting their strengths. It is important to note that, for short and very short beams, a major portion of the load capacity after inclined cracking is due to load transfer by the compression struts shown in Fig. 3.6. If the beam is not loaded on the top and supported on the bottom in the manner shown in Fig. 3.6, these compression struts will not form and failure occurs at, or close to, the inclined cracking load.
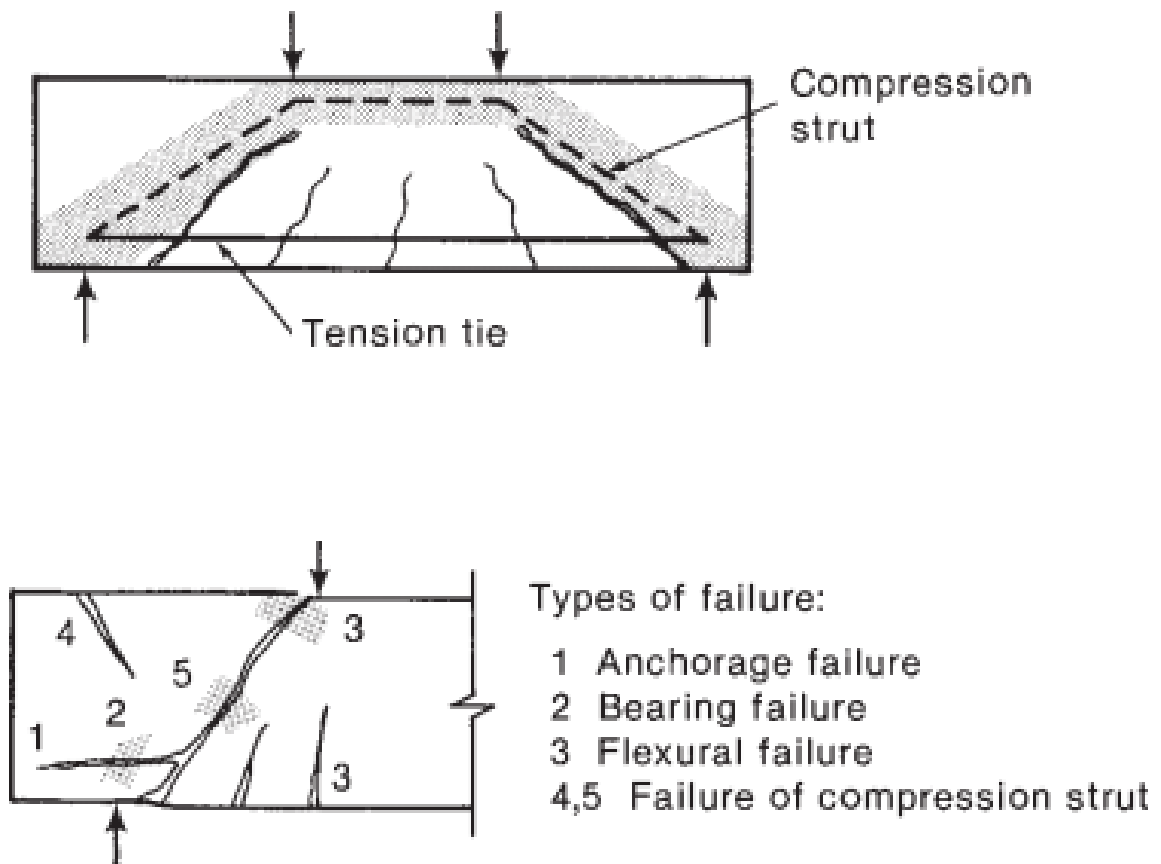
Figure 3.6: Modes of failure of deep beams, a/d=0.5 to 2.0
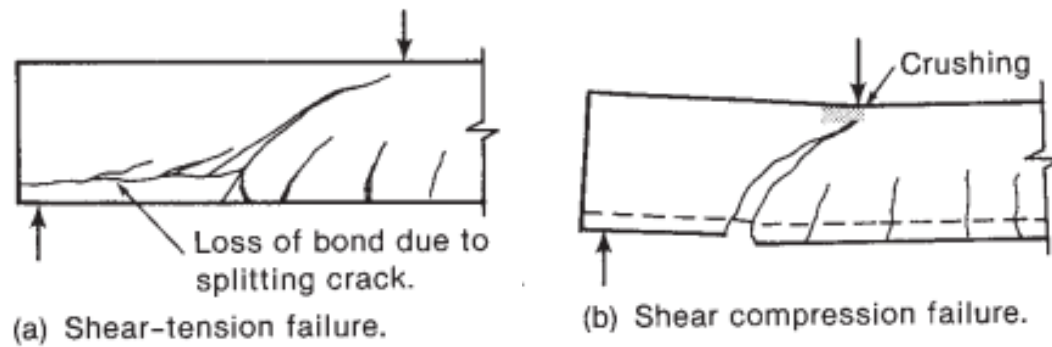
Figure 3.7: Modes of failure of short shear span, a/d=1.5 to 2.5

Because the moment at the point where the load is applied is for a beam loaded with concentrated loads, as shown in Fig. 3.5a. Figure 3.5b can be re-plotted in terms of shear capacity, as shown in Fig. 3.5c. The shear corresponding to a flexural failure is the upper curved line. If stirrups are not provided, the beam will fail at the shear given by the "shear failure" line. This is roughly constant for a/d greater than about 2. Again, the shaded area indicates the loss in capacity due to shear. Note that the inclined cracking loads of the short shear spans and slender shear spans are roughly constant. This is recognized in design by ignoring a/d in the equations for the shear at inclined cracking. In the case of slender beams, inclined cracking causes an immediate shear failure if no web reinforcement is provided.

3.5 Factors Affecting the Shear Strength of Beams without Web Reinforcement

Beams without web reinforcement will fail when inclined cracking occurs or shortly afterwards. For this reason, the shear capacity of such members is taken equal to the inclined cracking shear. The inclined cracking load of a beam is affected by five principal variables, some included in design equations and others not.

3.5.1 Tensile Strength of Concrete

Shear strength of concrete beam without web reinforcement that is a function of tension at inclined crack is directly affected by the tensile strength of concrete. As in the web of beams there exists a biaxial state of principal tension and compression stresses. Inclined cracking load is frequently related to strength obtained from a split-cylinder tension test as the similar

38

state of stresses as in the beam web exists such a test. Inclined cracking proceeds from flexural cracking interrupts the elastic-stress field to such an extent that inclined cracking occurs at a principal tensile stress roughly half of for the uncracked section.

3.5.2 Longitudinal Reinforcement Ratio

Amount of longitudinal steel reinforcement significantly influence the strength of concrete beam as shown in figure 3.8 that presents the shear capacities (psi units) of simply supported beams without stirrups as a function of the steel ratio. The practical range of steel ratio to develop the shear failures may range from 0.0075 to 0.025. For this range, shear strength of beam is approximated shown in below equation as indicated by the horizontal dashed line in Fig. 2.3 of chapter 2.

$$V_c = 2\lambda\sqrt{f_c^{'}} b_w d \qquad (3.5)$$

it is evident that this equation has a tendency to overestimate the shear strength for beams with small longitudinal steel ratio. The reason behind this is that, when the longitudinal steel ratio is relatively less, flexural cracks spread higher into the beam and open wider than would be the case for large values of steel ratio. An increase in crack width causes a reduction in shear that is being resisted due to aggregate interlock. Eventually, the resistance along the crack drops below that required resisting the loads, and the beam fails suddenly in shear.

3.5.3 Shear Span-to-Depth Ratio

Inclined cracking shear is also influenced by the shear span-to-depth ratio a/d, and portion of the member for which a/d is less than 2, as shown in Fig. 3.5c. For longer shear spans, where B-region behavior dominates, a/d has little effect on the inclined cracking shear, and can be neglected.

3.5.4 Lightweight Aggregate Concrete

Lightweight aggregate concrete has a lower tensile strength than normal weight concrete for a given concrete compressive strength. As shear strength of a concrete member without web reinforcement is directly related to the tensile strength of the concrete. This is handled in the ACI Code through the introduction of the factor λ, which accounts for the difference for the

tensile strength of lightweight concrete. ACI Code Section 8.6.1 states that for sand-lightweight concrete (i.e., concrete with normal weight small aggregates, and lightweight large aggregates), λ is to be taken as 0.85. For all lightweight concrete (i.e., both the large and small aggregate are lightweight materials), the same is taken as 0.75.

3.5.5 Size of Beam

An increase in the overall depth of a beam with very little (or no) web reinforcement results in a decrease in the shear at failure for a given and a/d. The width of an inclined crack depends on the product of the strain in the reinforcement crossing the crack and the spacing of the cracks. With increasing beam depth, the crack spacing and the crack widths tend to increase. This leads to a reduction in the maximum shear stress that can be transferred across the crack by aggregate interlock as shown in figure 2.1 of chapter 2.

An unstable situation develops when the shear stresses transferred across the crack exceed the shear strength, when this occurs, and the faces of the crack slip, one relative to the other It shows a significant decrease in the shear strengths of geometrically similar, uniformly loaded beams with effective depths d ranging from 4 in. to 118 in. and made with 0.1-in., 0.4-in., and 1-in. maximum size coarse aggregates.

The dashed lines show the variation in shear strength of beams without stirrups in tests. The beams were uniformly loaded and simply supported as shown in the inset. Each black circular dot in the figure corresponds to the strength of a beam having the section plotted directly below it.

3.5.6 Axial Force

Axial tensile forces tend to decrease the inclined cracking load, while axial compressive forces tend to increase it. As the axial compressive force is increased, the onset of flexural cracking is delayed, and the flexural cracks do not penetrate as far into the beam. Axial tension forces directly increase the tension stress, and hence the strain, in the longitudinal reinforcement. This causes an increase in the inclined crack width, which, in turn, results in a decrease in the maximum shear tension stress that can be transmitted across the crack. This reduces the shear failure load. A similar increase is observed in prestressed concrete beams.

The compression due to prestressing reduces the longitudinal strain, leading to a higher failure load.

3.5.7 Coarse Aggregate Size

As the size (diameter) of the coarse aggregate increases, the roughness of the crack surfaces increases, allowing higher shear stresses to be transferred across the cracks. As shown in Fig. 2.1 of chapter 2, a beam with 1-in. course aggregate and 40-in. Effective depth failed at about 150 percent of the failure load of a beam with and 0.1-in. maximum aggregate size. In high-strength concrete beams and some lightweight concrete beams, the cracks penetrate pieces of the aggregate rather than going around them, resulting in a smoother crack surface. This decrease in the shear transferred by aggregate interlock along the cracks reduces.

3.6 Behavior of Beams with Web Reinforcement

Inclined cracking causes the shear strength of beams to drop below the flexural capacity. The purpose of web reinforcement is to ensure that the full flexural capacity can be developed. Prior to incline cracking, the strain in the stirrups is equal to the corresponding strain of the concrete. Because concrete cracks at a very small strain, the stress in the stirrups prior to inclined cracking will not exceed 3 to 6 ksi. Thus, stirrups do not prevent inclined cracks from forming; they come into play only after the cracks have formed. The forces in a beam with stirrups and an inclined crack are shown in Fig. 3.8. The shear transferred by tension in the stirrups, does not disappear when the crack opens wider, so there will always be a compression force and a shear force acting on the part of the beam below the crack.

41
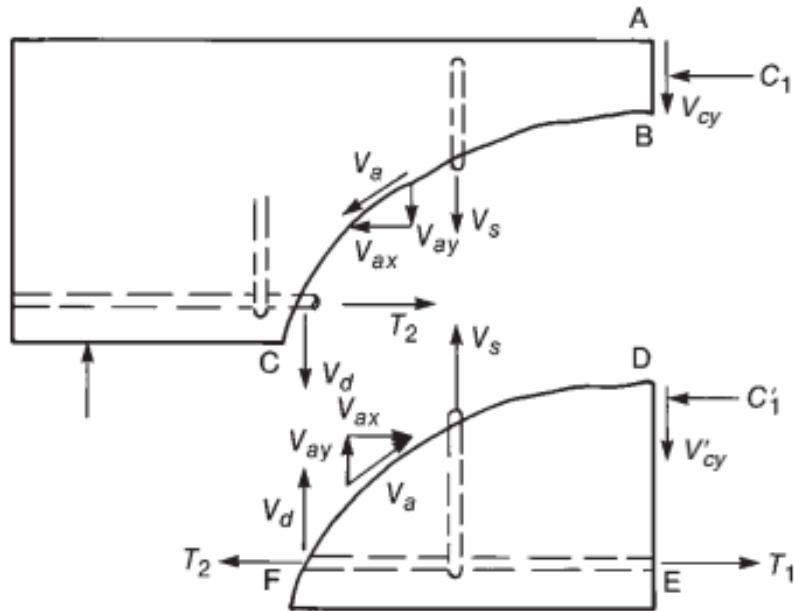
Figure 3.8: Internal forces in Cracked beam with stirrups.

3.7 Types of Cracks

There are three types of crack depending upon on the span-to-depth ratio of the beam and loading. Actually moment and shear along the beam span are influenced by these and others variables. If we consider a simply supported beam (without prestressing) under uniformly distributed load, fallowing types of cracks are identified.

3.7.1 Flexural Cracks

These cracks form formed when due to moment, flexure stress value increases from beam rupture modulus and their depth tend to increase towards the beam top. These are shown in figure 3.9a.

3.7.2 Web Shear Cracks

Web shear cracks formed in beams near neutral axis when due to combined flexure and shear action or only due increased shear stress value, these cracks are usually close the support and propagate inclined toward beam longitudinal axis as shown in figure 3.9b.

3.7.3 Flexure Shear Cracks

These cracks form at the bottom due to flexure and propagate due to both flexure and shear. In the following figure, the formation of cracks for a beam with large span-to-depth ratio and uniformly distributed loading is shown.

a) Initiation of flexural cracks

b) Growth of flexural cracks and formation of flexure shear and web shear cracks.

c) Cracks before failure
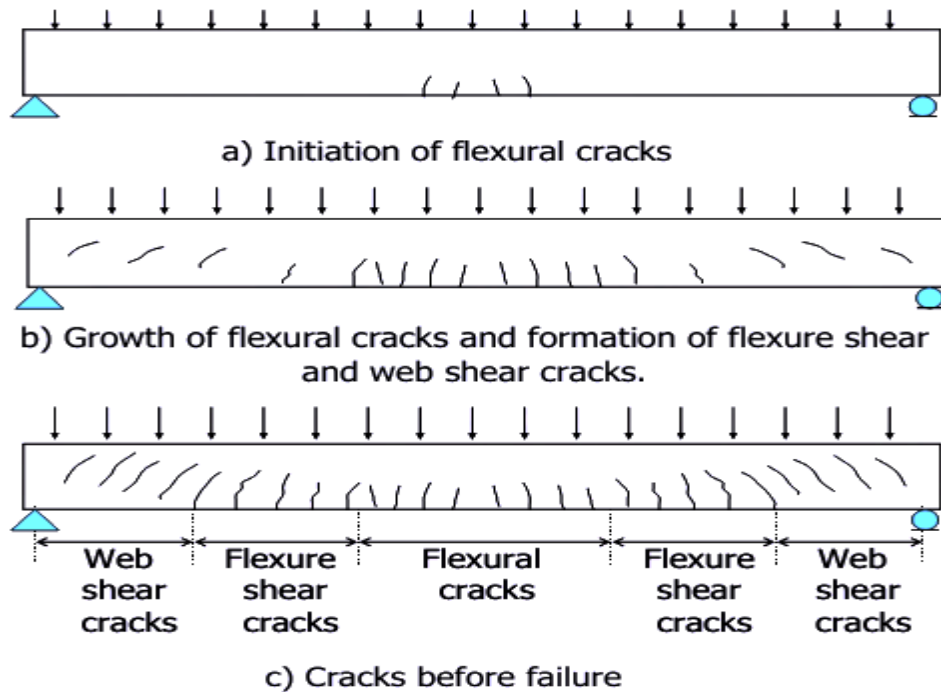
Figure 3.9: Formation of cracks in a reinforced concrete beam

3.8 Modes of Failure

Concrete beams under flexure load test may fail in different ways depending upon many factors. For many reasons shear failure may occurs including beams with low span-to-depth ratio or inadequate shear reinforcement. A shear failure is sudden and generally beam fails before reaching its flexure capacity. How beams will fail or occurrence of failure mode depends on the span-to-depth ratio, loading, cross-section of the beam, amount and anchorage of reinforcement. These failure modes are explained in next.

3.8.1 Diagonal Tension Failure

Concrete beam without web reinforcement may fail diagonal tension shear failure mode. Inclined cracks propagate rapidly towards beam depth due to inadequate shear reinforcement.
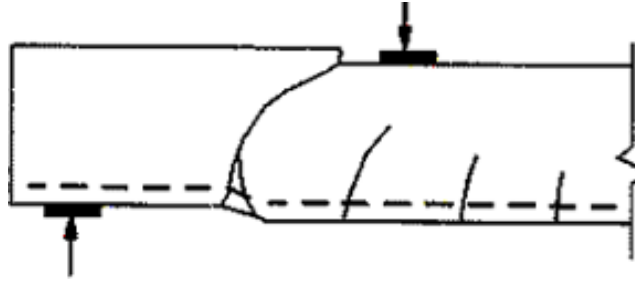
Figure 3.10: Diagonal tension failure.

3.8.2 Shear Compression Failure

In this failure mode beam may crushed near compression flange above the tip of inclined crack. The possible shape of this failure mode is shown in figure 3.11 below.
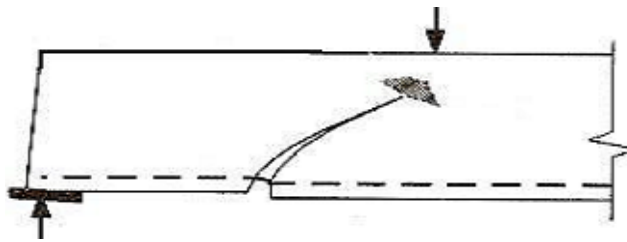
Figure 3.11: Shear Compression failure.

3.8.3 Shear Tension Failure

In this mode of failure because of inadequate development or anchorage of longitudinal steel bars at beam support, the diagonal cracks propagate horizontally along the bars.
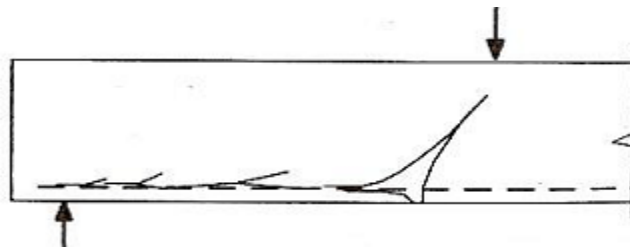
Figure 3.12: Shear tension failure.

3.8.4 Web Crushing Failure

Web of concrete may crushed due to insufficient thickness. This failure mode may occur in beam with expanded tension and compression flanges that usually have relatively lesser web thickness.
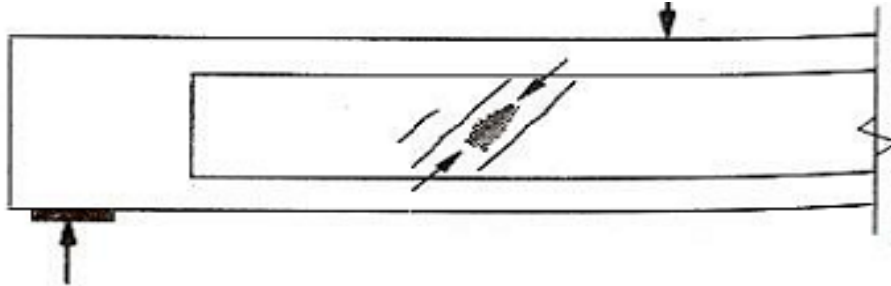
Figure 3.13: Web crushing failure

3.8.5 Arch Rib Failure

Arch rib type failure may occur generally in deep beams, in which web may crush due to buckling and subsequently may fail. There can be anchorage failure or failure of the bearing.
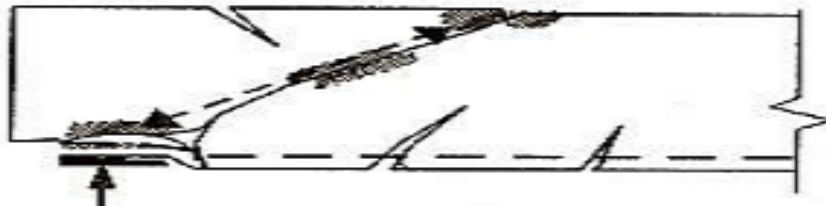
Figure 3.14: Arch rib failure.

3.9 Shear Theories

Shear forces and shear stresses will exist in those parts of a beam where the moment changes from section to section. By the traditional theory for homogeneous, elastic, uncracked beams, we can calculate the shear stresses, on elements 1 and 2 cut out of a beam (Fig. 3.17), using the equation

$$\upsilon = \frac{VQ}{Ib} \qquad (3.6)$$
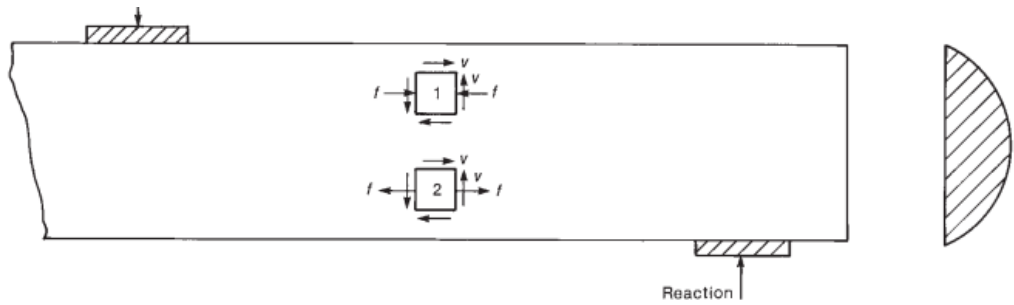
(a) Flexure and shear stresses acting on elements in the beam shear span

(b) Distribution of shear stresses
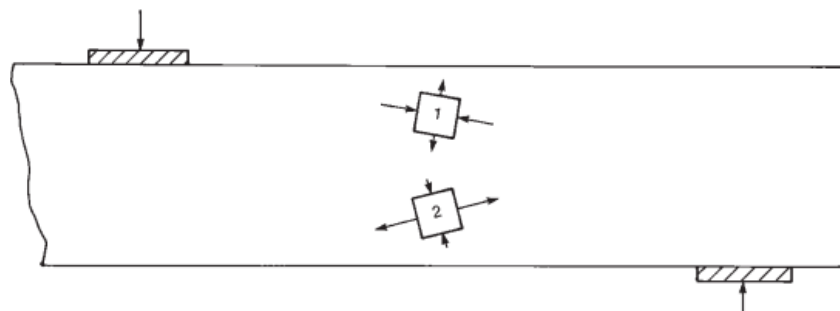
(c) Principal stresses on element in beam shear span

Figure 3.15: Normal shear and principle and shear stresses in homogeneous beam.

Where

V = Shear force on the cross section

I = Moment of inertia of the cross Section

Q = First moment about the centroidal axis of the part of the cross-sectional area lying farther from the centroidal axis than the point where the shear stresses are being calculated

b= Width of the member at the section where the stresses are being calculated

Equal shearing stresses exist on both the horizontal and vertical planes through an element, as shown in Fig. 3.15a. The shear stresses on the top and bottom of the elements cause a clockwise couple, and those on the vertical sides of the element cause a counterclockwise couple. These two couples are equal and opposite in magnitude and hence cancel each other out. The horizontal shear stresses are important in the design of construction joints, web-to-flange joints, and regions adjacent to holes in beams. For an uncracked rectangular beam, gives the distribution of shear stresses shown in Fig. 3.15b

The elements in Fig. 3.15a are subjected to combined normal stresses due to flexure, and shearing stresses. The largest and smallest normal stresses acting on such an element are referred to as principal stresses. The principal stresses and the planes they act on are found by using a Mohr's circle for stress.

The surfaces on which principal tension stresses act in the uncracked beam are plotted by the curved lines in Fig. 3.16a. These surfaces or stress trajectories are steep near the bottom of the beam and flatter near the top. This corresponds with the orientation of the elements shown in Fig. 3.15c. Because concrete cracks when the principal tensile stresses exceed the tensile strength of the concrete, the initial cracking pattern should resemble the family of lines shown in Fig. 3.16a.

The cracking pattern in a test beam with longitudinal flexural reinforcement, but no shear reinforcement, is shown in Fig. 3.16b. Two types of cracks can be seen. The vertical cracks occurred first, due to flexural stresses. These start at the bottom of the beam where the flexural stresses are the largest. The inclined cracks near the ends of the beam are due to combined shear and flexure. These are commonly referred to as inclined cracks, shear
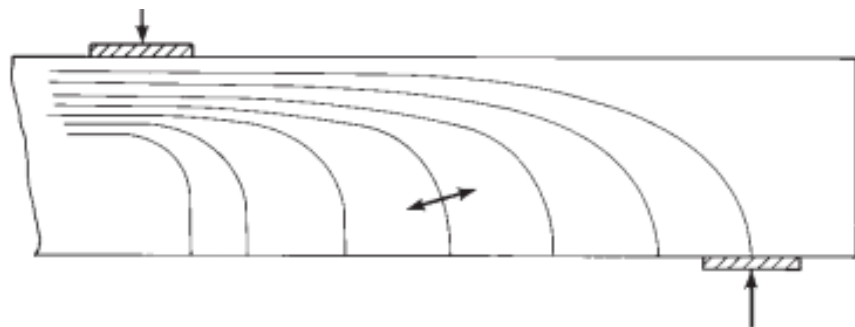
(a) Principal compressive stress trajectories in an uncracked beam.
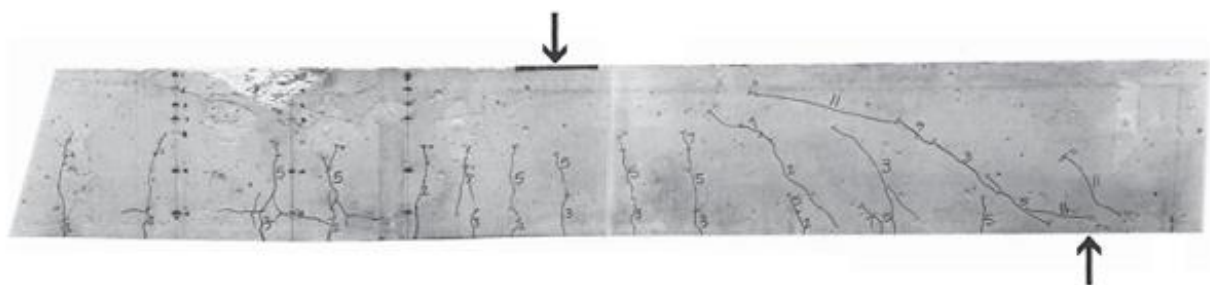
(b) Photograph of half of a cracked reinforced concrete beam.

Figure 3.16: Principle compressive stress trajectories and inclined cracks (James K. Wight and Macgregor 2012).

47

cracks, or diagonal tension cracks. Such a crack must exist before a beam can fail in shear. Some of the inclined cracks have extended along the reinforcement toward the support, weakening the anchorage of the reinforcement.

Although there is a similarity between the planes of maximum principal tensile stress and the cracking pattern, this relationship is by no means perfect. In reinforced concrete beams, flexural cracks generally occur before the principal tensile stresses at mid height become critical. Once a flexural crack has occurred, the tensile stress perpendicular to the crack drops to zero. To maintain equilibrium, a major redistribution of stresses is necessary. As a result, the onset of inclined cracking in a beam cannot be predicted from the principal stresses unless shear cracking precedes flexural cracking. This very rarely happens in reinforced concrete, but it does occur in some prestressed concrete beams.

3.10 Truss Model for Behavior of Slender RC Wide Beams Failing in Shear

The behavior of beams failing in shear must be expressed in terms of a mechanical mathematical model before designers can make use of this knowledge in design. The best model for beams with web reinforcement is the truss model.

In 1899 and 1902, respectively, the Swiss engineer Ritter and the German engineer Morsch, independently, published papers proposing the truss analogy for the design of reinforced concrete beams for shear. These procedures provide an excellent conceptual model to show the forces that exist in a cracked concrete beam
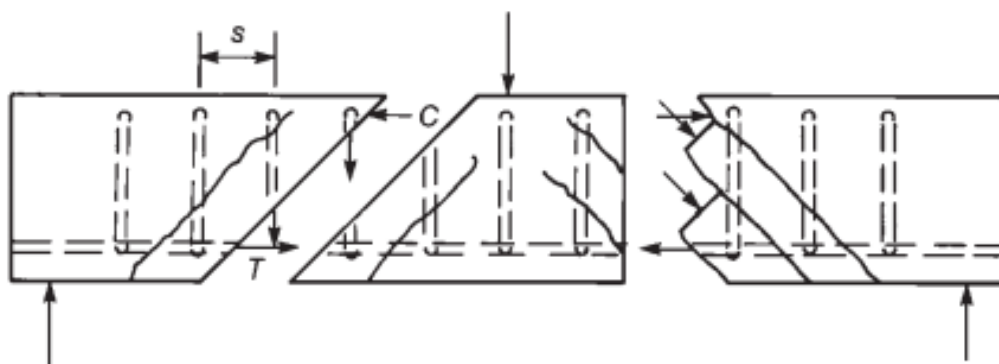
(a) Internal forces in a cracked beam.

48
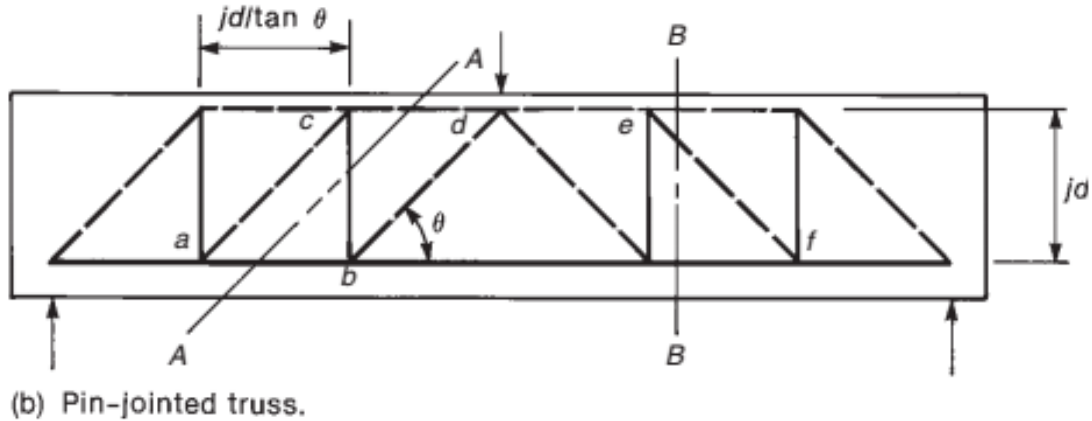
Figure 3.17: Truss analogy (James K. Wight and Macgregor 2012).

As shown in Fig. 3.17a, a beam with inclined cracks develops compressive and tensile forces, C and T, in its top and bottom "flanges," vertical tensions in the stirrups, and inclined compressive forces in the concrete "diagonals" between the inclined cracks. This highly indeterminate system of forces can be replaced by an analogous truss.

Several assumptions and simplifications are needed to derive the analogous truss. In Fig. 3.19b, the truss has been formed by lumping all of the stirrups cut by section A–A into one vertical member b–c and all the diagonal concrete members cut by section B–B into one diagonal member e–f. This diagonal member is stressed in compression to resist the shear on section B–B. The compression chord along the top of the truss is actually a force in the concrete but is shown as a truss member. The compressive members in the truss are shown with dashed lines to imply that they are really forces in the concrete, not separate truss members. The tensile members are shown with solid lines.

Figure 3.20a shows a beam with inclined cracks. The left end of this beam can be replaced by the truss shown in Fig. 3.18b. In design, the ideal distribution of stirrups would correspond to all stirrups reaching yield by the time the failure load is reached. It will be assumed, therefore, that all the stirrups have yielded and that each transmits a force of Av*fyt across the crack, where Av is the area of the stirrup legs and fyt is the yield strength of the transverse reinforcement. When this is done, the truss becomes statically determinate. The truss in Fig. 3.18b is referred to as a plastic-truss model, because we are depending on plasticity in the stirrups to make it statically determinate. The beam will be proportioned so

that the stirrups yield before the concrete crushes, so that it will not depend on plastic action in the concrete.

The compression diagonals in Fig 3.18b originating at the load at point A (AB, AD, and AF) are referred to as a compression fan. The number of diagonal struts in the fan must be such that the entire vertical load at A is resisted by the vertical force components in the diagonals meeting at A.
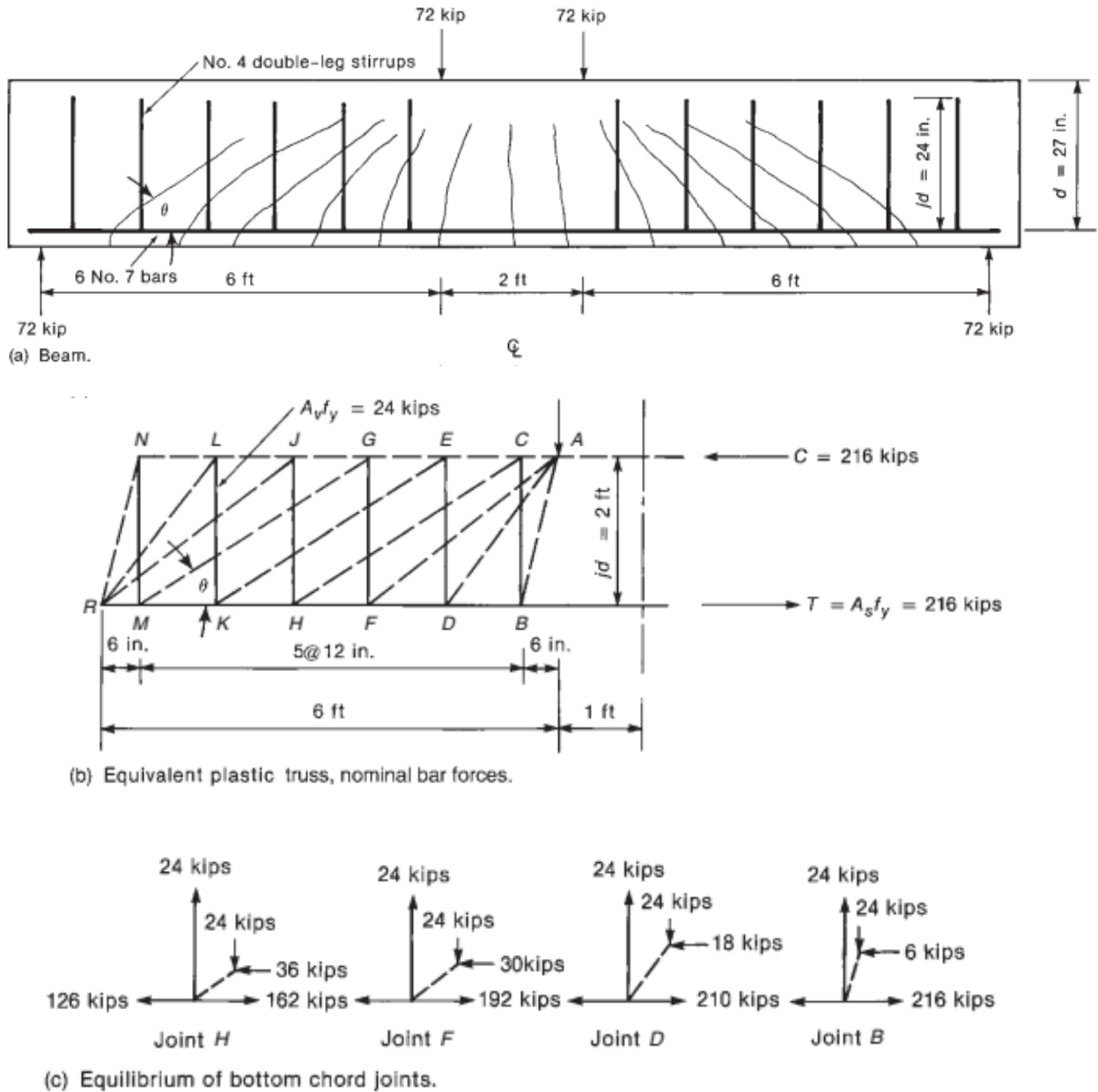
Figure 3.18: Construction of analogues plastic truss (James K. Wight and Macgregor 2012).

A similar compression fan exists at the support R (RN, RL, RJ). Between the compression fans is a compression field consisting of the parallel diagonal struts CH, EK, and GM. The angle of the compression field is determined by the number of stirrups needed to equilibrate the vertical loads in the fans. Each of the compression fans occurs in a D-region (discontinuity region). The compression field is a B-region (beam region).

3.11 Simplified Truss Analogy

A statically determinate truss analogy can be derived via the method suggested by Marti Figures 3.21a and b show a uniformly loaded beam with stirrups and a truss model incorporating all the stirrups and representing the uniform load as a series of concentrated loads at the panel points. The truss in Fig. 3.21b is statically indeterminate, but it can be solved if it is assumed that the forces in each stirrup cause that stirrup to just
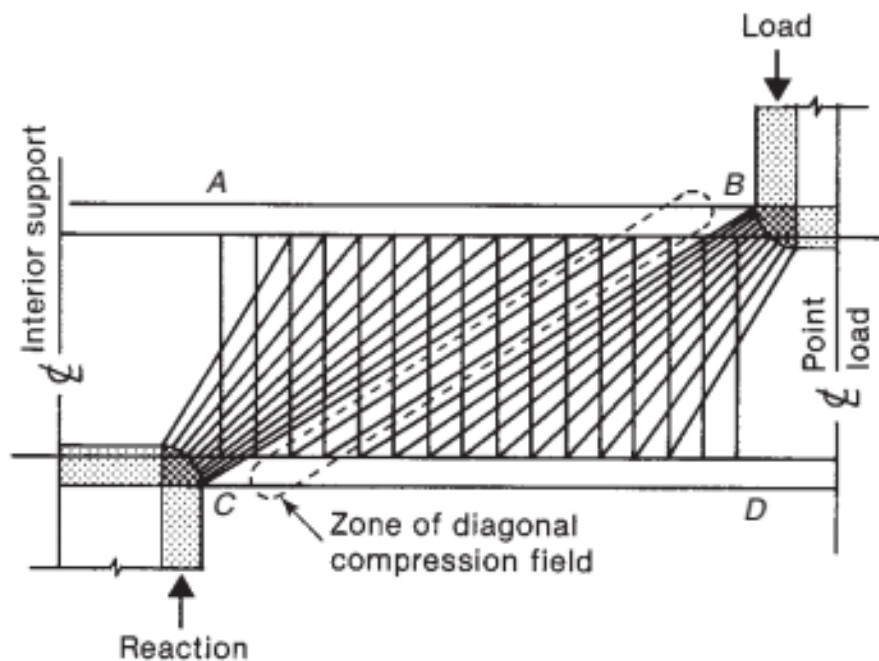
Figure 3.19: Crack patterns and truss model for two span beams (James K. Wight and Macgregor 2012).
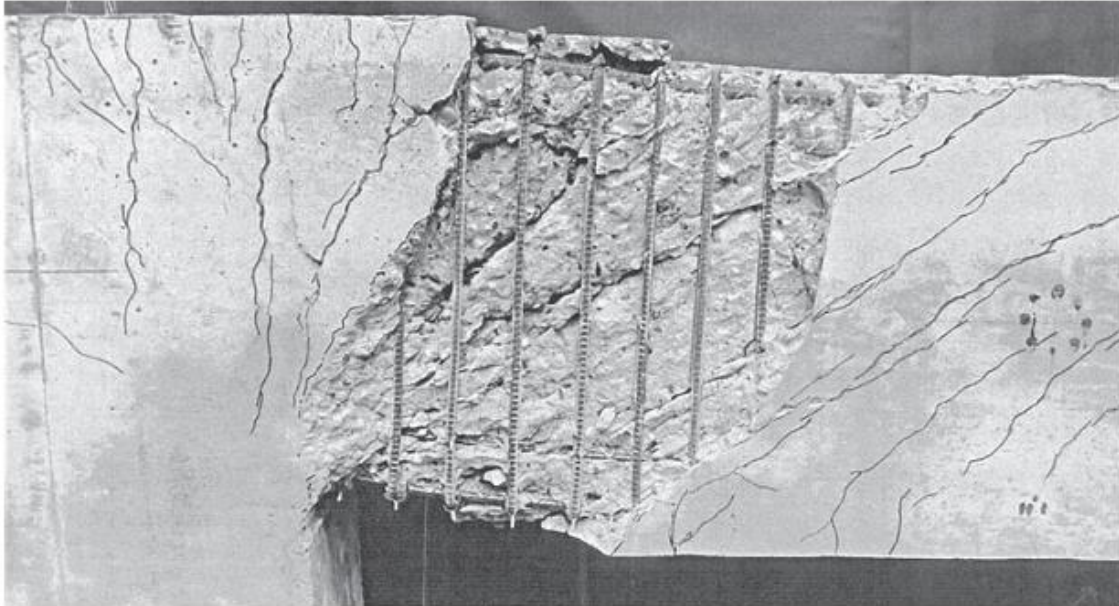
Figure 3.20: Compression fan shown at interior support of beam (James K. Wight and Macgregor 2012).
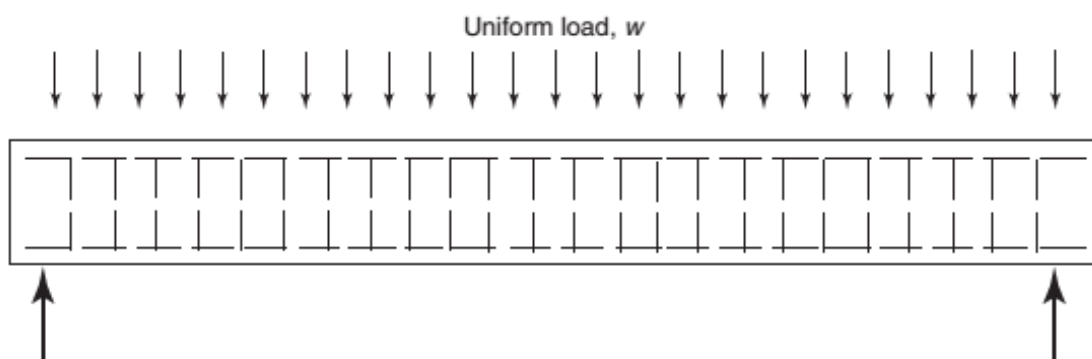
(a) Beam and reinforcement.

(b) Truss model.

(c) Statically determinate truss.
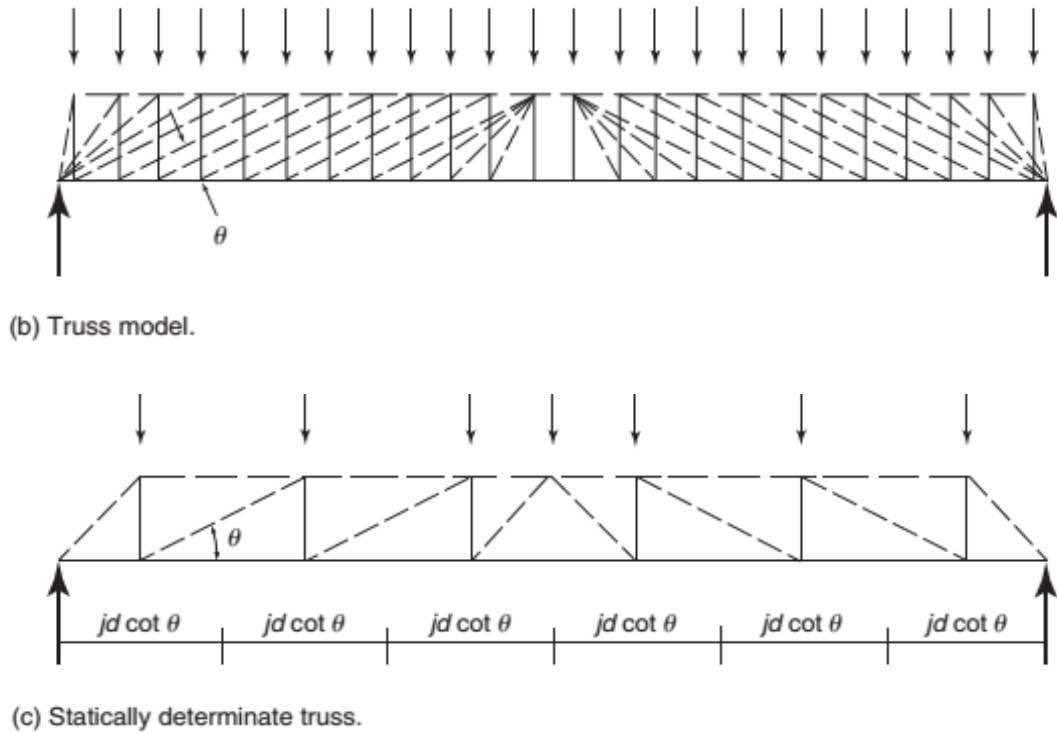
Figure 3.21: Truss model for design (James K. Wight and Macgregor 2012)

reach yield, as was done in the preceding paragraphs. For design, it is easier to represent the truss as shown in Fig. 3.21c, where the tension force in each vertical member represents the force in all the stirrups within a length Similarly, each inclined compression strut represents a width of web equal to The uniform load has been idealized as concentrated loads of acting at the panel points. The truss in Fig. 3.21c is statically determinate

3.12 Compression Field Theories

This theory is the inverse of the tension field theory developed by Wagner in 1929 for the design of light-gauge plates in metal airplane fuselages. If a light gauge metal web is loaded in shear, it buckles due to the diagonal compression in the web. Once buckling has occurred, further increases in shear require the web shear mechanism to be replaced by a truss or a field of inclined tension forces between the buckles in the web. This diagonal tension field in turn requires a truss that includes vertical compression struts and longitudinal compression chords to resist the reactions from the tension diagonals in the web.

The compression field theory (CFT) is just the opposite of the tension field theory. In the CFT, the web of the beam cracks due to the principal tension stresses in the web. Cracking reduces the ability of the web to transmit diagonal tension forces across the web. After cracking, loads are carried by a truss-like mechanism with a field of hypothetical diagonal compression members between the cracks and tensions in the stirrups and the longitudinal chords.

The CFT from the 1984 Canadian Concrete Code did not have a term. Instead, stirrups were provided for the full shear. In designing a structure, it was necessary to check web crushing by using stresses and strains derived from Mohr's circles. In design, the angle was assumed and was used to compute web stresses and the capacity of the concrete. In the CFT, the angle could have any value between 15 and 75°, as long as the same angle was used for all the calculations at a given section.

MODELING AND ANALYSIS OF RC BEAMS

4.1 Concrete Material Matrix

Constitutive relation for plane stress problems is presented below for concrete model. For stress combinations inside the initial yield surface, concrete is assumed to be a homogeneous, linear isotropic material. Stress strain relation for plane stress problems has the simple form:

$$\begin{Bmatrix} \sigma_x \\ \sigma_y \\ \tau_{xy} \end{Bmatrix} = \frac{E}{1-v^2} * \begin{bmatrix} 1 & v & 0 \\ v & 1 & 0 \\ 0 & 0 & \frac{1-v}{2} \end{bmatrix} * \begin{Bmatrix} \varepsilon_x \\ \varepsilon_y \\ \gamma_{xy} \end{Bmatrix}$$

where E is the initial elastic modulus of concrete and v is Poisson's ratio.

4.2 Steel Material Matrix

One dimensional truss element is widely used as reinforcement steel. Beam element can also be used with three degrees of freedom connected with concrete element. In both cases one dimensional reinforcing bar elements can be easily superimposed on the three-dimensional concrete element mesh. Stiffness matrix for one dimensional truss element is given by

$$\begin{Bmatrix} P1 \\ P2 \end{Bmatrix} = \frac{AE}{L} * \begin{bmatrix} 1 & -1 \\ -1 & 1 \end{bmatrix} * \begin{Bmatrix} d1 \\ d2 \end{Bmatrix}$$

where, A the cross-sectional area, L the length of the bar element and E is the modulus of elasticity. P1 and P2 are axial end forces and d1 and d2 are axial end displacements of the reinforcing bar.

4.3 Finite Element Modeling and Analysis of RC beams

Fallowing four phases are involved from beam modeling and analysis of results

a) Pre-processor phase

b) Solution phase

c) General post processor phase

d) Time history post processor phase

4.4 Pre-Processor Phase

In pre-processor phase nonlinear finite element modeling of eight numbers RC beams referred in Table 1.1 of chapter 1, for which sketches are shown bellows, were carried out. For this purpose ANSYS 14 multifunction finite element package were used. To create the finite element model, ANSYS 14 involve multiple tasks that have to be completed to run the model properly. This section describes the different tasks and entries into used to create FE models of beams. Just for simplification, different label numbers are used to represent element type, real constants and material model described below from those in actual ANSYS modeling.
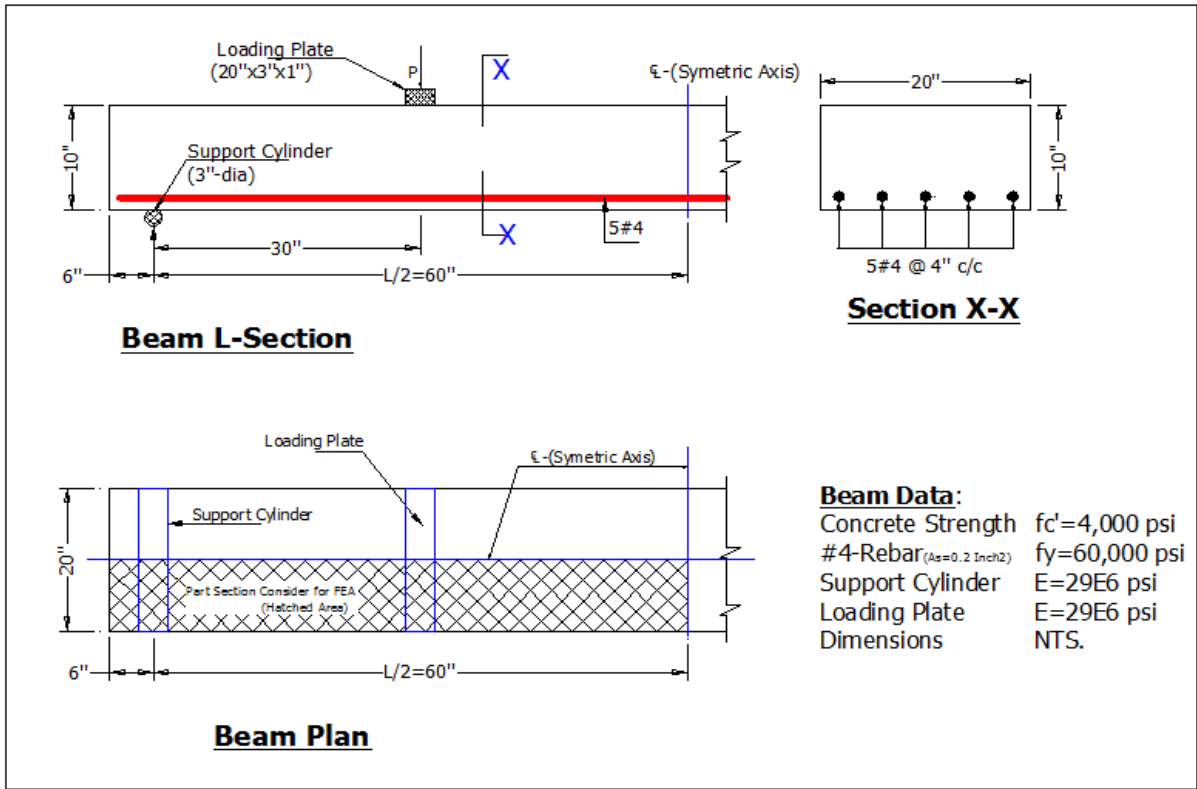
Figure 4.1: Schematic sketch of Beam BXL1
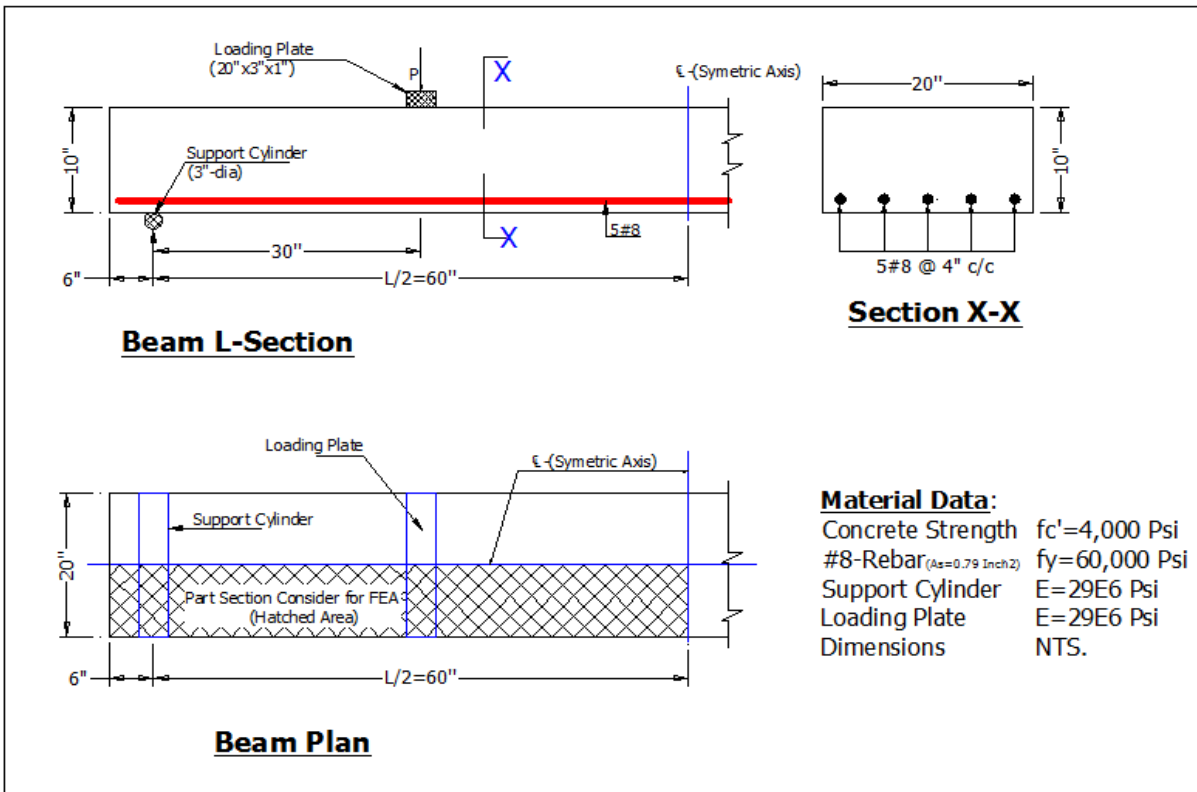
Figure 4.2: Schematic sketch of Beam BXL2
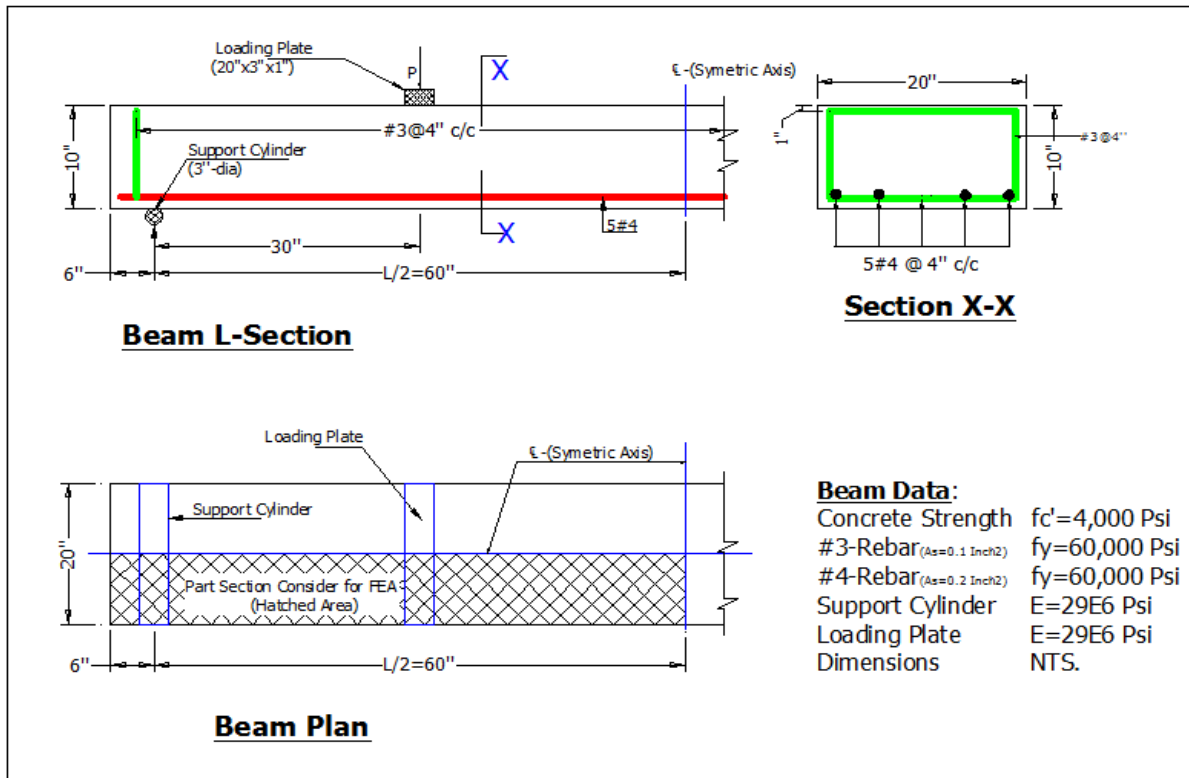
Figure 4.3: Schematic sketch of Beam BXL1W.
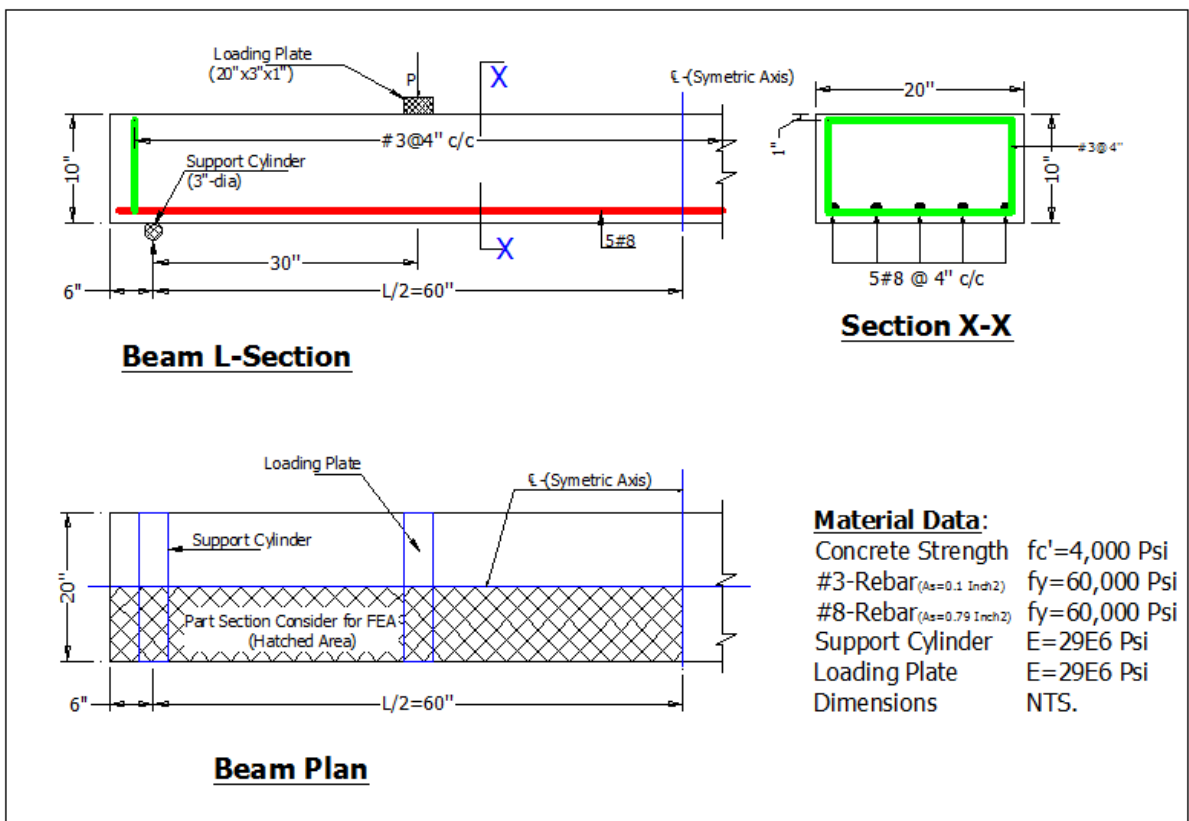
Figure 4.4: Schematic Sketch of Beam BXL2W

58
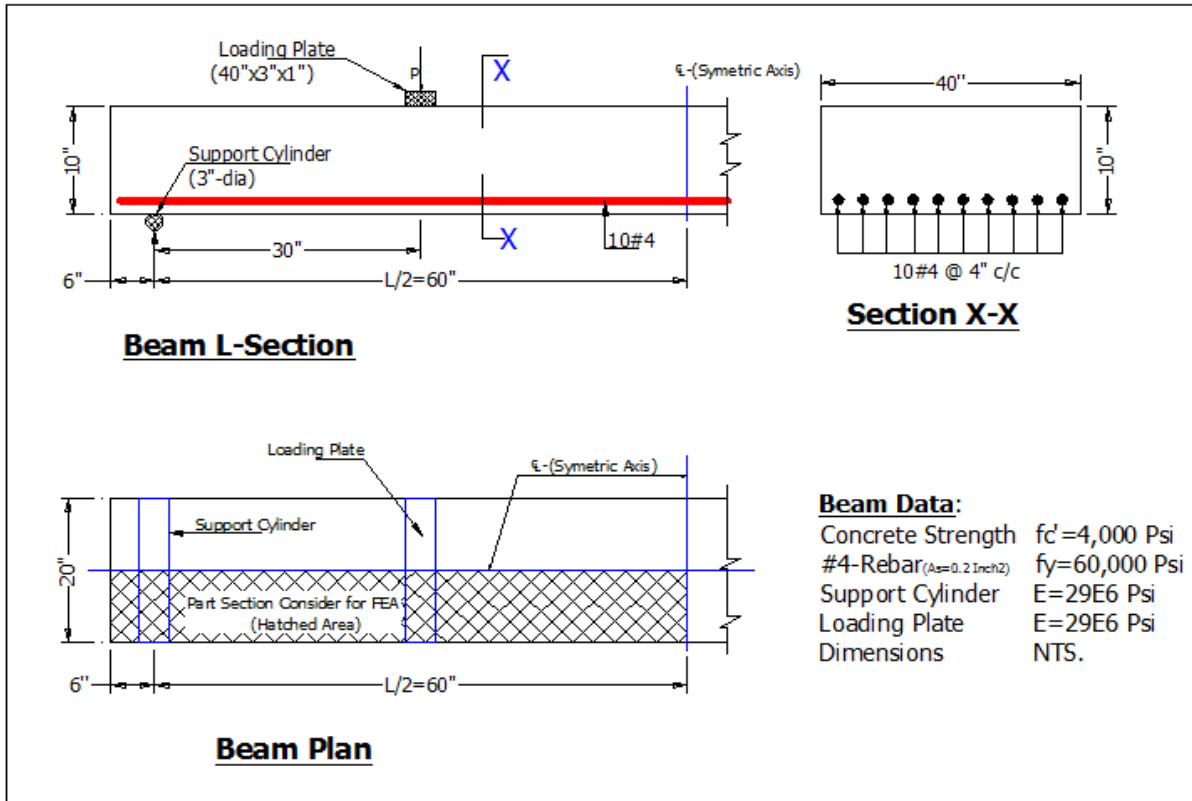
Figure 4.5: Schematic sketch of Beam BZL1.
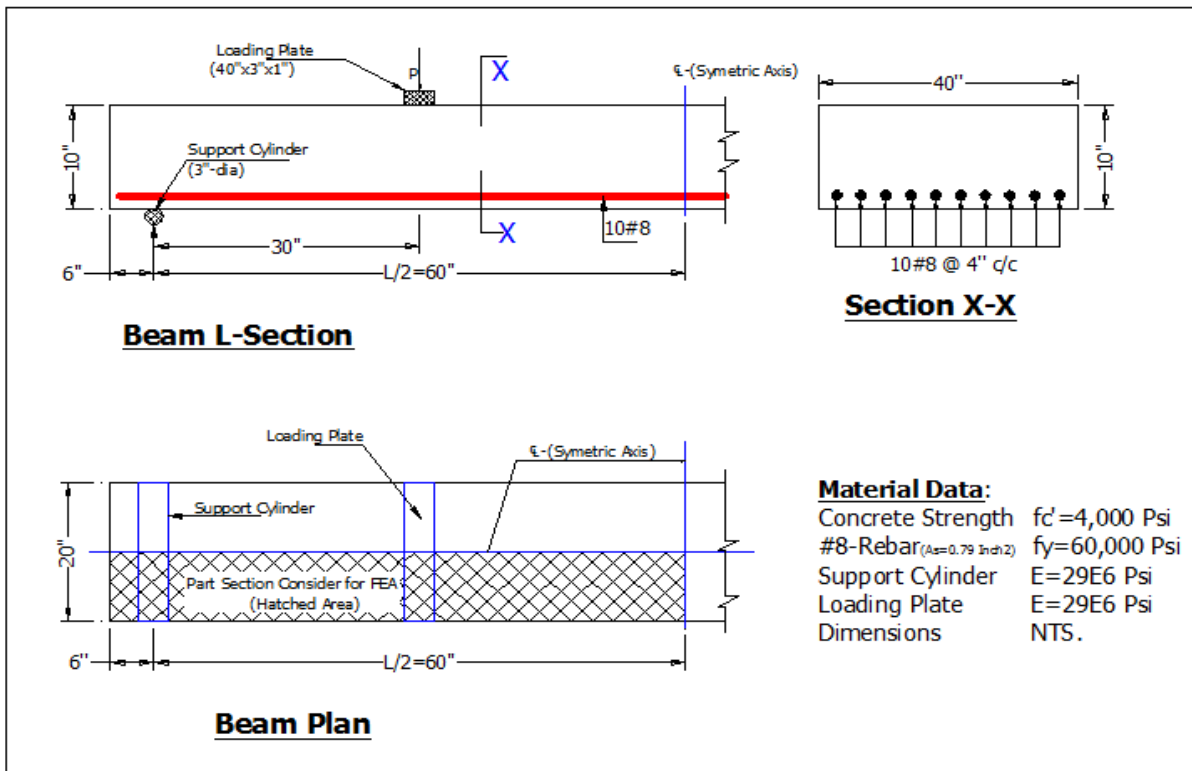
Figure 4.6: Schematic sketch of Beam BZL2.
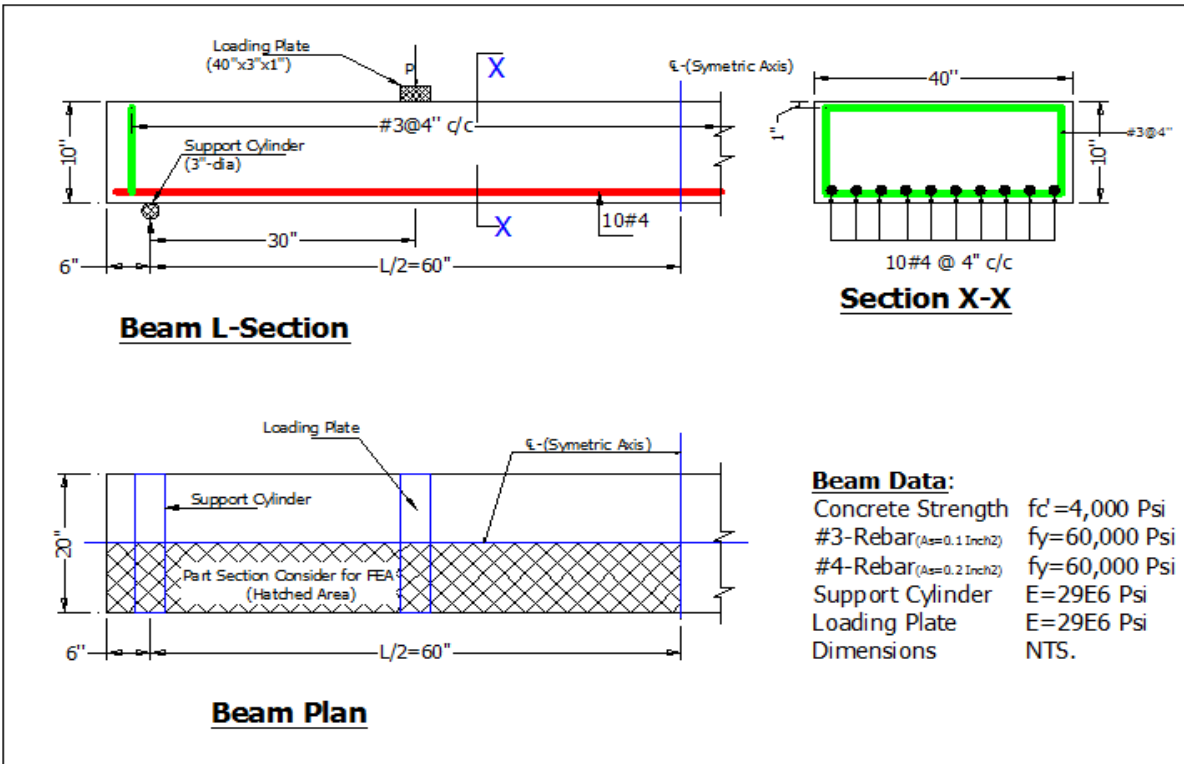
Figure 4.7: Schematic sketch of Beam BZL1W.
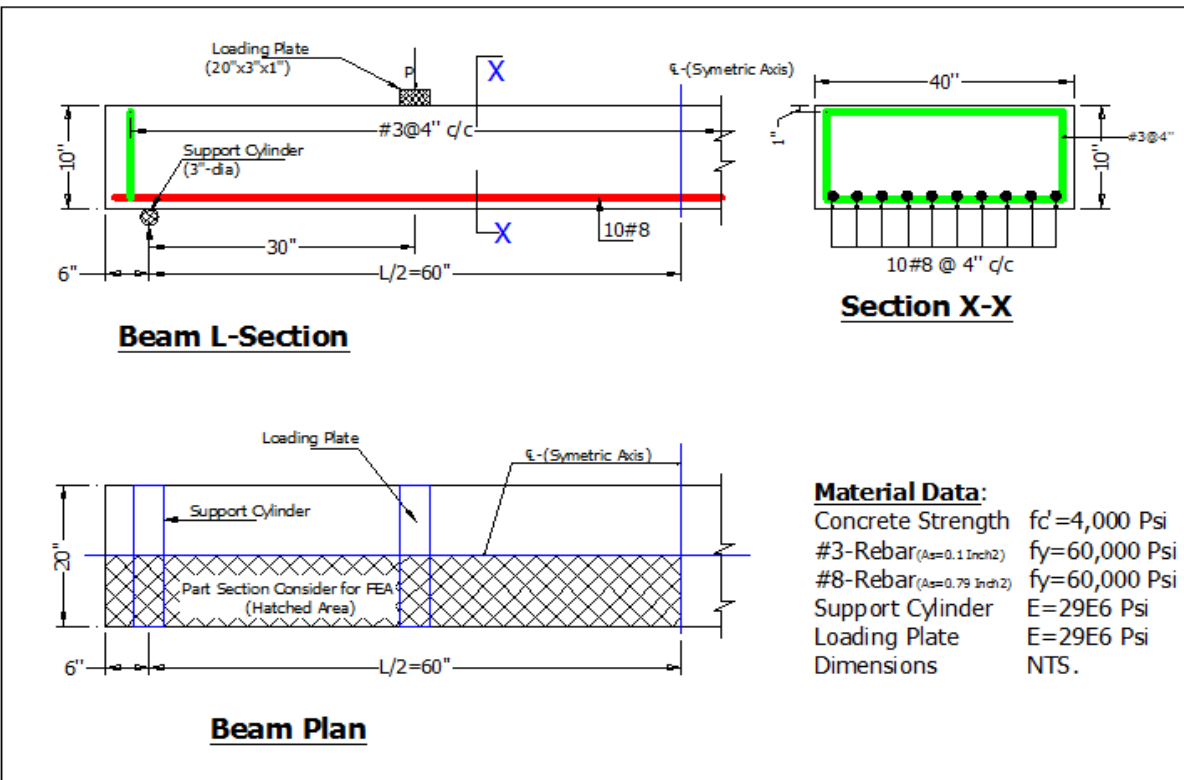
Figure 4.8: Schematic sketch of Beam BZL2W.

4.4.1 Element Types

More than about 180 elements with different formulations are the part of ANSYS element library. Each element is identified by its name, such as Solid65; that consist of group label (Solid) and a unique number (65) that identify that particular element.

Element Type for Concrete: For concrete three dimensional modeling, Solid65 element was used. Eight nodded solid65 elements have three translational degrees of freedom U_x, U_y and U_z in three orthogonal X, Y and Z direction at each node. This element is capable to crack in three orthogonal directions, plastic deformation, and crushing. A schematic and type of used elements to represent concrete is shown in fig 4.9
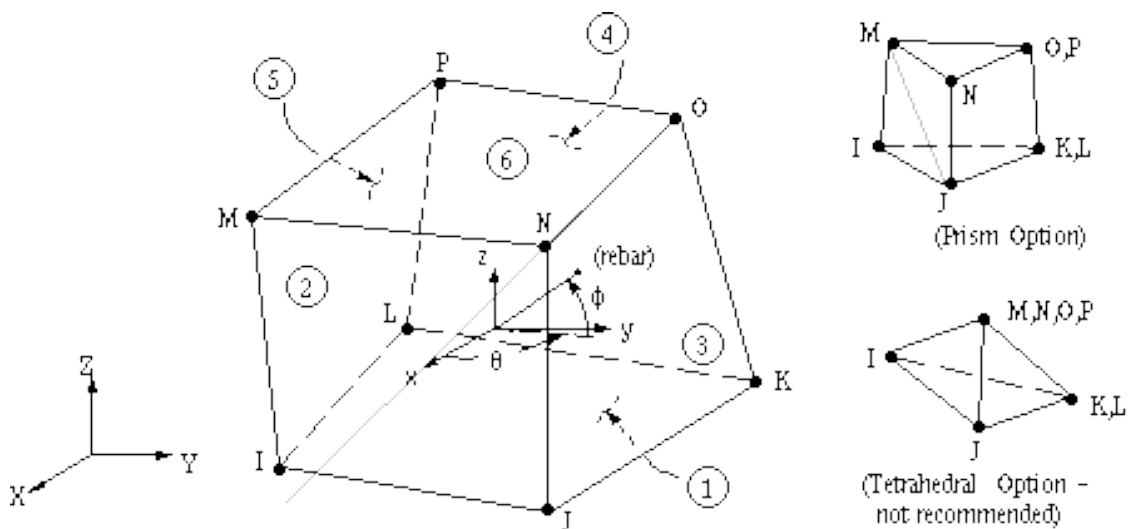
Figure 4.9: Solid65 element used for concrete(ANSYS-Multiphysics 2011).

Element Type for Steel Plates: Like solid65 element used for concrete, Solid185 is also three dimensional elements with eight node having three translational degrees of freedom at each node in x, y and z direction. This was used for steel cylinder and plates at the supports and loading positions of beams. The node location and geometry of this element are shown in Figure 4.10

61
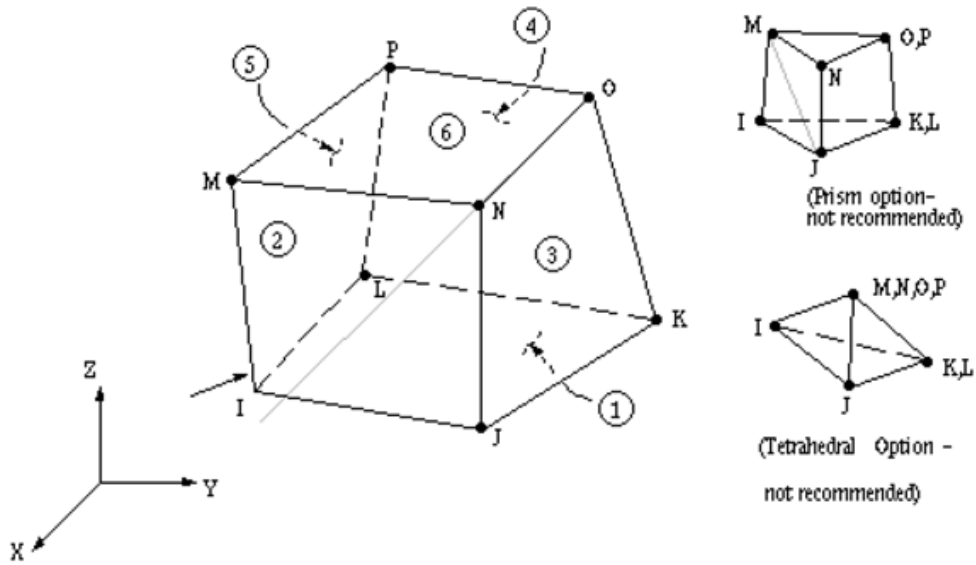
Figure 4.10: Solid185 elements used for steel plates (ANSYS-Multiphysics 2011).

Element Type for Rebar: LINK180 is a uniaxial tension –compression spar element spar which can be used in many of the engineering applications such as to model trusses, sagging cables, links, springs, etc. This element has three translational degrees of freedom in x, y and z directions. In a beam this element was used to model longitudinal and web steel rebar. Bending resistance of the element is neglected and creep plasticity, rotation, large deflection, and large strain capabilities are included. Schematic sketch of this element is shown in Figure 4.11.
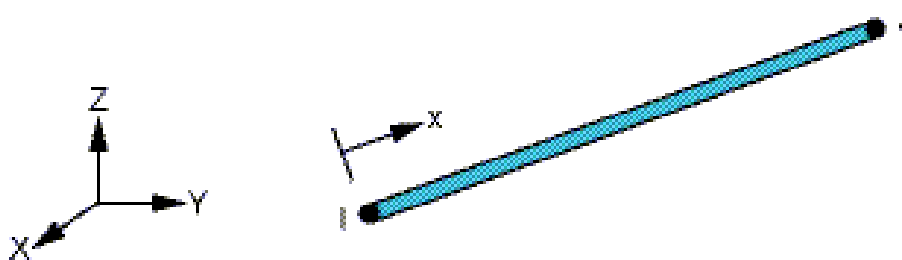
Figure 4.11: Link 180 element used for steel rebar (ANSYS-Multiphysics 2011).

4.4.2   Real Constants

Real constants are the data which are required for element stiffness matrix calculation, but cannot be determined from the material properties or node locations. Properties such as cross

sectional area of the steel rebar are input as real. Typical real constants include area, thickness, inner diameter, outer diameter, etc. The set of real constants used for considered twelve beams data are shown in Table 4.1

Table 4.1: : Real Constants for beams.

Type	Real Constant.	Element Type	Constants		Rebar 1	Rebar 2	Rebar 3
Concrete	1	Solid 65	Material Number		0	0	0
			Volume ratio		0	0	0
			Orientation angle		0	0	0
#3-bar	2	Link 180	Cross-Sectional area (inch2)		0.11	----	----
#4-bar	3	Link 180	Cross-Sectional area (inch2)		0.2	----	----
#8-bar	4	Link 180	Cross-Sectional area (inch2)		0.79	----	----

For solid 65 elements, real Constant Set 1 is used. It requires real constants for rebar assuming a smeared model. Values can be entered for Material Number, Volume Ratio, and Orientation Angles. The material number refers to the type of material for the reinforcement. The volume ratio refers to the ratio of steel to concrete in the element. The orientation angles refer to the orientation of the reinforcement in the smeared model.

In the present study all beams discrete approach to model reinforcement steel has been used. Therefore, to turn off the smeared reinforcement capability of solid65 element, a value of zero was entered for all real constants. Similarly for link180 element real Constant Sets with

number 2, 3, and 4 are defined corresponding to rebar #3, #4 and #8. At symmetric location half of these mentioned real constant values were used numbered and defined accordingly.

4.4.3 Material Properties

Depending on the application, most element types require material properties. These properties may be:

- Linear or nonlinear
- Isotropic, orthotropic, or anisotropic
- Constant temperature or temperature-dependent.

Each set of material properties has a material reference number, as with element types and real constants. The table of material reference numbers versus material property sets is called the material table. Multiple sets of material properties within one analysis can be used (to correspond with multiple materials used in the model). ANSYS classifies each set with a particular reference number.

Parameters needed to define the material models can be found in Table 4.2. There are multiple parts of the material model for each element.

Table 4.2: 2 Material Model for beams.

Material Number	Element type	Material Properties		
1	Solid 65	**Linear isotropic**		
		EX	3.60E+06	
		PRXY	0.2	
		Multi-linear isotropic		
			Stress	Strain
		Point 1	0.0001	360
		Point 2	0.0003	1062
		Point 3	0.0008	2552
		Point 4	0.0012	3347
		Point 5	0.0016	3795
		Point 6	0.002	3978
		Point 7	0.0022	4000
		Point 8	0.003	4000
		Concrete		
		Op-Shr-coef.	0.3	
		Cl-Shr-coef.	0.8	
		Un-tens St.	474	
		Bi-Comp-St.	0	
		Hydro-Prs.	0	
		Bi-hydro-St.	0	
		Uni-hydro-St.	0	
		Ten-Cr-Fac.	0.6	
2	Solid 185			**Linear isotropic**
			EX	29E6 psi
			PRXY	0.3
3	Link 180			**Bilinear Isotropic**
			Yield Stress	60,000 psi
			Tang Mod	0

The uniaxial compressive stress-strain relationship for the concrete model was obtained using the following equations to compute the multilinear isotropic stress-strain curve for the concrete (James K. Wight and Macgregor 2012).

$$f_c = \frac{E_c \varepsilon}{1 + \left[\dfrac{\varepsilon}{\varepsilon_o}\right]^2} \quad , \quad \varepsilon_o = \frac{2f_c}{E_c} \quad \text{and} \quad E_c = \frac{f}{\varepsilon}$$

Where f = Stress at any strain

ε = Strain at any stress f

$\varepsilon_{o \, = \, Strain}$ at ultimate compressive stress

The multilinear isotropic constituent relation of the material i.e. stress-strain data implemented requires that first point of the curve to be defined by the user and it must obey Hooke's Law. Plot of stress-strain curve for concrete and steel are shown in figure 4.12.
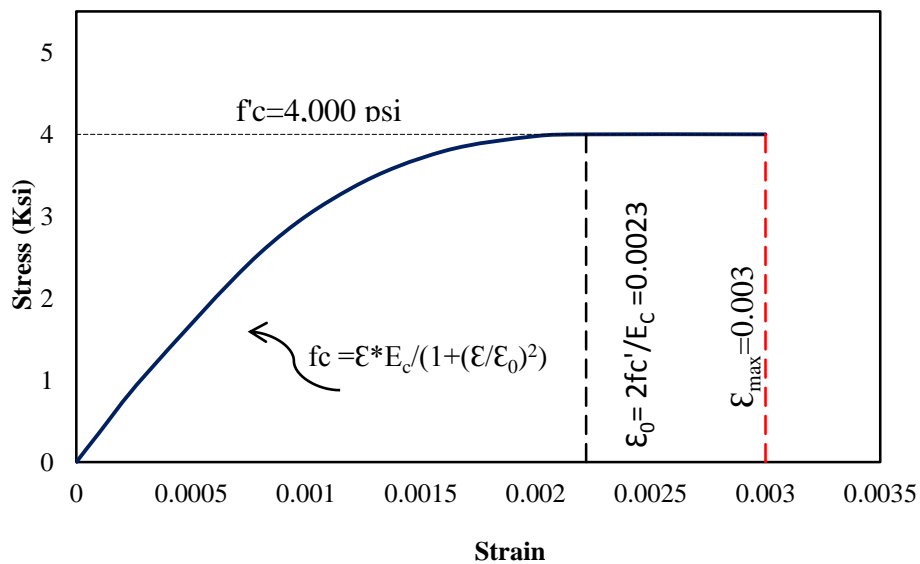
a): Plot of stress strain relations of concrete.
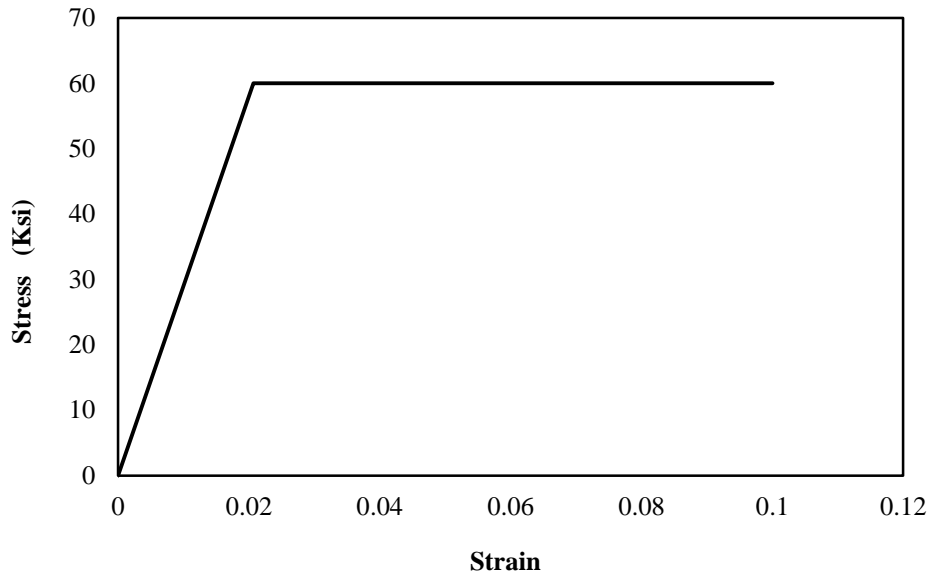
b): Plot of stress strain relations of steel rebar.

Figure 4.12: Plot of stress strain relations of concrete.

As shown in figure 4.12 maximum concrete strain at failure $\varepsilon_{(max)}$ =0.003 indicating traditional crushing strain for unconfined concrete recommended by ACI code.

Shear transfer coefficient values, that represent the part of shear resisted at crack by aggregate interlock. Shear transfer coefficients range from 0.0 to 1.0. Bottom value of 0.0 represent a smooth crack that means thorough loss of shear resistance at crack location and similarly maximum value of 1.0 represents a rough crack which means no loss of shear at crack. Convergence problems may arise when the shear transfer coefficient for the open crack falls below 0.2. In present research work value of 0.3 have beam used for all beams.

The uniaxial tensile cracking stress that is based upon the modulus of rupture is determined using,

$$f_{cr} = 7.5\sqrt{f_c'} \qquad (4.1)$$

The f_{cr} value from above equation comes out to be 474 psi. This uniaxial tensile crushing stress in this model was based on the uniaxial unconfined compressive strength (f_c'). The value of uniaxial crushing strength at above serial number four was put equal -1, which

turned off the crushing capability of the soild65 concrete element. Convergence problems have been frequently occurred when the crushing capability was turned on.

Material Model Number 2 refers to the Solid185 element and same was used for steel plate and cylinder at loading and support positions. This material properties of this element is modeled as a linear isotropic with a modulus of elasticity for the steel (E_s) same as of steel (E_s=29E6 psi), and poison's ratio (0.3).

Similarly to represent the steel reinforcement in the beams, material model Number 3 was defined that refers to the Link180 element. Material model for Link180 is a bilinear isotropic and same will be used for all the steel reinforcement in the beams and. Failure criteria of Bilinear isotropic material is based on the von Misses theory. The bilinear material model requires the yield stress f_y, as well as the hardening modulus of the steel to be defined. The yield stress was defined as 60,000 psi, and the hardening modulus was 0.

4.4.4 Modeling

The beam, plates, and cylinder supports were modeled as volumes. Taking advantage of symmetry only quarter of the beam are being modeled; all beams are of eleven feet length including 6'' offset from each support and of 10'' high with 20'', and 40'' wide. The zero values for the X, Y and Z coordinates coincide bottom left of the cross-section for the concrete beam.

Steel Rebar: As referred above to model all steel rebar Link 180 elements were used to create the flexural and shear reinforcement. For this purpose volumes were so divided that lines were created at locations where these reinforcement exists at a plane of symmetry and in the beam. The half steel area was used for bars located at symmetric locations.

Three dimensional finite element models of concrete beams considered for analysis in the study are presented in figures 4.13 to figure 4.16.
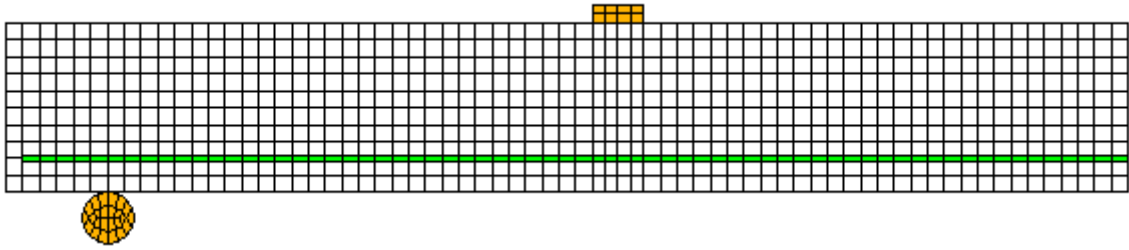
a): L-section beam BXL1 and BXL2.
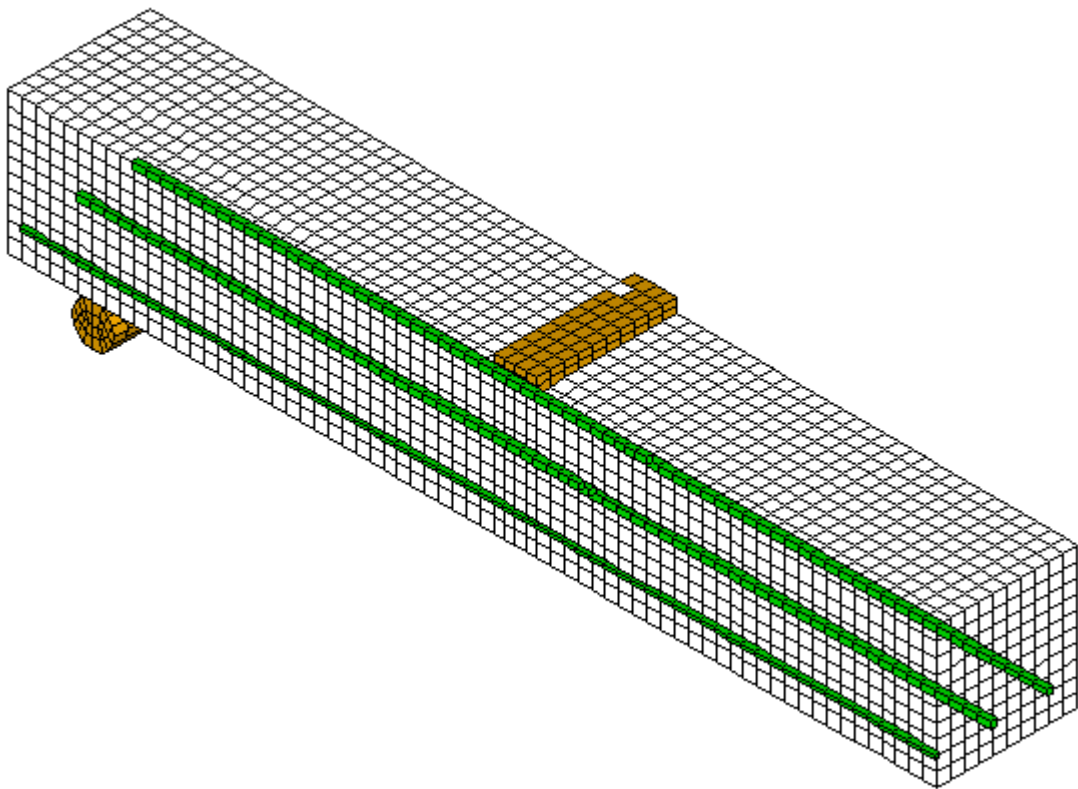
b): Isomeric view of beam BXL1 and BXL2.

Figure 4.13: Plan view of ANSYS FE Model for BXL1 and BXL2 beams.
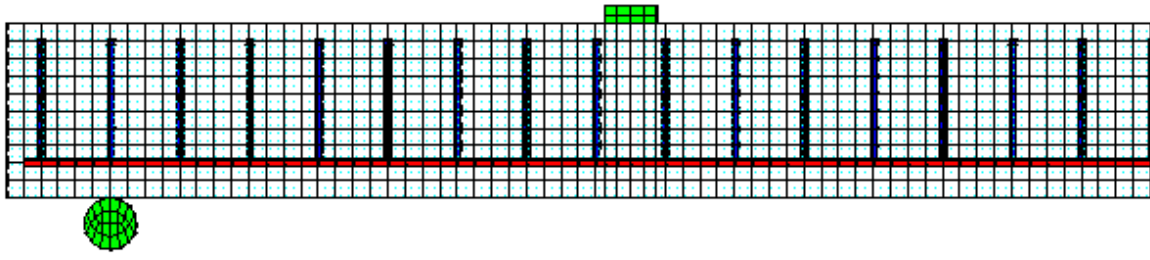
a): L-section beam BXL1W and BXL2W.
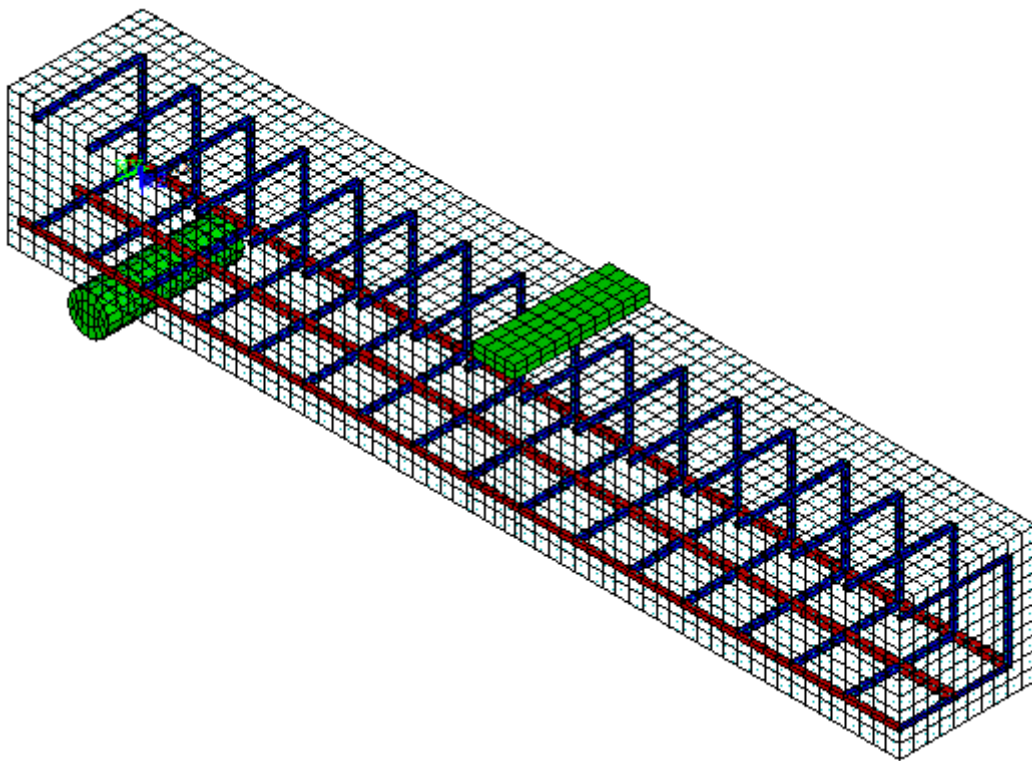
b): Isomeric view of beam BXL1W and BXL2W.

Figure 4.14: Isomeric view of ANSYS FE Model for BXL1Wand BXL2W beams.
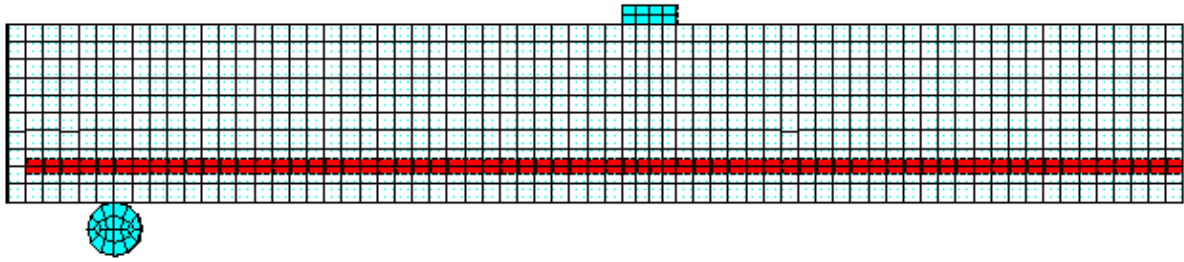
a): L-section beam BZL1 and BZL2.
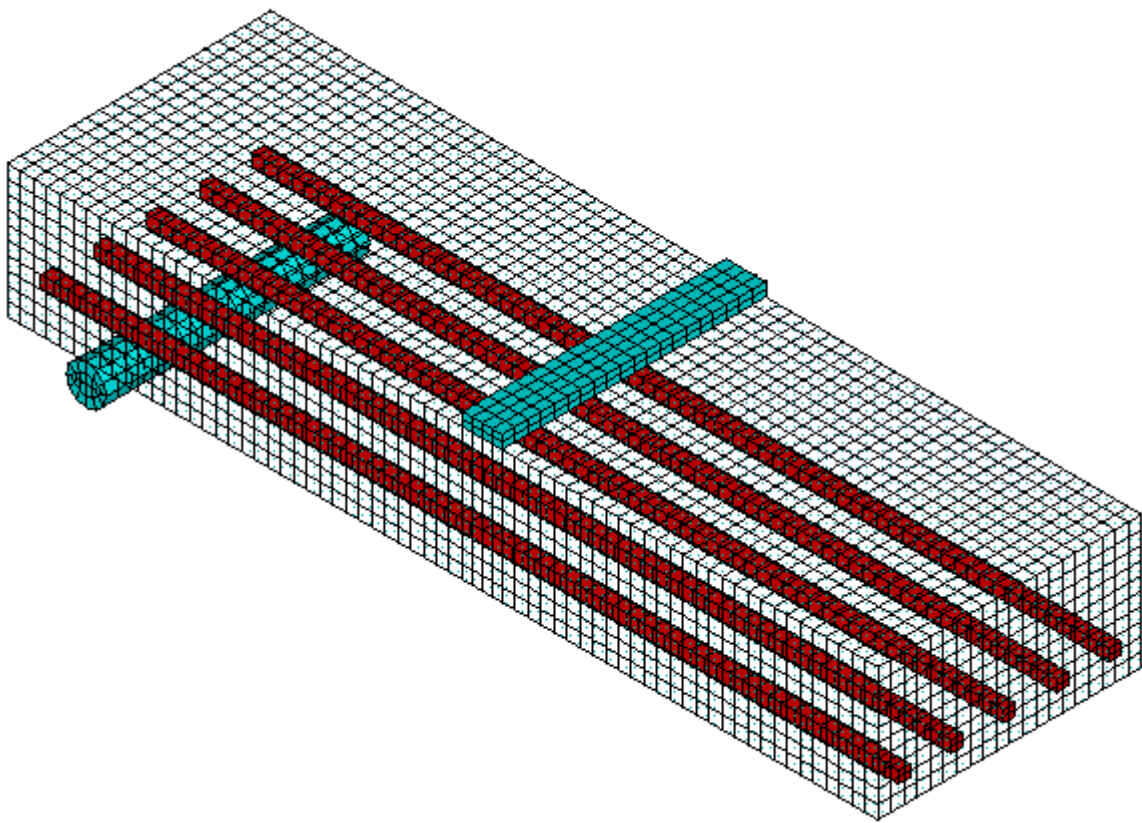
b): Isomeric view of beam BZL1 and BZL2.

Figure 4.15: Isomeric view of ANSYS FE Model for BZL1Wand BZL2W beams.
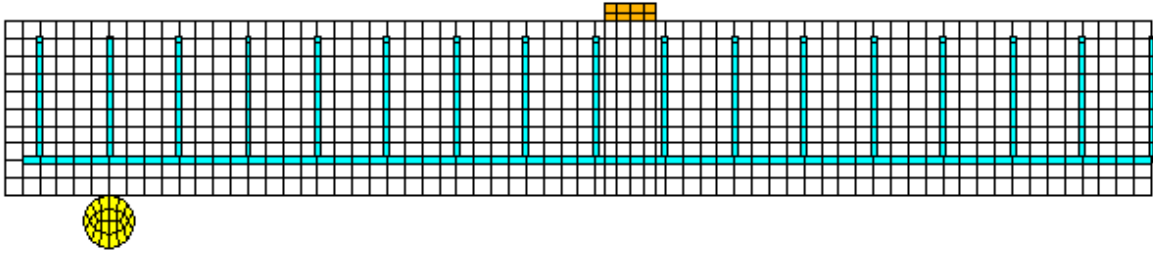
a): L-section beam BZL1W and BZL2W.
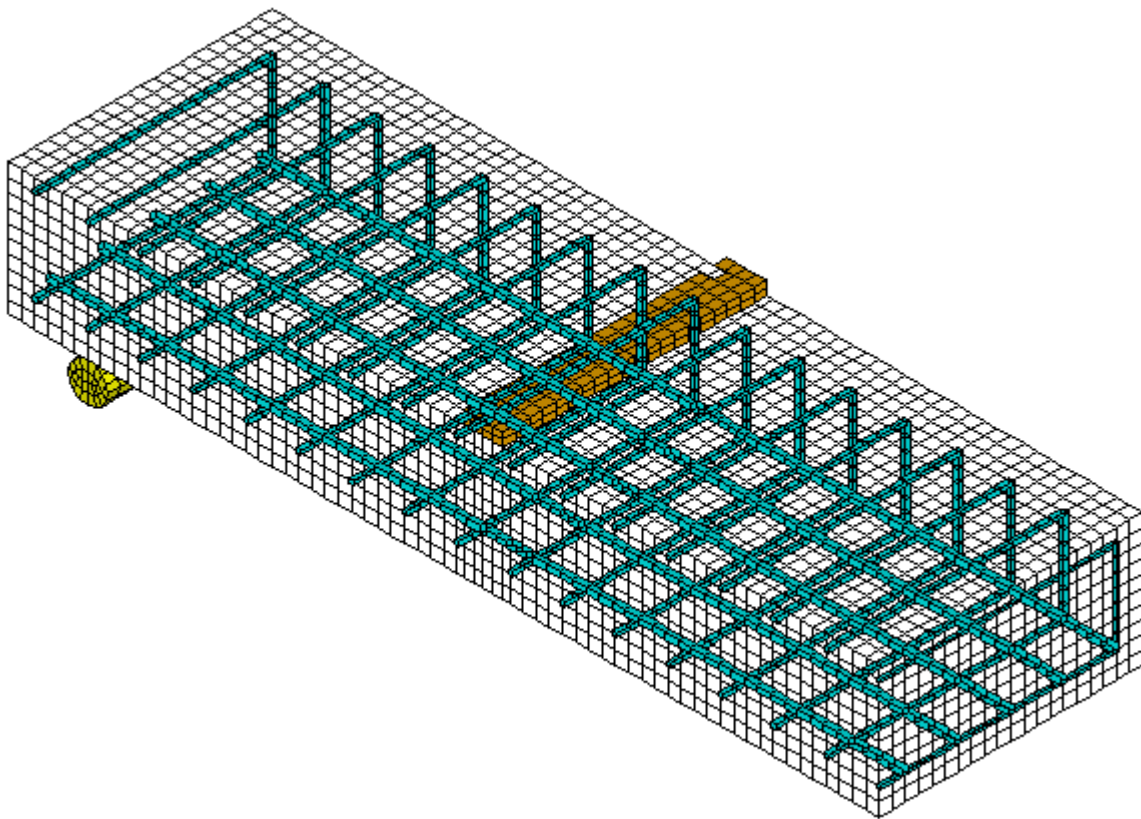
b): Isomeric view of beam BZL1W and BZL2W.

Figure 4.16: Isomeric view of ANSYS FE Model for BZL1Wand BZL2W beams.

4.4.5 Meshing

The option of use of a rectangular mesh for solid65 element is recommended to obtain good results. Therefore, all steel and concrete volumes and attached lines were so divided that the mesh was set up such that square or rectangular elements were formed. For this purpose the volume sweep command was used to mesh the steel cylinder at support and plate at loading location. This option properly sets the length and width of finite elements in the plates and cylinder to be consistent with the elements and nodes in the concrete portions of the model. The meshed volume of the concrete, support cylinder and plate, are shown in figures 4.16 to figures 4.19. After meshing volumes, all lines which have been attributed rebar properties were selected and meshed. The meshing of the reinforcement is a special case compared to the volumes.

4.4.6 Numbering Controls

Separate entities that have the same location are merged by numbering control command. By using this command items will then be merged into single entities. Merging key points before nodes can result in some of the nodes becoming "orphaned"; that is, the nodes lose their association with the solid model. The orphaned nodes can cause certain operations (such as surface load transfers, boundary condition transfers, and so on) to fail. While executing numbering control merges command, one must be careful when merging entities in a already meshed model because the merging order is significant. All entities were merged in a proper way as taking above precautions.

4.5 Solution Phase

In this phase loads, boundary conditions at support, loading plates, at symmetric locations, analysis types and solutions controlling parameters are selected.

4.5.1 Loads and Boundary Conditions

To obtained unique solution, displacement boundary conditions are needed to constrain the model. To ensure that the model behaves the same way as the assumed beams boundary conditions need to be applied at support and at the points where plane of symmetry exist. In present case there are two symmetric locations in beams parallel to X and Z axis. The

boundary conditions for the beams at both planes of symmetry and at loading plate and support cylinder are shown in Figure 4.17 to figure 4.20.
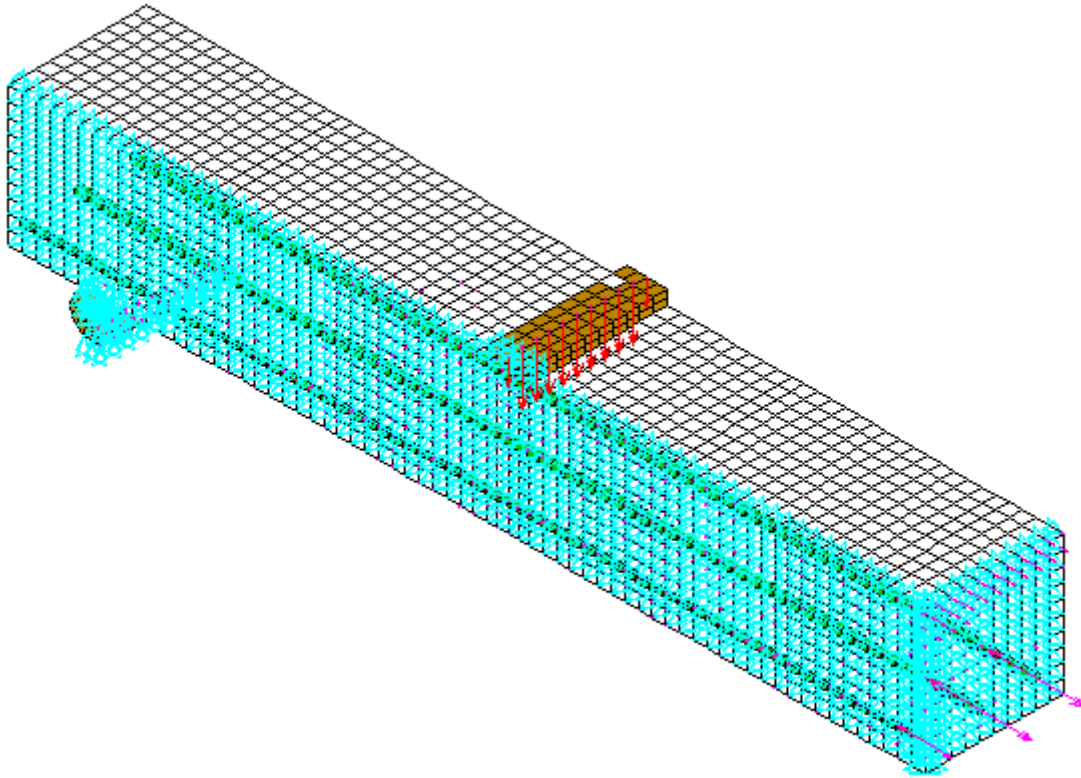
Figure 4.17: Loads and boundary Conditions on both planes of symmetry and at support and loading plates for beams BXL1 and BXL2.
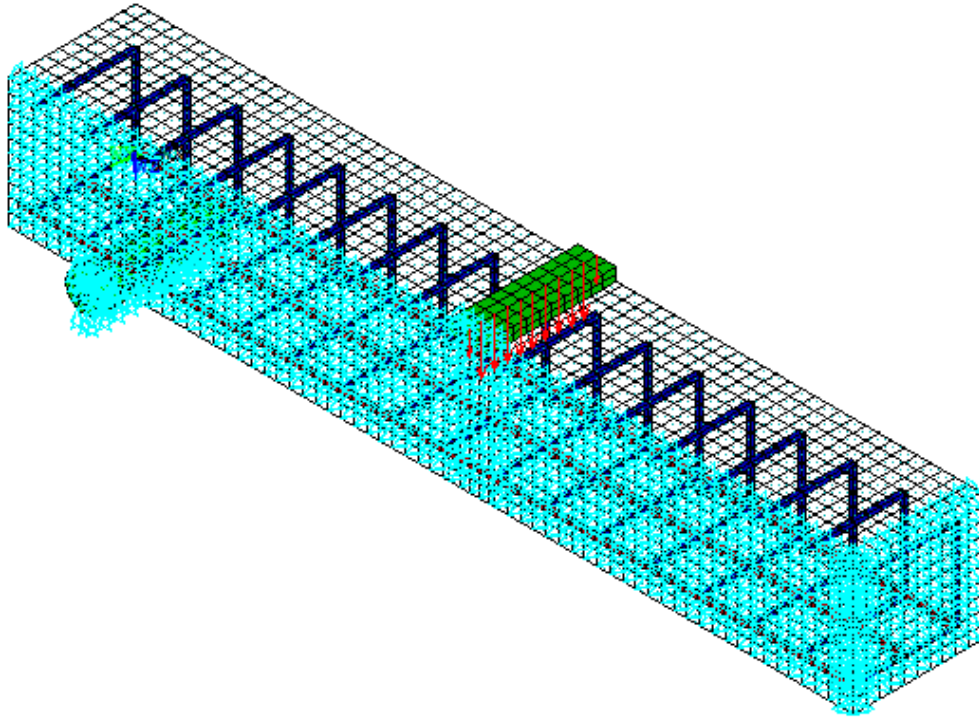
Figure 4.18: Loads and boundary Conditions on both planes of symmetry and at support and loading plates for beams BXL1W and BXL2W.
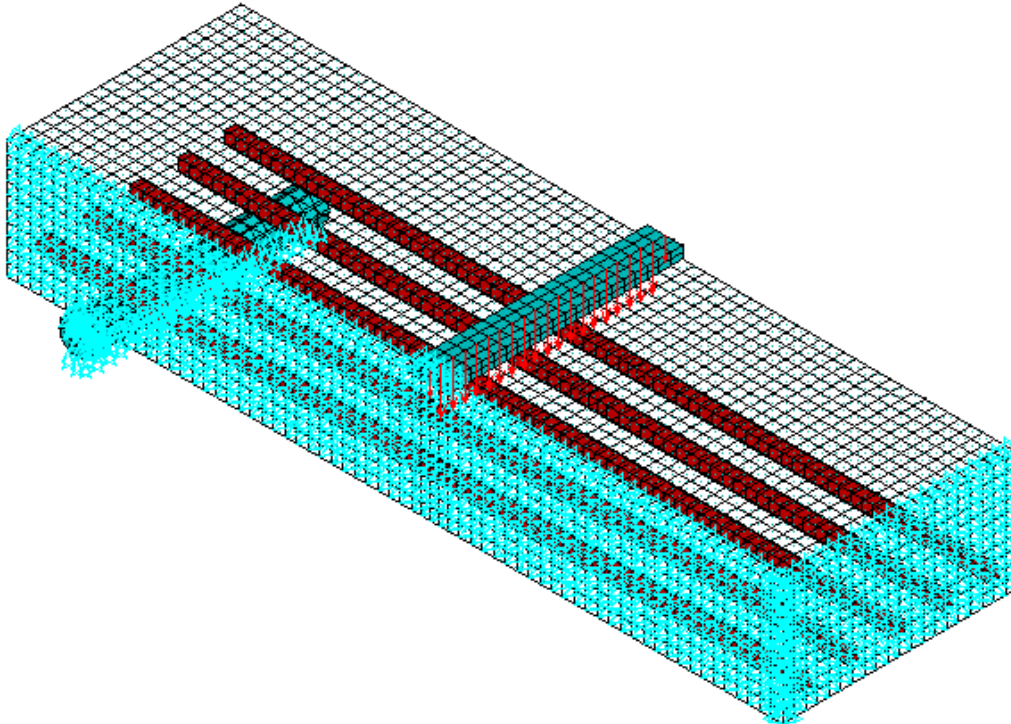
Figure 4.19: Loads and boundary Conditions on both planes of symmetry and at support and loading plates for beams BZL1 and BZL2.
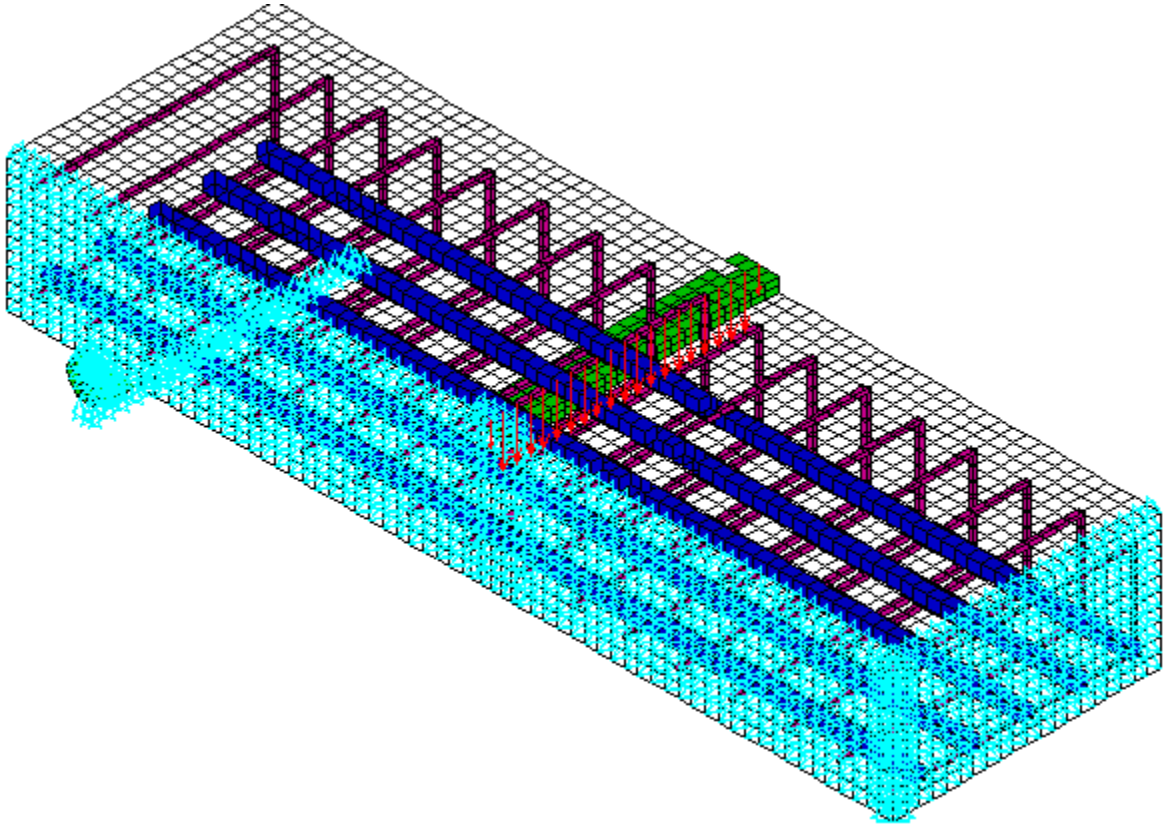
Figure 4.20 Loads and boundary Conditions on both planes of symmetry and at support and loading plates for beams BZL1W and BZL2W.

Boundary conditions for planes of symmetry constraint in the X and Z-directions. At these symmetric locations on above two mentioned planes, nodes on the planes must be constrained in the perpendicular direction. To do this nodes on the planes, were restrict to move in X and Z direction i.e. $U_x = 0$ and $U_z=0$. The cylinder support was modeled in a way that a rotational degree of freedom was allowed about Z-axis. Three lines of nodes on the cylinder were given constraint in the Y-directions. By doing this, the beam will be allowed to rotate and stable at the support. The force P at the steel plate is applied across the entire centerline of the plate.

4.5.2   Analysis Type and Process

In the present study nonlinear finite element analysis of simple beams are being performed under transverse loading. Static analysis command was used for these beams. The Newton-Raphson method of analysis was used to compute the nonlinear response To run the solution up to end, after the one load step has been ended, restart command was used to start next load step. Small displacement and static analysis was performed until failure or the yielding of

76

steel whichever reached first occur. Load increment used to complete the one load step is a sub step and results of each subs step analysis was recorded in result file. A convergence criterion for each load step was set to defaults except for the tolerances. The tolerance value for displacement was set equal to 0.25 from the start of solution to end, which is five times the default value. For this tolerance value, ANSYS analysis results were in good co-relation with elastic beam theory analysis when applied uncracked elastic beam of equaling concrete cross section. A listing of the load steps, sub steps, and loads applied per restart files for analyzed beams are shown in Table 4.3 to Table 4.6.

Table 4.3: Load increment details for beam BXL1and BXL2 for ANSYS analysis

Load increment details for beam BXL1				
Step No.	**Time @ Start**	**Time @ End**	**Increment**	**No of Sub Steps.**
1	0	5,500	500	11
2	5,500	5,850	350	1
3	5,850	6,000	1	150
4	6,000	12,500	100	65
5	12,500	**14,300**	50	36
Analysis stopped at load P=14,300 lbs. due to convergence issue.				
Load increment details for beam BXL2				
Step No.	**Time @ Start**	**Time @ End**	**Increment**	**No of Sub Steps.**
1	0	6,500	500	13
2	6,500	6,875	375	1
3	6,875	7,000	1	125
4	7,000	25,000	100	180
5	25,000	30,000	50	100
6	30,000	**31,800**	50	70
Analysis stopped at load P=31,800 lbs. due to convergence issue.				

Table 4.4: : Load increment details for beam BXL1and BXL2 for ANSYS analysis

Load increment details for beam BXLIW				
Step No.	**Time @ Start**	**Time @ End**	**Increment**	**No of Sub Steps.**
1	0	5,500	500	11
2	5,500	5,850	350	1
3	5,850	6,000	1	150
4	6,000	12,500	100	65
5	12,500	**14,400**	50	38
Analysis stopped at tensile steel yielding load P=14,400 lbs				
Load increment details for beam BXL2W				
Step No.	**Time @ Start**	**Time @ End**	**Increment**	**No of Sub Steps.**
1	0	6,500	500	13
2	6,500	6,875	375	1
3	6,875	7,000	1	125
4	7,000	25,000	100	180
5	25,000	40,000	100	150
6	40,000	**42,900**	100	29
Analysis stopped at load P=42,900 lbs. due to convergence issue.				

Table 4.5: Load increment detail for beam BZL1and BZL2 for ANSYS analysis

Load increment details for beam BZL1				
Step No.	**Time @ Start**	**Time @ End**	**Increment**	**No of Sub Steps.**
1	0	11,000	1000	11
2	11,000	11,700	700	1
3	11,700	11,800	2	50
4	11,800	25,000	200	66
5	25,000	**26,300**	100	13
Analysis stopped at load P=26,300 lbs. due to convergence issue.				
Load increment details for beam BZL2				
Step No.	**Time @ Start**	**Time @ End**	**Increment**	**No of Sub Steps.**
1	0	13,000	1000	13
2	13,000	13,750	750	1
3	13,750	13,800	2	25
4	13,800	50,000	200	181
5	50,000	**52,900**	100	29
Analysis stopped at load P=52,900 lbs. due to convergence issue.				

Table 4.6: Load increment detail for beam BZL1Wand BZL2W for ANSYS analysis.

Load increment details for beam BZL1W				
Step No.	**Time @ Start**	**Time @ End**	**Increment**	**No of Sub Steps.**
1	0	11,000	1000	11
2	11,000	11,700	700	1
3	11,700	11,800	2	50
4	11,800	25,000	200	66
5	25,000	**28800**	100	38
Analysis stopped at load P=28,800 lbs. due to convergence issue.				
Load increment details for beam BZL2W				
Step No.	**Time @ Start**	**Time @ End**	**Increment**	**No of Sub Steps.**
1	0	13,000	1000	13
2	13,000	13,750	750	1
3	13,750	13,800	2	25
4	13,800	50,000	200	181
5	50,000	80,000	200	150
6	80,000	90,000	200	50
7	90,000	**98,400**	100	84
Analysis stopped at tensile steel yielding load P=98,400 lbs.				

4.6   General and Time History Postprocessor

Post processor which includes results will be discussed in chapter 5.

CHAPTER 5

RESULTS and DISCUSSIONS

The ANSYS analysis results for flexure and shear response parameters are presented and discussed in next pages of chapter 5. In the table 5.1, list of beams is reproduced for ready reference.

Table 5.1 List of beams considered for ANSYS finite element analysis

S.N0	Series	Beam Type	Size (bxh)	Flexure Rebar	ρ (Long)	depth-d	Conc $f_c^{'}$ (psi)	Shear Rebar
1	X	BXL1	40"x10"	10#4	0.50%	8"	4,000	-----
2		BXL2	40"x10"	10#8	1.98%	8"	4,000	-----
3		BXL1W	40"x10"	10#4	0.5%	8"	4,000	# 3 @ 4"
4		BXL2W	40"x10"	10#8	1.98%	8"	4,000	# 3 @ 4"
5	Z	BZL1	20"x10"	5#4	0.50%	8"	4,000	-----
6		BZL2	20"x10"	5#8	1.98%	8"	4,000	-----
7		BZL1W	20"x10"	5#4	0.50%	8"	4,000	# 3 @ 4"
8		BZL2W	20"x10"	5#8	1.98%	8"	4,000	# 3 @ 4"

5.1 Flexure and Shear Response Parameters Results

5.1.1 Plots of Bending Stress-S_X along Depth of Beams
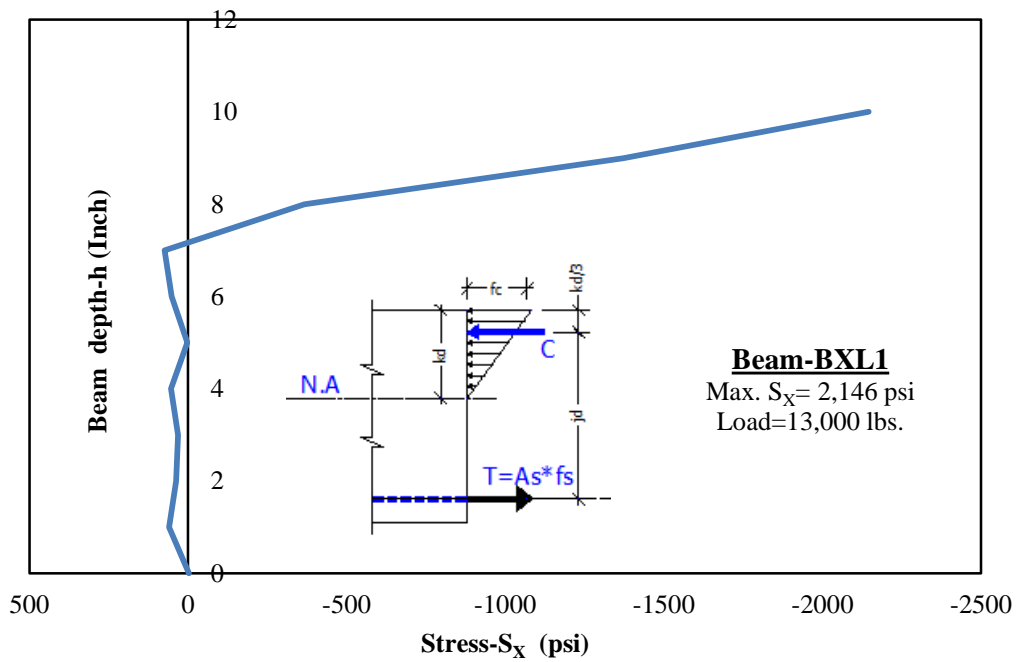
Figure 5.1: Plots of stress-S_X along depth of beam BXL1
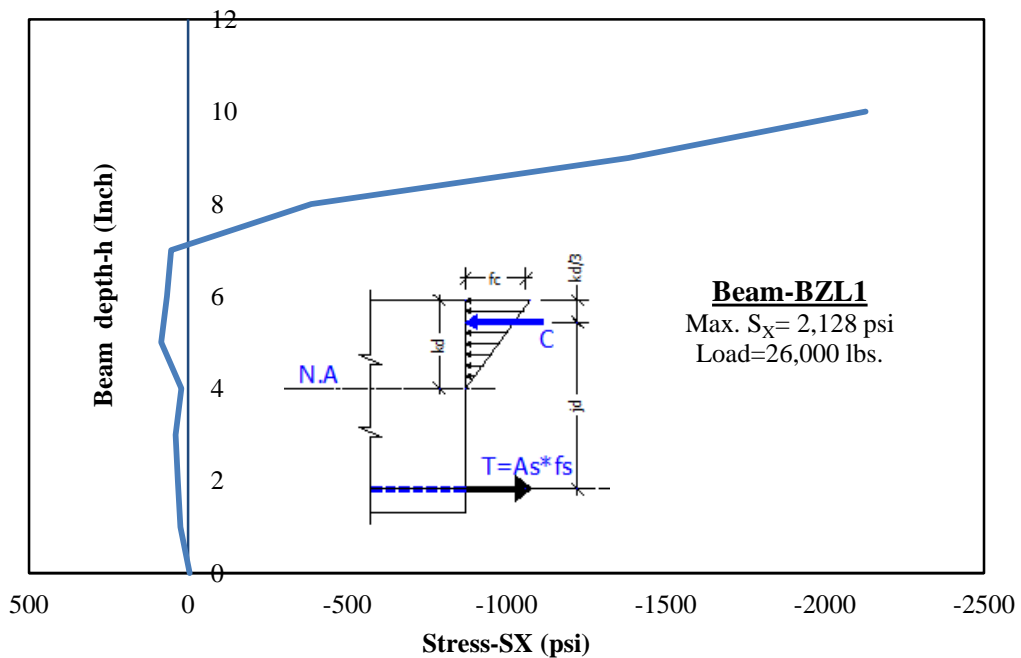
Figure 5.2: Plots of stress-S_X along depth of beam BZL1
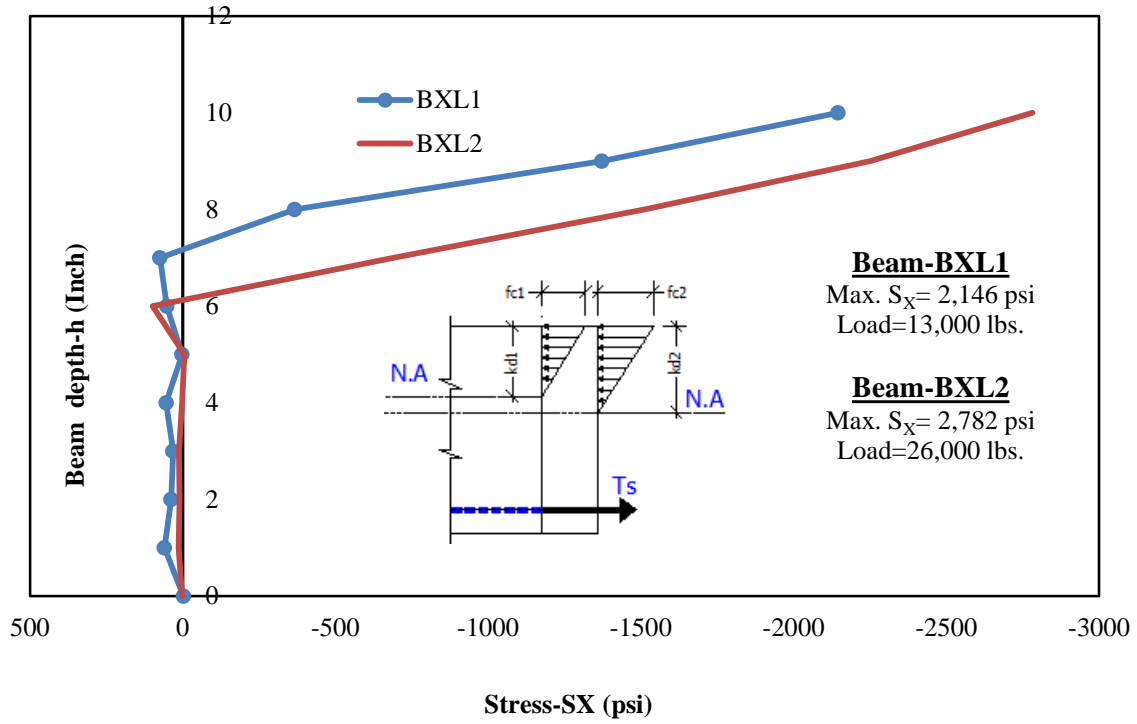
Figure 5.3: Plots of stress-S_X along depth of beams (BXL1 & BXL2)
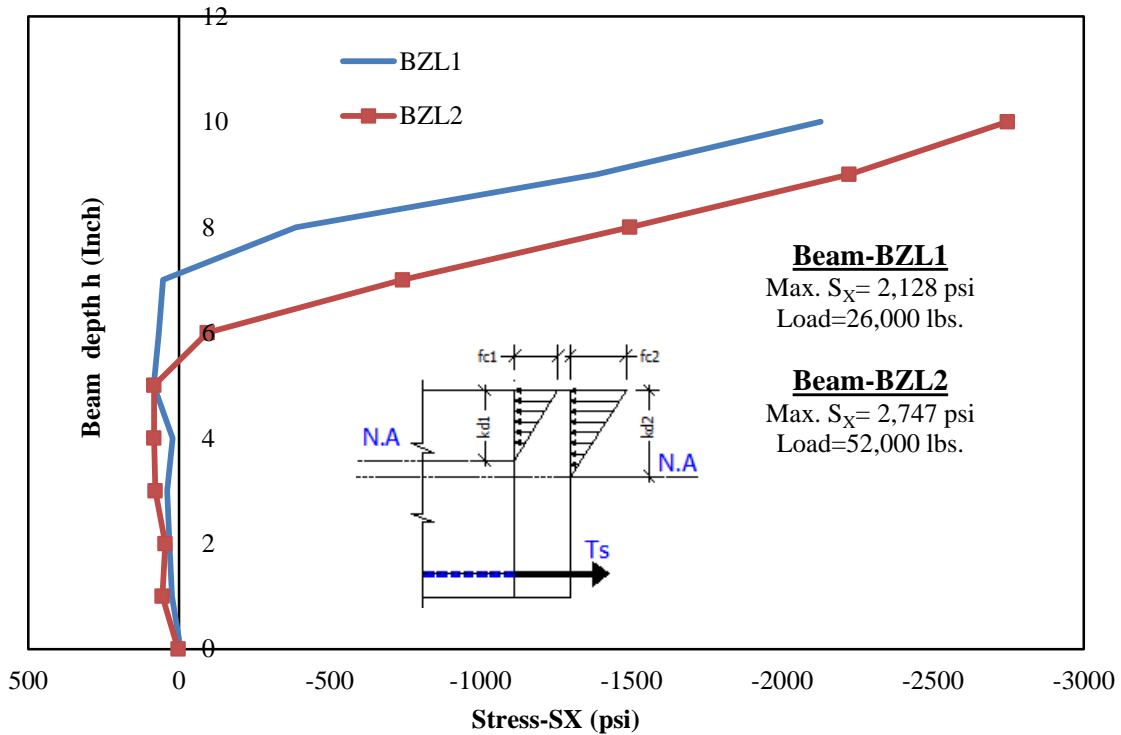
Figure 5.4: Plots of stress-S_X along depth of beam (BZL1 & BZL2)

84
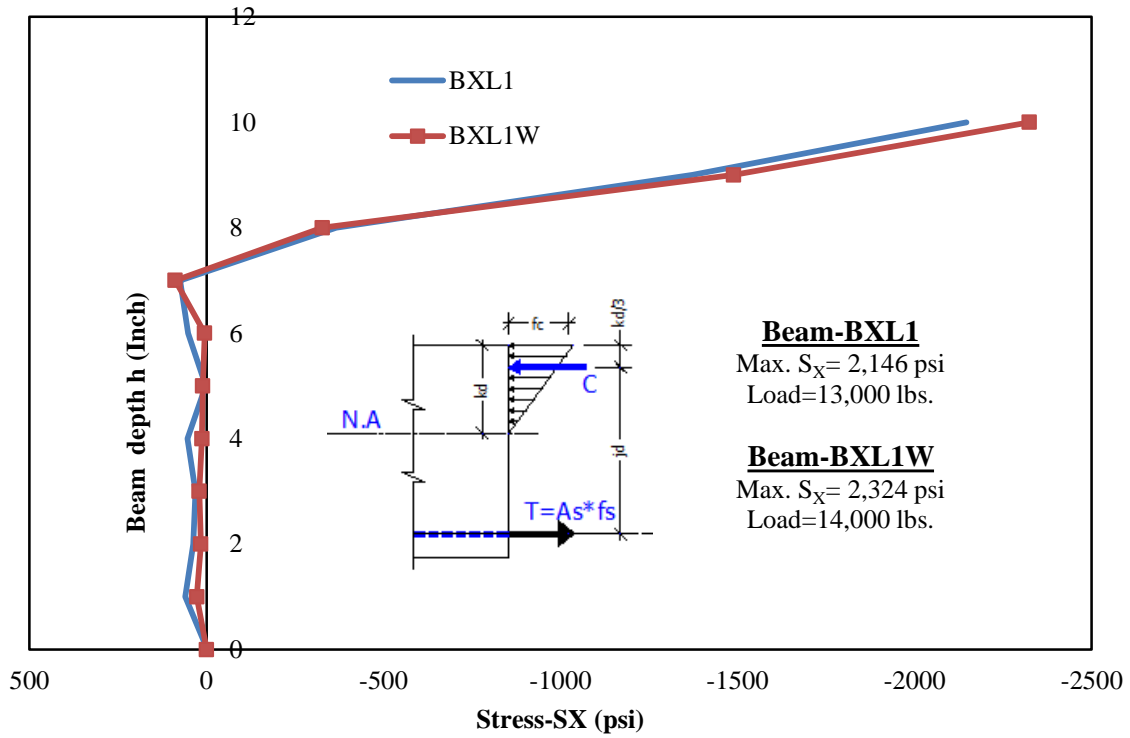
Figure 5.5: Plots of stress-S_X Along depth of beams (BXL1 &BXL1W)
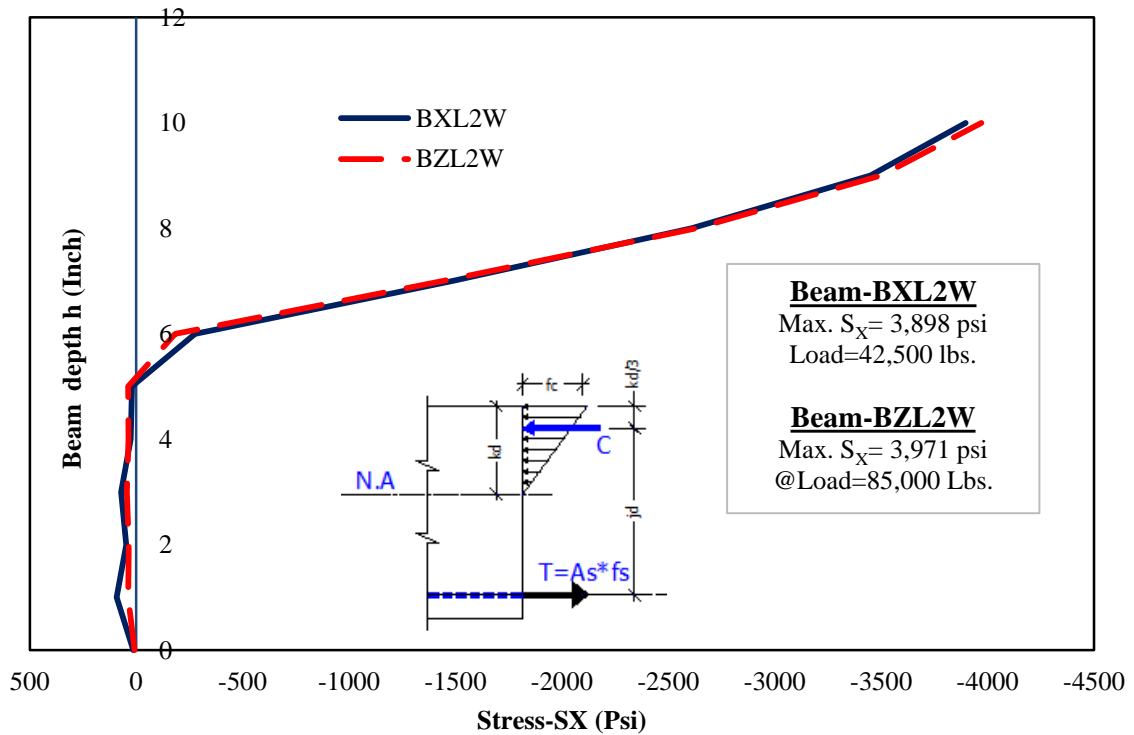
Figure 5.6: Plots of stress-S_X along depth of beams (BXL2W &BZL2W)

5.1.2   Crack Pattern for Beam- BXL1
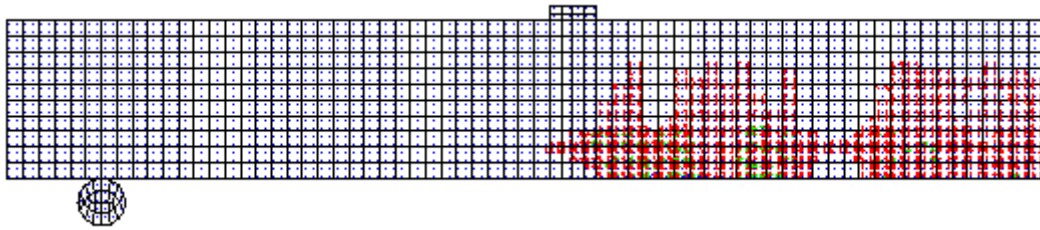
(a): Crack pattern for beam BXL1 at load P= 6,000 lbs.
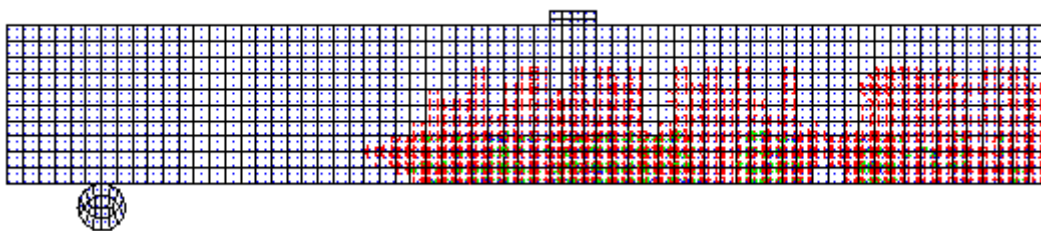
(b): Crack pattern for beam BXL1 at load P= 10,000 lbs.
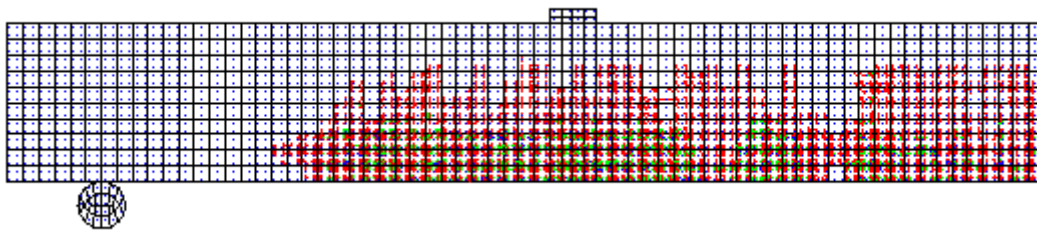
(c): Crack pattern for beam BXL1 at load P= 13,000 lbs.
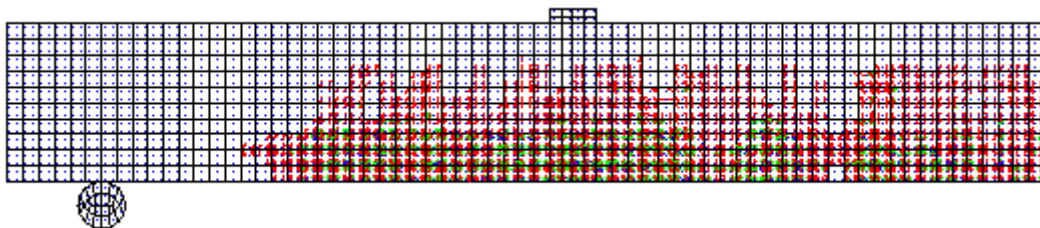
(d): Crack pattern for beam BXL1 at load P= 14,300 lbs.

Figure 5.7: Crack pattern for beam BXL1 at different load values

5.1.3   Crack Pattern for Beam- BXL2
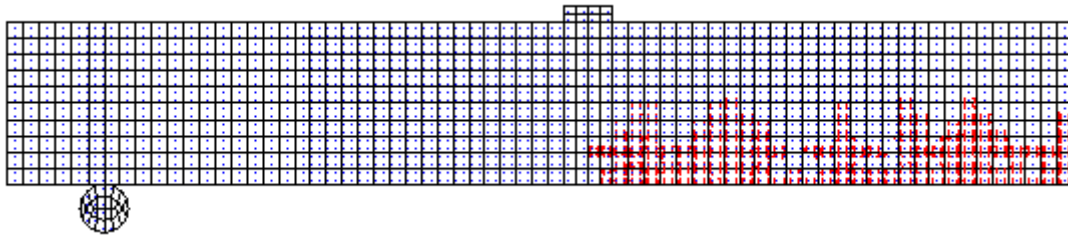
(a): Crack pattern for beam BXL2 at load P= 7,000 lbs.
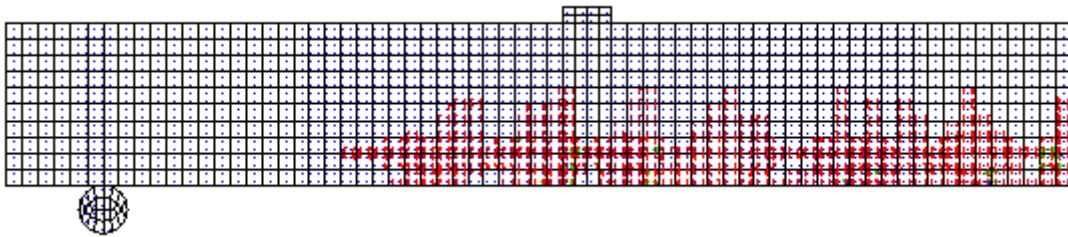
(b): Crack pattern for beam BXL2 at load P= 13,000 lbs.
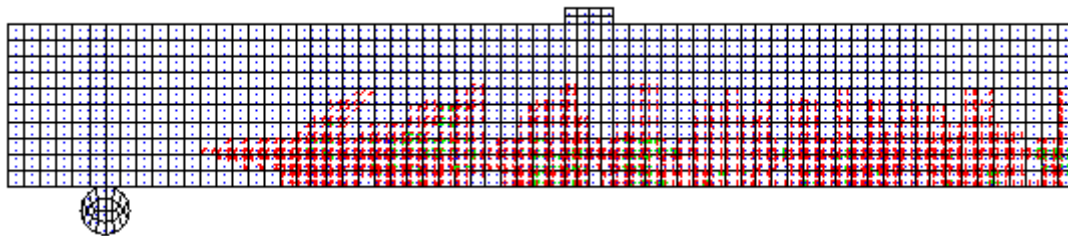
(c): Crack pattern for beam BXL2 at load P= 20,000 lbs.
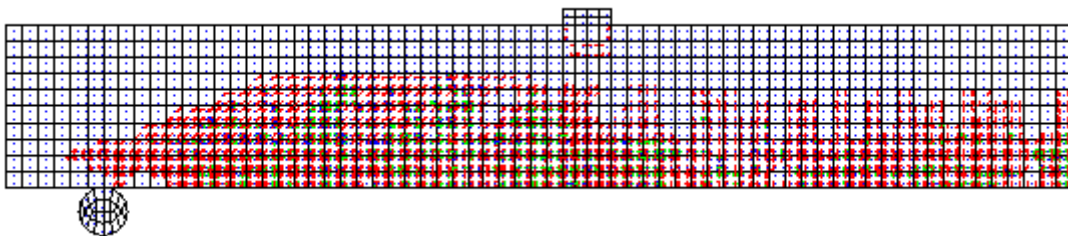
(d): Crack pattern for beam BXL2 at load P= 31,800 lbs.

Figure 5.8: Crack pattern for beam BXL2 at different load values

5.1.4   Crack Pattern for Beam- BXL1W
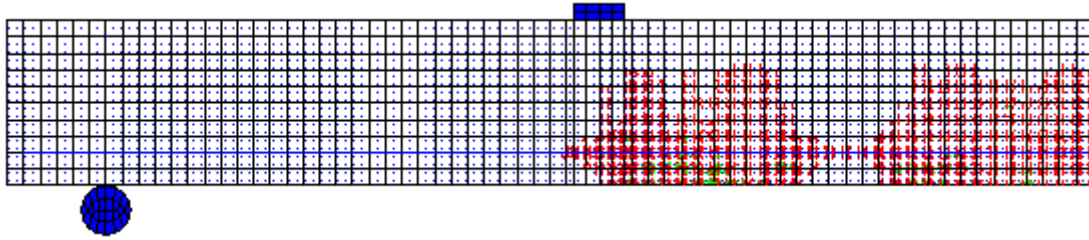
(a): Crack pattern for beam BXL1W at load P= 6,000 lbs.
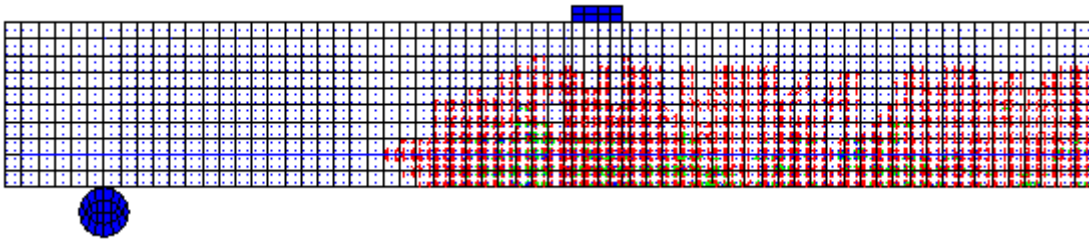
(b): Crack pattern for beam BXL1W at load P= 10,000 lbs.
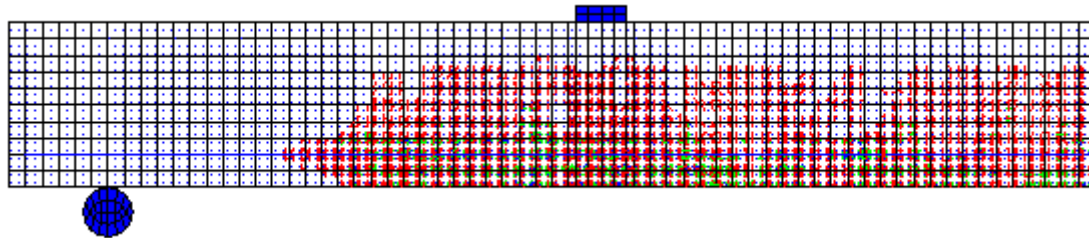
(c): Crack pattern for beam BXL1W at load P= 13,000 lbs.
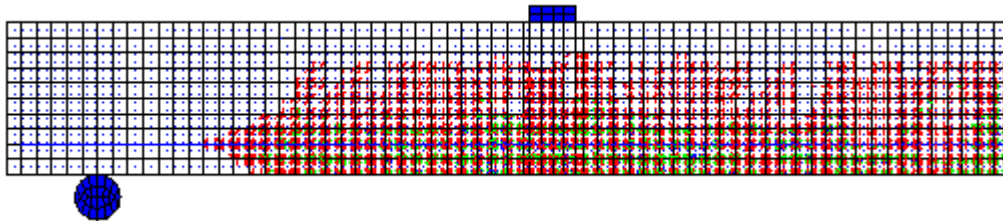
(d): Crack pattern for beam BXL1W at load P= 15,120 lbs.

Figure 5.9: Crack pattern for beam BXL1W at different load values

5.1.5   Crack Pattern for Beam- BXL2W
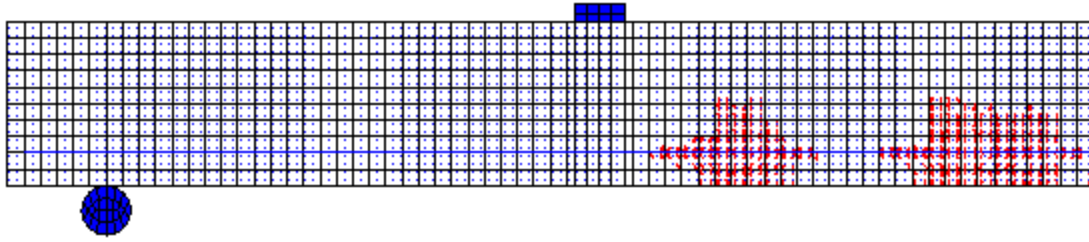
(a): Crack pattern for beam BXL2W at load P= 7,000 lbs.
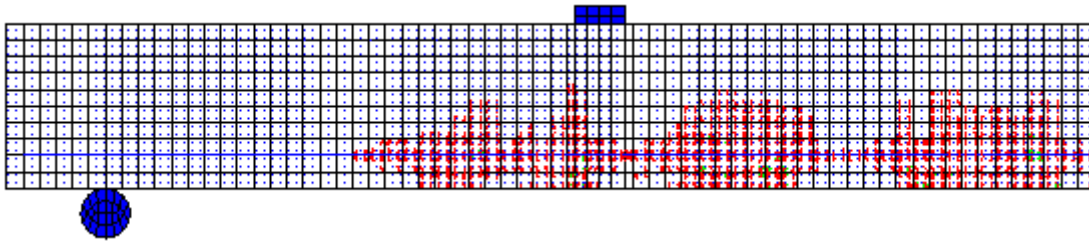
(b): Crack pattern for beam BXL2W at load P= 13,000 lbs.
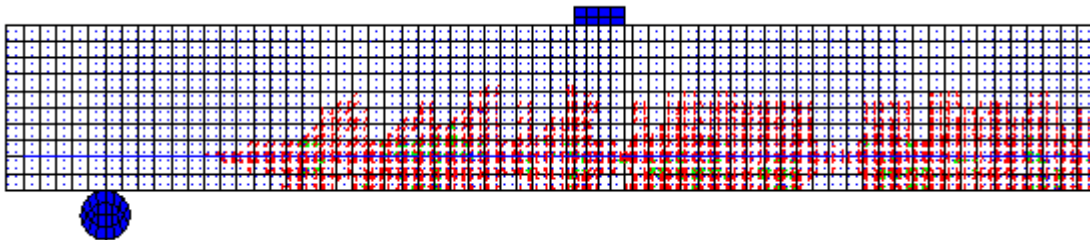
(c): Crack pattern for beam BXL2W at load P= 20,000 lbs.
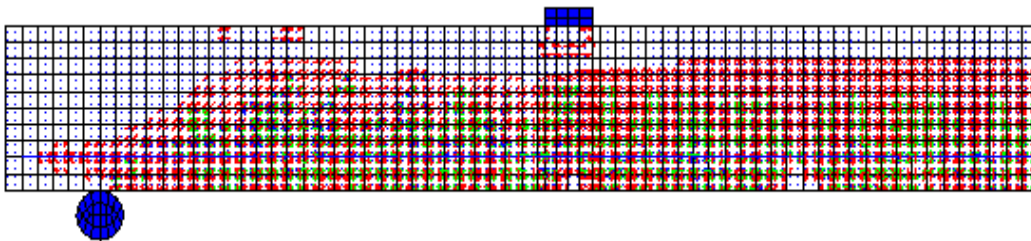
(d): Crack pattern for beam BXL2W at load P= 42,900 lbs.

Figure 5.10: Crack pattern for beam BXL2W at different load value

5.1.6 Plots of Stress-S_X and S_Z along width of beams

Beam-BXL2
Max. S_X=2,796 psi
Min. S_X=2,746 psi
Load=26,000 lbs.

As=5#8

Beam-BXL1
Max. S_X=2,167 psi
Min. S_X=2,103 psi
Load=13,000 lbs

As=5#4
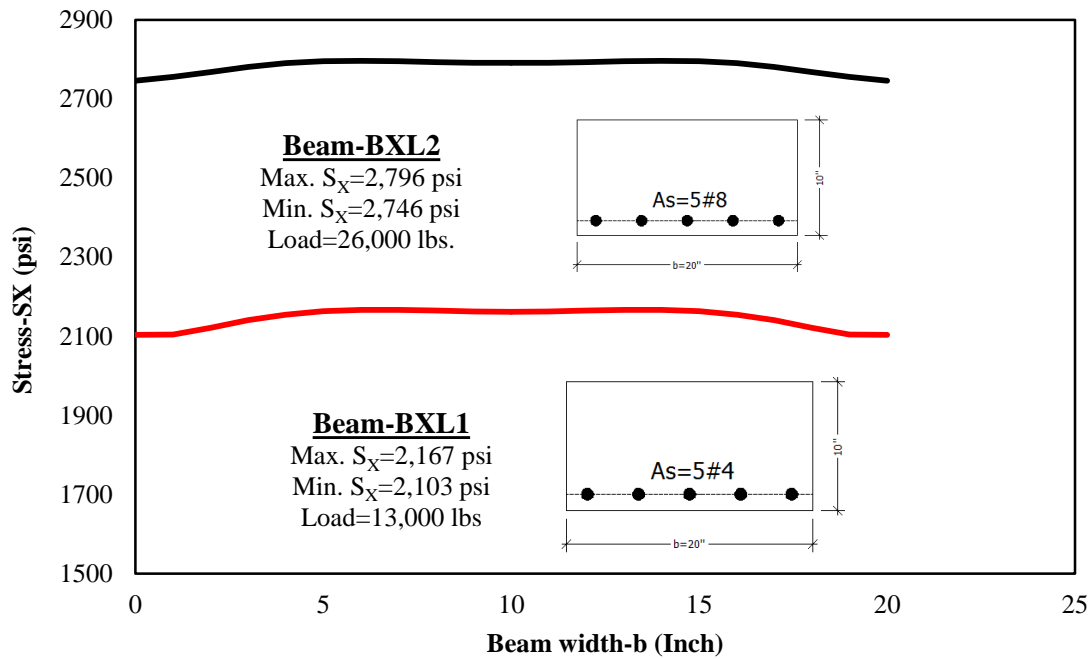
Figure 5.11: Plots of Stress-S_X along width of beams at top of middle Centre (BXL1 &BXL2)

Beam-BZL2
Max. S_X= 2,790 psi
Min. S_X=2,663 psi
Loads=52,000 lbs.

As=10#8

Beam-BZL1
Max. S_X= 2,153 psi
Min. S_X=2,078 psi
Load=26,000 lbs.

As=10#4
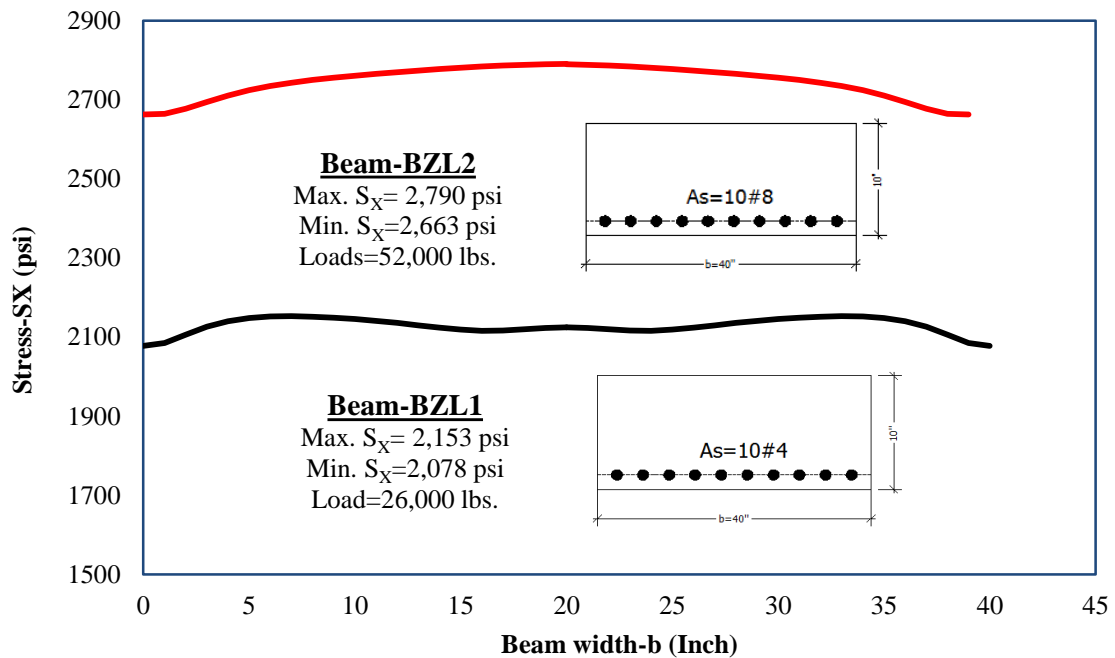
Figure 5.12: Plots of Stress-S_X along width of beams at top of middle center (BZL1 & BZL2)

90

5.1.7   Plots of shear stress S$_{XY}$ along width of beams BXL1, BZL2 and BZL1
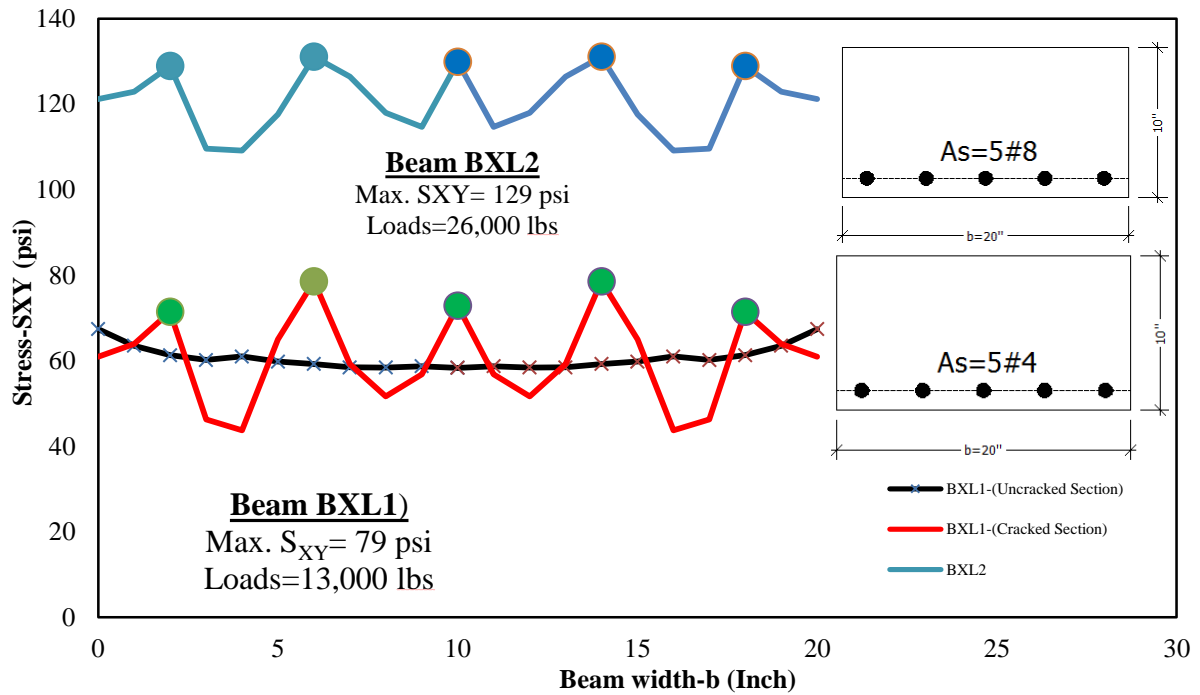
Figure 5.13: Plots of shear Stress-S$_{XY}$ along width of beam-BXL1 and BXL2
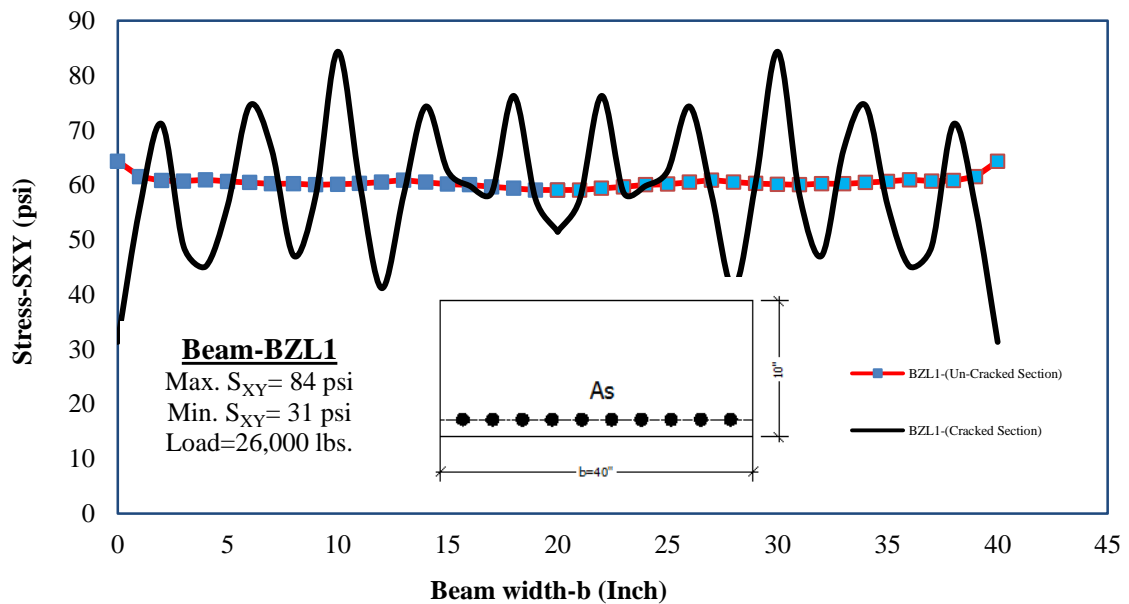
Figure 5.14: Plots of shear Stress-S$_{XY}$ along width of beam-BZL1

91

5.2 Interpretation and discussion of beams flexure and shear results

Flexure response of the concrete beam is influenced by many factors such longitudinal reinforcement ratio, presence of compression steel and web reinforcement, material strength, loading pattern, beam size and geometry etc. Similarly factors such as concrete tensile strength, longitudinal reinforcement steel ratio, shear span to depth ratio (a/d), light weight aggregate, beam and coarse aggregate size and axial force effect shear response of concrete beams. Because of limited scope of the present research, only fallowing three flexure and shear response affecting factors are discussed below.

5.2.1 Longitudinal steel Reinforcement Ratio ρ_w.

Flexure and shear response parameters of concrete beams are considerably affected by amount of flexure steel reinforcement ratio. This fact can easily be realized from cracking and failure load values of beams considered and analyzed in this research presented in table 5.2 and 5.3 and graphical plots as shown in figure 5.3 and 5.4. It is also observed that concrete beams with same dimensions but with different longitudinal reinforcement ratio have different neutral axis and crack depth at certain load values. From result data of the tables 5.2, it is observed that cracking loads and corresponding deflections calculated by elastic beam theory applied to uncracked elastic concrete cross section made up of homogeneous material are in good co-relation with result obtained from ANSYS analysis. Beam BXL1 with 0.5% longitudinal steel ratio has more crack depth and less neutral axis depth with relatively little compression zone depth compares to beam BXL2 with 1.98% longitudinal steel reinforcement ratio. This fact may be the one of the reasons for more shear strength for beam BXL2 than beam BXL1. Similarly beam BZL1 and BZL2 shows the same behaviour as described above for beam BXL1 and BXL2.

It is also observed that magnitude of deflection just after onset of cracking is higher, due to sudden cracking of beam tensile zone (60-inch length) with slight additional load increment as the same has already been stressed to cracking stress-f_{cr}, located in constant moment region between two loading points. Further at onset of cracking, instant increase in deflection is more in beams with low flexure steel ratio due to relatively higher stresses in steel re-bars, once the section has been cracked.

Table 5.2: Cracking loads and deflections results from beam theory and ANSYS analysis

S. No	Beam Type	Beam Theory Result		ANSYS Analysis	
		Cracking Load (lbs.)	Deflection (Inch)	Cracking Load (lbs.)	Deflection (Inch)
1	BXL1	5,620	0.044	5,870	0.047
2	BXL2	6,590	0.047	6,895	0.050
3	BXL1W	5,620	0.044	5,874	0.047
4	BXL2W	6,590	0.047	6,899	0.050
5	BZL1	11,240	0.044	11,712	0.047
6	BZL2	13,180	0.047	13,754	0.050
7	BZL1W	11,240	0.044	11,718	0.047
8	BZL2W	13,180	0.047	13,756	0.050

Table 5.3: Theoretical and ANSYS analysis failure loads and moments results

S. No	Beam Type	Beam Theory		ANSYS Analysis	
		Load Capacity P_n (lbs.)	Moment (Kip-ft)	Load Capacity P_n (lbs.)	Moment (Kip-ft)
1	BXL1	15,100	37.75	14,300	35.75
2	BXL2	49,400	123.5	31,800	79.5
3	BXL1W	15,100	37.75	14,400	36
4	BXL2W	49,400	123.5	42,900	107.25
5	BZL1	30,200	75.5	26,300	65.75
6	BZL2	59,200	148	52,900	132.25
7	BZL1W	30,200	75.5	28,800	72
8	BZL2W	98,800	247	98,400	246
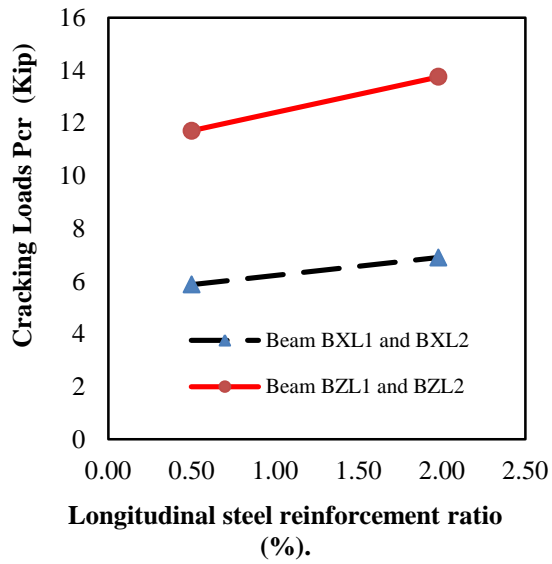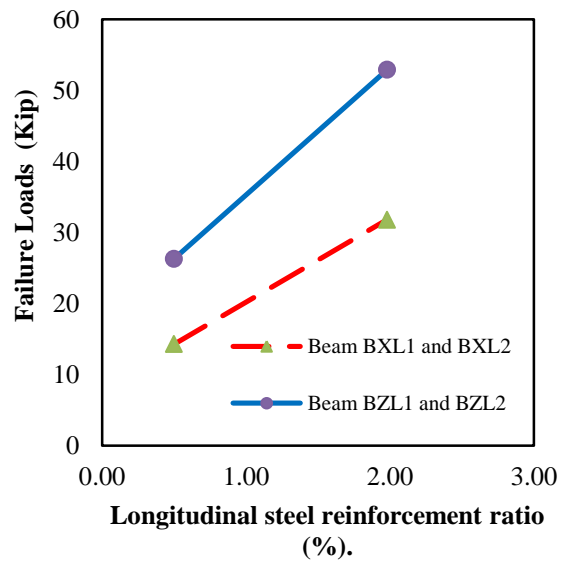
(a)   (b)

Figure 5.135: Effect of reinforcement steel ratio, on cracking and failure load for concrete beams.
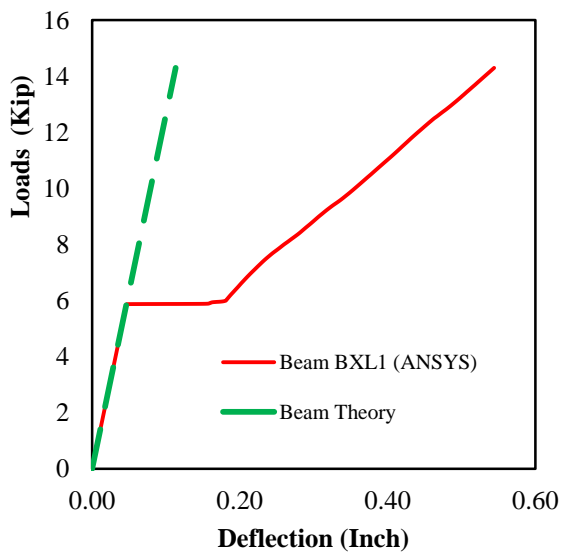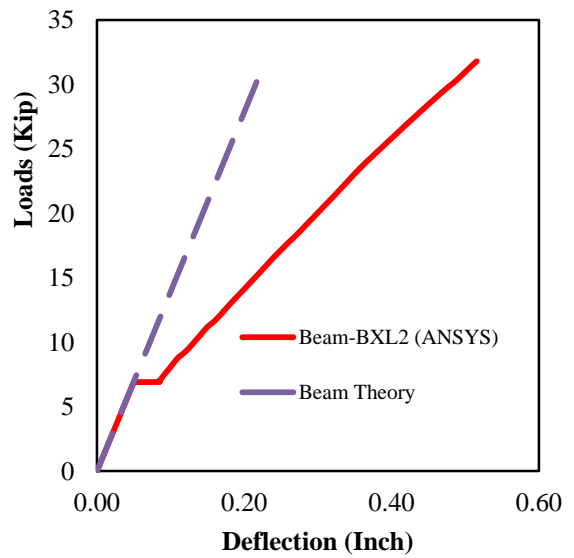
(a)   (b)
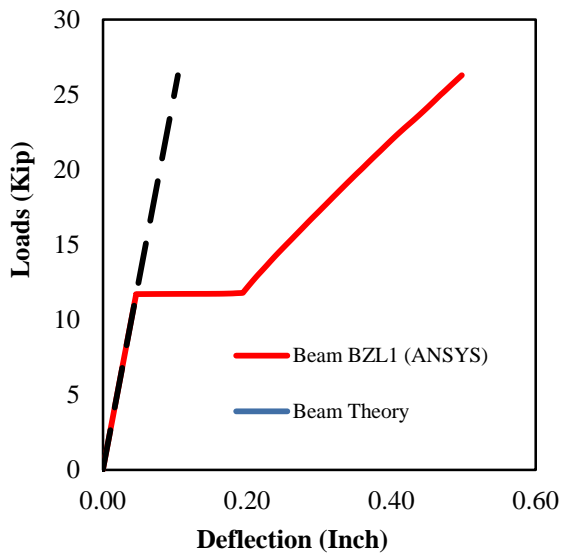
(c)
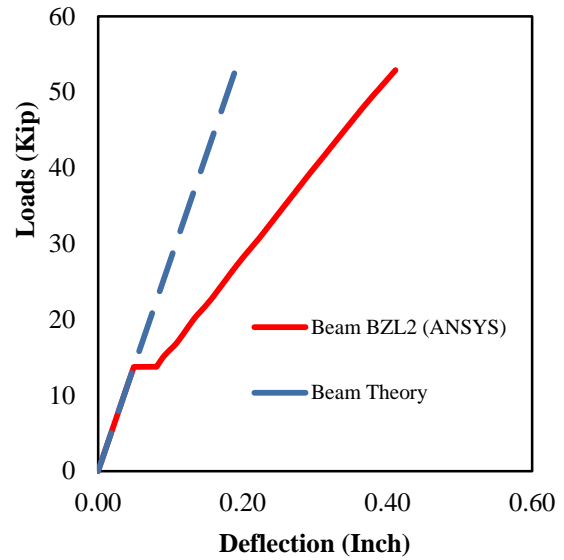
(d)
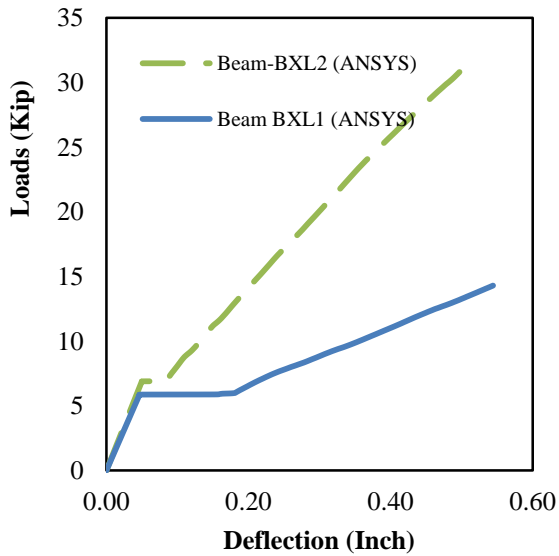
(e)
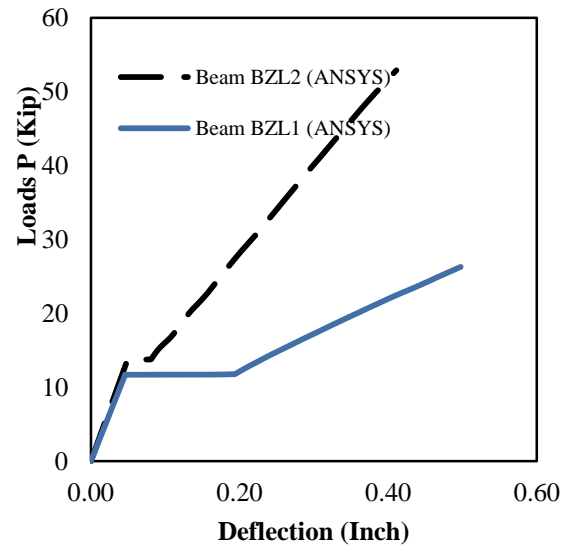
(f)

Figure 5.1614: Loads versus deflection plots for beams

The longitudinal reinforcement steel ratio significantly affect the shear strength of beams as shown in Figure 5.17, that   presents the shear capacities (psi units) of simply supported beams without stirrups as a function of the steel ratio. Generally the practical range of longitudinal reinforcement ratio for developing shear failure ranges from 0.0075 to 0.025. In this range, as indicated by horizontal dashed line, the shear strength is approximately given by ACI equation as:

$$V_c = 2\sqrt{f_c'}b_w d \qquad (5.1)$$
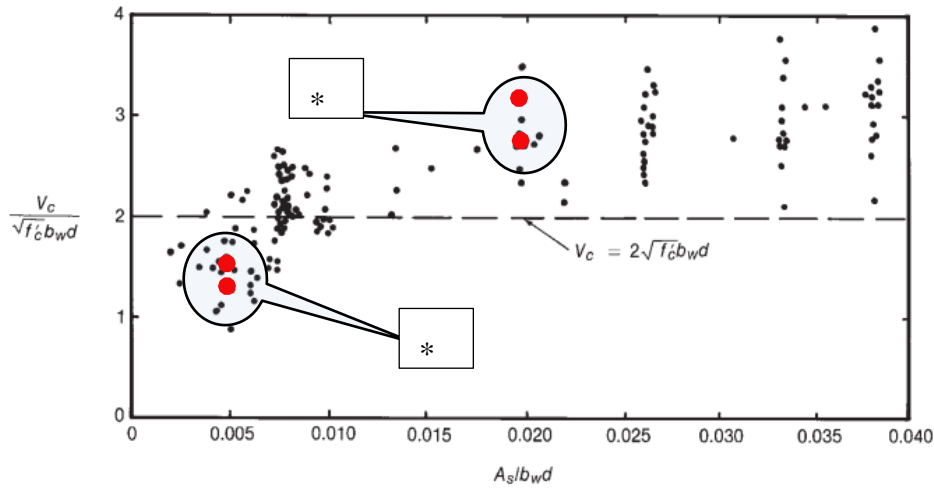
Figure 5.1715: Effect of reinforcement ratio ρ_w, on shear capacity V_c of the beams
constructed with normal weight concrete and without stirrups (ACI-ASCE Committee 426).

* Beam BXL1 $\dfrac{V_c}{\sqrt{f_c^{'}b_wd}} = 1.41,$ and   Beam BZL1 $\dfrac{V_c}{\sqrt{f_c^{'}b_wd}} = 1.30$

** Beam BXL2 $\dfrac{V_c}{\sqrt{f_c^{'}b_wd}} = 3.14,$ and   Beam BZL2 $\dfrac{V_c}{\sqrt{f_c^{'}b_wd}} = 2.61$

Shear capacity when calculated by above equation 5.1 tend to be overestimate for beams with small longitudinal steel ratio particularly less than 0.010. For relatively small ratio of ρ_w, flexural cracks extend higher into the beam and open wider than would be the case for large values of ρ_w. The maximum values of the components of shear that are transferred across the inclined cracks by dowel action or by shear stresses on the crack surfaces decreases as cracks width increases. Eventually, the resistance along the crack drops below that required for resisting the loads, and the beam fails suddenly in shear. The effect of deeper crack with relatively more widen cracks can easily be observed from results of beams BXL1 with longitudinal steel reinforcement ratio $\rho_w = 0.005$ and also for beams BXL2 with longitudinal steel reinforcement ratio $\rho_w = 0.0198$ plotted in figure 5.7 and 5.8 and similarly for beam BXL1W and BXL2W in figure 5.9 and 5.10. Shear strength factor $\dfrac{V_c}{\sqrt{f_c^{'}b_wd}}$ are found as under

and the same are plotted in figure 5.17 that agrees well with experimental result data.

96

For beam BXL1 $\rightarrow$ $\dfrac{V_c}{\sqrt{f_c'}\,b_w d} = 14{,}300/\,(\sqrt{4{,}000}*20*8)$ $= 1.41$

For beam BZL1 $\rightarrow$ $\dfrac{V_c}{\sqrt{f_c'}\,b_w d} = 26{,}300/\,(\sqrt{4{,}000}*40*8)$ $= 1.30$

For beam BXL2 $\rightarrow$ $\dfrac{V_c}{\sqrt{f_c'}\,b_w d} = 31{,}800/\,(\sqrt{4{,}000}*20*8)$ $= 3.14$

For beam BZL2 $\rightarrow$ $\dfrac{V_c}{\sqrt{f_c'}\,b_w d} = 52{,}900/\,(\sqrt{4{,}000}*40*8)$ $= 2.61$

5.2.2 Size of Beam

In wide RC beams, shear strength decreases with increase in width, as shear strength in beam BXL1 (20 in wide) was 8% higher than similar beam BZL1 (40 in wide). Collins, Kuchma (Collins and Kuchma 1999) and Kani (Kani 1967) have experimentally shown that increasing the depth of beam with little or no web reinforcement results in a decrease in the shear for given load shear span to depth ratio (a/d) at failure. Crack width is affected by strain in reinforcement at cracked location and the spacing of the cracks. With increasing beam depth, the crack spacing and the crack widths tend to increase. This is the main reasons that lead to a reduction in the maximum shear stress that can be transferred across the crack by aggregate interlock. When shear stress transferred across the crack due to aggregate interlock exceeds the shear strength, unstable situation may develop. When this occurs, the concrete faces slip on the crack, one relative to the other. Figure 2.1 of chapter 2 shows a significant decrease in the shear strengths of beams with increasing depth from 4-icnh to 118-inch and beam width ranging from 6 inch to 59 inch made with 0.1 inch, 0.4 and 1 inch maximum aggregate size inch, uniformly loaded.

Although in research by Collins and Kuchma, it has been described that decrease in shear strength is mainly due to increase in beam depth. But on the other hand it is fact that beams width b were not kept constant for tests beams, perhaps it has been considered that beam width did not affect the shear strength.

Very little experimental research has been performed that described absolute role of beam width on shear strength of concrete beams. Kani, Collins and Lubel et al (Collins and Kuchma 1999; Kani 1967; Lubell et al. 2004) in their research have shown that influence of

beam width on shear strength is negligible. Hadi Nasir Ghadhban (Ghadhban 2007) by statistical regression analysis performed on 689 reinforced concrete beams results selected from the literature for which beam width b_w ranges from 5 inch to 24 inch. Out of 689 beams, 402 were without web reinforcement and 287 with web reinforcement. All beams were tested under two equal top point with a/d > 2. The plot of beam width versus Vexp/Vaci in terms of relative shear strength values (RSSV) is shown below in figure 5.19.
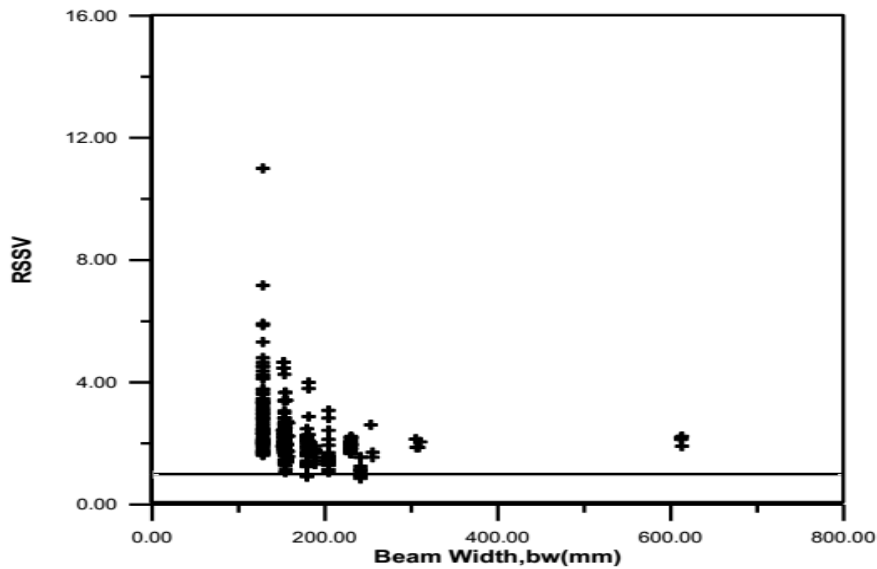
Figure 5.18: Effect of beam width on shear strength of beam without web reinforcement (Ghadhban 2007).

From the plots of figure 5.18, it is evident that shear strength value RSSV is affected by beam width and the same tends to be decrease as the beam width increases. This results of this research also supports the finding of Hadi Nasir Ghadhban as for beams BXL1 and BZL1 and similarly for beams BXL2 and BZL2 with 0.5% and 1.98% longitudinal steel reinforcement ratio respectively shear strength are relatively more for beams with less width i.e. beam BXL1 and BXL2 with 20 inch width than beams BZL1 and BZL2 with 40 inch width as shown in ANSYS analysis shear failure loads presented in table 5.3.

5.2.3 Web Reinforcement

Before the start of cracking the role of web reinforcement is to resist shear and its contribution to enhance the beam stiffness is negligible. This result of cracking loads and corresponding deflection for beams with and without shear reinforcement are presented in

table 5.2, which clearly indicate that function of web reinforcement is negligible before the flexure cracks are formed.

The role of web reinforcement comes into play when flexure cracks start and its helps to prevent spreading of cracks towards the compression zone of concrete and to achieve full flexure strength and preventing pre mature failure due to shear. It is observed that beams without web reinforcement like BXL1, BZL2, BXL2, and BZL2 fails before reaching it full flexure capacity, while on other hand when same beams like BXL1W, BZL1W, BXL2W and BZL2W equipped with web reinforcement almost attain their full flexure strength as reflected in failure load values presented in table 5.3 and figure 5.19a to 5.19d. Further when we examine cracking load results values presented in table 5.2, it is observed that initial cracking load values are same for beams with and without web reinforcement ignorable differences.

(a)

(b)
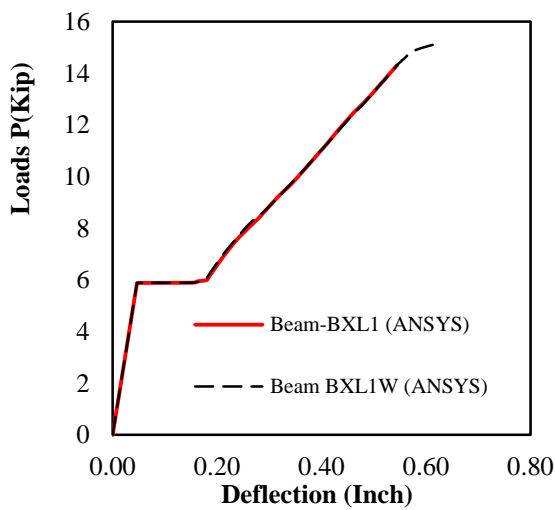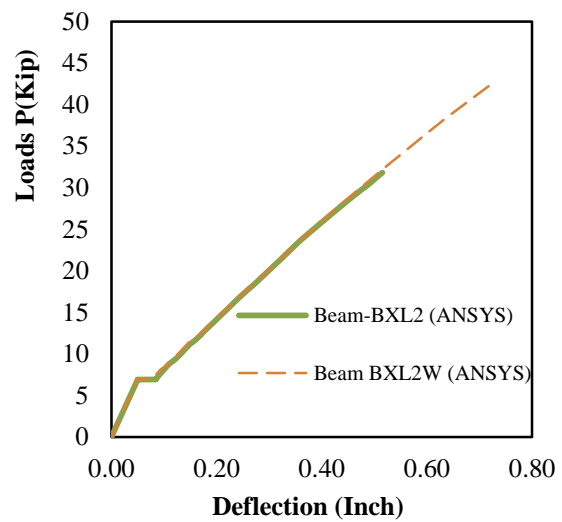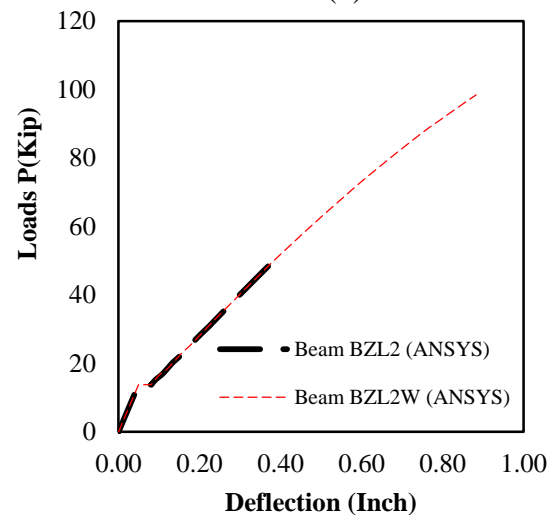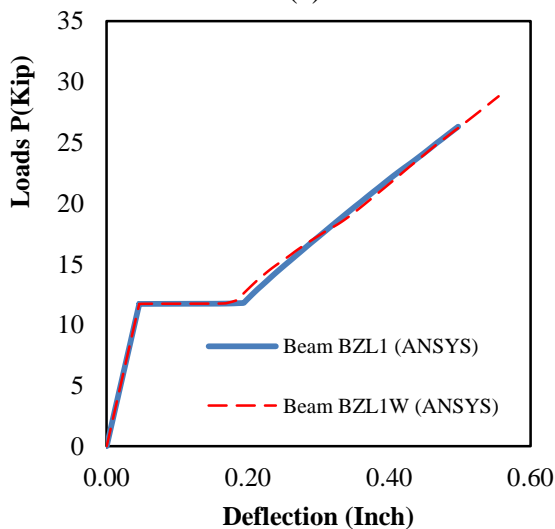
Figure 5.20: Effect of web reinforcement on shear strength of beam.

Beams provided with little or at least the minimum required web reinforcement show improved shear behaviour than those without web reinforcement. Web reinforcement holds the crack faces together so that the shear transfer across the cracks by aggregate interlock is not lost.

The shear capacity of concrete beams without web reinforcement drop below the flexural strength due to inclined. Before inclined cracking occurs, strain in the stirrups is equal to the corresponding strain of the concrete due to perfect bond assumption. Concrete tensile strength is very less than compressive strength as a result its cracks at a very small strain, the stress in the stirrups prior to inclined cracking usually in the range of 3 to 5 ksi. Due to these reasons, web reinforcement does not prevent inclined cracks from forming; they come into play only after the cracks have formed.

Beams not provided with web reinforcement fails as inclined cracking occurs or shortly afterwards. In the table 5.4 shown below, it is obvious that the beams BXL1W, BXL2W, BZL1W and BZL2W provided with #3@4 inch c/c, fails at higher load values and almost attain their full flexure strength before failure as compared to those beams without web reinforcement like BXL1, BXL2, BZL1 and BZL2 that failed in shear before developing their full flexure strength. The failure loads of these beams are shown table below.

Table 5.4: Failure loads for beams with and without web reinforcement

S. No.	Beam Label	Size (bxh) (Inch)	Web reinforcement	ANSYS Failure load (lbs.)
1	BXL1	20 x 10	------	14,300
2	BXL2	20 x 10	------	31,800
3	BXL1W	20 x 10	#3 @ 4'' c/c	14,400
4	BXL2W	20 x 10	#3 @ 4'' c/c	42,900
5	BZL1	40 x 10	------	26,300
6	BZL2	40 x 10	------	52,900
7	BZL1W	40 x 10	#3 @ 4'' c/c	28,800
8	BZL2W	40 x 10	#3 @ 4'' c/c	98,400

5.3 Conclusions

Followings are findings and recommendation concluded from this research work:

1. Shear strength of RC beams is significantly influenced by flexure steel ratio, values of factor $\left(V_c \Big/ \sqrt{f_c' \, b_w d} \right)$ for RC wide beams ranges from 1.3 to 3.14 for beams with 0.5% and 1.98% flexure steel ratio respectively.

2. ACI shear strength equation for concrete beams ($V_c = 2\sqrt{f_c' \, b_w d}$, with coefficient equal to 2), gives conservative shear strength values for lightly reinforced wide RC beams.

3. In wide RC beams, shear strength decreases with increase in width, as shear strength in beam BXL1 (20 in wide) was 8% higher than similar beam BZL1 (40 in wide).

4. Although shear strength of RC wide beams without web reinforcement increases with the increase in flexure steel ratio, however to protect the premature shear failure in wide beams (that might be sudden and without warning), web reinforcement must be provided in RC wide beams.

5. In wide RC beams, shear stress variation along its width at un-cracked cross-section is relatively uniform; however once the section cracks, shear resisting pattern is disturbed, beam cross sectional strips located at flexure re-bars position show higher shear stiffness and resist more shear than those in-between the re-bars.

5.4 Recommendations

It is recommended that, the effect of bar spacing seems to be noticeable in beam shear response, indicating that shear strength can be enhanced by decreasing flexure bar spacing, thus making relatively more uniform shear stress distribution along member width. This effect is required to be experimentally checked and examined.

APPENDIX-A

(Theoretical Calculations and Stresses Results from ANSYS Analysis)

1-Theoretical analysis of beams BXL1 and BXL1W

<table>
<tr><td colspan="6" align="center">Beam BXL1=10"x20"</td></tr>
<tr><td>Beam X-Section</td><td>(b x h) =</td><td>20"x 10"</td><td>,</td><td>Conc. Strength f'_c =</td><td>4,000 psi</td></tr>
<tr><td>Span Length</td><td>L =</td><td>10 ft</td><td>,</td><td>Rebar strength f_y =</td><td>60,000 psi</td></tr>
</table>

Beam L-Section   Section X-X

$A_{s(Provided)}$ =	5 *#4* → A_s=	1.00 Inch^2 →	d= 8 "	$\rho = A_s/bd$ =	0.50%
E_c = 57000 x $(f'_c)^{1/2}$ =	3604997 psi		n=E_s/E_c= 8.04	→ ρ_b =	2.83%

nA_s = 8.04 Inch^2 → A_t = A_g+nA_s = 208.04 Inch^2

Y_t = $\sum(Ay/2)A_t$ = 5.12 " , Y_b = 4.88 " , $I_{(tr)}$ = $\sum (bh^3/12+A\,d^2)$ = 1736 Inch^4

Stress Elastic and Section Un-Cracked:

Point Load   P (ANSYS) =   5620   lbs   @X=   30 "   (From Support)

Bending Moment	M=P*X=	169	K-Inch
Max Concrete Stress at bottom	f_{cb} =M*Y_b/I =	**474**	psi
Max Conc. Stress at top	f_{ct} = M *Y_t/ I =	**497**	psi
Max Steel Stress (+)	f_s= n x M * (d-Y_t)/ I =	**2253**	psi
Max Deflection	d_{max} = P*X/24EI*(3L^2-4X^2) =	**0.0444**	Inch

fcr=7.5*fc$^{1/2}$ = 474psi and corresponding cracking load Pcr=5,620Lbs

Stress Elastic and Section Cracked:

Point Load   P =   6000   Lbs

Bending Moment   M= P*X =   180 " Kip-Inch   Steel ratio $\grave\rho$= A_s/bh =   0.005

K = $\sqrt{((n\rho)^2 + 2n\rho)}$ - nρ =   0.25   →   J = 1 -K/3 =   0.9179 →   kd =   1.97 "

Conc Stress @Top	f_{ct}= 2M/(KJbd^2) =	**1244**	psi
Re-bar Steel Stress	f_s= M/As*Jd =	**24512**	psi

Strength Analysis:

Stress Block depth	a= A_s*f_y / (0.85f'_c*b) =	0.88	Inch
Moment Capacity	M_n = A_s*f_y * (d-a/2) =	454	K-Inch
Load Capicity	P_n = M_n/x ≈	15100	lbs φP_n= 13590 lbs

Shear Design:

Acting Shear force	V_u =φ P_n =	13590	Kips $V_u \leq$ φV_c
Conc. shear capacity = φV_c=0.75*2*$\sqrt{f'_c}$*bd =		18974	Kips φ = 0.75
Provided web reinforcement		*Nill	

* A web reinforcement #3@4" c/c was provided in beam BXL1W.

2-Theoretical analysis of beams BXL2 and BXL2W
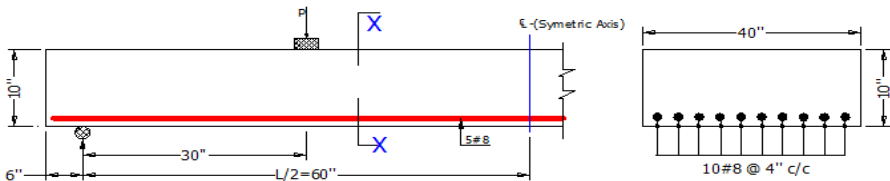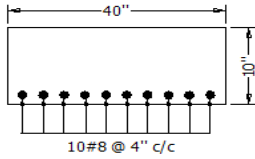
Beam BXL2=10"x20"

Beam X-Section	(b x h) =	20"x 10"	,	Conc. Strength	f'_c =	4,000 psi
Span Length	L =	10 ft	,	Rebar strength	f_y =	60,000 psi

Beam L-Section

Section X-X

5#8 @ 4" c/c

$As_{(Provided)}$ =	5 #8	→	As=	3.95 Inch^2	→	d=	8 "	ρ =As/bd = 1.98%
$E_c = 57000 \times (f'_c)^{1/2}$ =	3604997 psi			n=Es/Ec=	8.04			→ ρ_b = 2.83%

nA_s = 31.78 Inch^2 → $A_t = A_g + nA_s$ = 231.78 Inch^2

$Y_t = \sum(Ay/2)A_t$ = 5.41 " , Y_b = 4.59 " , $I(tr) = \sum (bh^3/12 + A\,d^2)$ = 1913 Inch^4

Stress Elastic and Section Un-Cracked:

Point Load   P = 6590 lbs @X= 30 " (From Support)

Bending Moment	M=P*X=	198	K-Inch
Max Concrete Stress at bottom	$f_{cb} = M*Y_b/I$ =	**474**	psi
Max Conc. Stress at top	$f_{ct} = M*Y_t/I$ =	**559**	psi
Max Steel Stress (+)	$f_s = n \times M * (d-Y_t)/I$ =	**2152**	psi
Max Deflection	$d_{max} = P*X/24EI*(3L^2-4X^2)$ =	**0.0473**	Inch

Beam Rupture Modulus $f_{cr} = 7.5*f_c^{1/2} = 474$ psi and corresponding Ccacking load Pcr=6,590 lbs

Stress Elastic and Section Cracked:

Point Load   P = 7000 lbs

Bending Moment   M= P*X = 210 " Kip-Inch   Steel ratio $\rho = A_s/bh$ = 0.020

$K = \sqrt{((n\rho)^2 + 2n\rho)} - n\rho$ = 0.43 → J = 1 - K/3 = 0.8577 → kd = 3.41 "

Conc Stress @Top	$f_c = 2M/(KJbd^2)$ =	**896**	psi
Re-bar Steel Stress	$f_s = M/As*Jd$ =	**7748**	psi

Strength Analysis:

Stress Block depth	$a = A_s*f_y / (0.85f'_c*b)$ =	3.49	Inch		
Moment Capacity	$M_n = A_s*f_y* (d-a/2)$ =	1483	K-Inch	X =	30 "
Load Capicity	$P_n = M_n/x \approx$	49400	lbs	φP_n=	44460 lbs

Shear Design:

Acting Shear force	$V_u = \varphi P_n$ =	44460	Kips		$V_u \geq \varphi V_c$
Conc. shear capacity = $\varphi V_c = 0.75*2*\sqrt{f'_c}*bd$ =		15179	Kips	φ =	0.75
Provide web reinforcement		*Nill			

* A web reinforcement #3@4" c/c was provided in beam BXL2W.

3-Theoretical Analysis of beams BZL1 and BZL1W

Beam BZL1=10"x40"

Beam X-Section	(b x h) =	40"x 10"	, Conc. Strength	$f_c =$	4,000 psi
Span Length	L =	10 ft	. Rebar strength	$f_r =$	60,000 Ksi

Beam L-Section

Section X-X

10#4 @ 4" c/c

$A_{s(Provided)} =$	10 *#4*	→	$A_s=$	2.00 Inch^2	→	d=	8 "	$\rho = A_s/bd =$	0.50%
$E_c = 57000 \times (f_c)^{1/2} =$		3604997 psi		$n=E_s/E_c=$	8.04			→ $\rho_b =$	2.83%

$nA_s =$ 16.09 Inch^2	→	$A_t =$ $A_g+nA_s =$		416.09 Inch^2	
$Y_t = \sum(Ay/2)A_t =$ 5.12 "	, $Y_b =$ 4.88 "	,	$I_{(tr)} = \sum (bh^3/12+A\,d^2) =$		3473 Inch^4

Stress Elastic and Section Un-Cracked:

Point Load	P = 11240 lbs	@X= 30 " (From Support)			
Bending Moment		M=P*X=	337	K-Inch	
Max Concrete Stress at bottom		$f_{cb} = M*Y_b/I =$	**474**	psi	$f_{cr} = 7.5*fc^{1/2} =$ 474psi and corresponding cracking load Pcr=11,240 lbs
Max Conc. Stress at top		$f_{ct} = M*Y_t/I =$	**497**	psi	
Max Steel Stress (+)		$f_s= n \times M * (d-Y_t)/I =$	**2253**	psi	
Max Deflection		$d_{max} = P*X/24EI*(3L^2-4X^2) =$	**0.0444**	Inch	

Stress Elastic and Section Cracked:

Point Load	P =	12000 lbs			
Bending Moment	M= P*X =	360 " Kip-Inch	Steel ratio	$\rho= A_s/bh =$	0.005
$K = \sqrt{((n\rho)^2 + 2n\rho)} - n\rho =$	0.25	→	$J = 1 -K/3 =$ 0.9179 →	kd =	1.97 "
Conc Stress @Top	$f_{ct}= 2M/(KJbd^2) =$	**1244**	psi		
Re-bar Steel Stress	$f_s= M/As*Jd =$	**24512**	psi		

Strength Analysis:

Stress Block depth	$a= A_s*f_y / (0.85f_c*b) =$	0.88	Inch		
Moment Capacity	$M_n = A_s*f_y* (d-a/2) =$	907	K-Inch		
Load Capicity	$P_n = M_n/x \approx$	30200	lbs	$\varphi P_n=$	27180 lbs

Shear Design:

Acting Shear force	$V_u =\varphi P_n =$	27180	Kips	$V_u \le \varphi V_c$	
Conc. shear capacity = $\varphi V_c =0.75*2*\sqrt{f_c}*bd =$		37947	Kips	$\varphi =$	0.75
Provided web reinforcement		*Nill			

* A web reinforcement #3@4" c/c was provided in beam BZL1W.

4-Theoretical Analysis of beams BZL2 and BZL2W

Beam BZL2=10"x40"

Beam X-Section	(b x h) =	40"x 10"	, Conc. Strength	f_c =	4,000 psi
Span Length	L =	10 ft	, Rebar strength	f_y =	60,000 Ksi

Beam L-Section

Section X-X

10#8 @ 4" c/c

$A_{s(Provided)}$ =	10 #8	→ A_s =	7.90 Inch^2	→ d=	8 "	$\rho = A_s/bd$ =	1.98%
E_c = 57000 x $(f_c)^{1/2}$ =		3604997 psi		n=E_s/E_c=	8.04	→ ρ_b =	2.83%

nA_s = 63.55 Inch^2 → $A_t = A_g + nA_s$ = 463.55 Inch^2

$Y_t = \sum(Ay/2)A_t$ = 5.41 " , Y_b = 4.59 " , $I_{(tr)} = \sum(bh^3/12 + A d^2)$ = 3827 Inch^4

Stress Elastic and Section Un-Cracked:

Point Load P = 13180 lbs @X= 30 " (From Support)

Bending Moment	M=P*X=	395	K-Inch	
Max Concrete Stress at bottom	f_{cb} = M*Y_b/I =	**474**	psi	fcr=7.5*fc$^{1/2}$ = 474 psi and Corresponding Cracking Load Pcr=13,180Lbs
Max Conc. Stress at top	f_{ct} = M *Y_t/ I =	**559**	psi	
Max Steel Stress (+)	f_s= n x M * (d-Y_t)/ I =	**2152**	psi	
Max Deflection	d_{max} = P*X/24EI*(3L^2-4X^2) =	**0.0473**	Inch	

Stress Elastic and Section Cracked:

Point Load P = 14000 lbs

Bending Moment M= P*X = 420 " Kip-Inch   Steel ratio ρ= A_s/bh = 0.020

K = $\sqrt{((n\rho)^2 + 2n\rho)}$ - nρ = 0.43 → J = 1 -K/3 = 0.8577 → kd = 3.41 "

Conc Stress @Top	f_{ct}= 2M/(KJbd^2) =	**896**	psi
Re-bar Steel Stress	f_s= M/As*Jd =	**7748**	psi

Strength Analysis:

Stress Block depth	a= A_s*f_y / (0.85f_c*b) =	3.49	Inch
Moment Capacity	$M_n = A_s*f_y* (d-a/2)$ =	2966	K-Inch
Load Capicity	P_n = M_n/x ≈	98800	lbs	φP_n= 88920 lbs

Shear Design:

Acting Shear force	V_u =φ P_n =	88920	Kips	$V_u \geq \varphi V_c$
Conc. shear capacity = φV_c=0.75*2*$\sqrt{f_c}$*bd =		37947	Kips	φ = 0.75
Provided web reinforcement		*Nill		

* A web reinforcement #3@4" c/c was provided in beam BZL2W.

Table A1: Cross Sectional Values of Bending Stress S_X (psi) for Beam-BXL1 at Load P=13,000 lbs. (Middle Centre)

		Beam width →										
		0''	1''	2''	3''	4''	5''	6''	7''	8''	9''	10''
Beam depth-h (from bottom) →	0''	0	0	0	0	0	1	89	-72	0	-1	-44
	1''	-95	35	98	111	200	91	13	38	-2	5	164
	2''	153	51	29	23	51	19	5	-1	4	69	12
	3''	164	19	97	42	-1	2	8	8	6	0	0
	4''	76	169	197	129	15	7	9	-1	-5	-2	-2
	5''	-54	-28	-23	-3	147	-1	1	-6	-3	-2	-2
	6''	-17	-38	17	3	88	201	130	108	78	1	1
	7''	35	52	107	138	70	106	28	20	65	108	88
	8''	-389	-394	-377	-375	-368	-365	-353	-348	-351	-359	-358
	9''	-1374	-1365	-1360	-1360	-1366	-1374	-1379	-1381	-1381	-1381	-1381
	10''	-2103	-2104	-2121	-2141	-2155	-2163	-2167	-2167	-2165	-2163	-2162

107

Table A2: Cross Sectional Values of Shear Stress S_{XY} (psi) for Beam-BXL1 at Load P=13,000 lbs. (15'' from Support)

		Beam width $\rightarrow$										
		0''	1''	2''	3''	4''	5''	6''	7''	8''	9''	10''
Beam depth-h (from bottom) $\downarrow$	0''	-2	-35	-7	45	73	-19	-5	19	-13	31	36
	1''	-15	-49	29	64	13	20	-49	43	4	66	-25
	2''	-90	-77	-110	-45	-31	-68	-72	-59	0	-31	-75
	3''	-99	-69	-198	-99	-54	-105	-149	-103	-11	-115	-134
	4''	-51	-32	-83	-47	-53	-69	-56	-49	-42	-78	-84
	5''	1	-28	-19	-19	-30	-48	-81	-28	-10	-10	-39
	6''	-12	-34	-30	-28	-21	-39	-38	-39	-53	-50	-46
	7''	-86	-89	-89	-96	-89	-88	-103	-112	-113	-108	-103
	8''	-144	-134	-129	-131	-133	-137	-144	-152	-156	-156	-155
	9''	-106	-96	-93	-94	-96	-100	-103	-106	-108	-109	-109
	10''	-67	-60	-58	-59	-61	-63	-64	-66	-66	-67	-67

Table A3: Cross Sectional Values of Bending Stress S_X (psi) for Beam-BXL2 at Load P=26,000 lbs. Middle Centre)

		Beam width →										
		0''	1''	2''	3''	4''	5''	6''	7''	8''	9''	10''
Beam depth-h (from bottom) ↓	0''	1	1	13	1	1	0	0	0	0	0	0
	1''	17	2	6	2	-1	1	6	25	38	44	11
	2''	-2	4	-12	-6	1	-3	10	7	58	14	43
	3''	19	12	7	6	4	8	5	44	13	9	7
	4''	-4	2	4	2	2	2	3	4	3	1	1
	5''	-12	-7	-6	-6	-6	-6	-4	-2	-2	-2	-2
	6''	131	149	146	144	127	111	89	68	50	37	30
	7''	-703	-677	-667	-665	-669	-678	-689	-701	-712	-719	-721
	8''	-1533	-1519	-1511	-1507	-1506	-1506	-1507	-1509	-1511	-1513	-1514
	9''	-2245	-2247	-2249	-2251	-2253	-2253	-2253	-2252	-2252	-2251	-2251
	10''	-2746	-2756	-2768	-2781	-2791	-2795	-2796	-2795	-2793	-2792	-2791

Table A4: Cross Sectional Values of Shear stress S_{XY} (psi) for Beam-BXL2 at Load P=26,000 lbs. (15'' from Support)

		Beam width $\rightarrow$										
		0''	1''	2''	3''	4''	5''	6''	7''	8''	9''	10''
Beam depth-h (from bottom) $\downarrow$	0''	20	6	-22	12	6	-5	1	-18	-16	4	-35
	1''	54	-41	24	1	12	-30	10	-51	-39	-21	-9
	2''	66	-56	-141	-33	-35	-29	-106	-65	-45	-49	-130
	3''	-149	-118	-219	-90	-77	-134	-221	-139	-80	-111	-156
	4''	-230	-186	-153	-174	-171	-175	-201	-189	-192	-211	-199
	5''	-256	-209	-203	-225	-209	-211	-216	-212	-224	-185	-229
	6''	-251	-220	-207	-201	-221	-205	-207	-212	-197	-191	-180
	7''	-204	-185	-175	-173	-182	-177	-171	-172	-171	-165	-157
	8''	-179	-167	-159	-158	-159	-160	-161	-162	-163	-162	-162
	9''	-125	-110	-104	-103	-104	-105	-106	-107	-108	-108	-108
	10''	-78	-65	-61	-61	-61	-62	-63	-64	-64	-65	-65

110

Table A5: Cross Sectional Values of Bending stress S_X (psi) for Beam-BXL1W at Load P=14,000 lbs (Middle Centre)

		Beam width $\rightarrow$										
		0''	1''	2''	3''	4''	5''	6''	7''	8''	9''	10''
Beam depth-h (from bottom) $\downarrow$	0''	-3	0	0	0	0	0	0	0	0	0	0
	1''	-29	-10	-9	-1	15	51	1	-5	105	74	108
	2''	-5	-2	-2	-5	-6	7	8	30	40	75	36
	3''	0	0	4	3	5	6	18	34	9	75	74
	4''	3	1	3	-1	2	13	7	11	35	29	42
	5''	-2	-2	-2	-1	5	0	36	38	25	24	-2
	6''	-10	-9	-9	-11	-7	-1	-3	0	72	30	7
	7''	134	113	120	139	170	191	90	29	10	-14	-7
	8''	-407	-389	-371	-356	-351	-346	-283	-256	-262	-281	-294
	9''	-1478	-1466	-1471	-1479	-1487	-1494	-1499	-1501	-1500	-1501	-1502
	10''	-2250	-2259	-2274	-2295	-2320	-2339	-2353	-2362	-2368	-2370	-2371

Table A6: Cross Sectional Values Shear Stress S_{XY} (psi) for Beam-BXL1W at Load P=14,000 lbs (15'' from Support)

		Beam width $\rightarrow$										
		0''	1''	2''	3''	4''	5''	6''	7''	8''	9''	10''
Beam depth-h (from bottom) $\downarrow$	0''	153	8	-86	-1	139	-23	-55	99	-25	3	-75
	1''	19	10	-47	13	25	35	-58	46	76	33	-66
	2''	0	-100	-93	-20	-36	-52	-33	-29	-5	-36	-134
	3''	-64	-148	-99	-141	-39	-32	-115	-111	-84	-122	-81
	4''	-200	-110	-103	-91	-94	-94	-105	-132	-134	-111	-85
	5''	-186	-46	-55	-32	-49	-164	-68	-76	-71	-30	-130
	6''	-154	-110	-78	-45	-11	-31	-21	-35	-44	-21	-8
	7''	-114	-97	-83	-59	-62	-66	-69	-84	-77	-72	-71
	8''	-122	-113	-111	-114	-117	-121	-126	-130	-132	-130	-129
	9''	-96	-88	-90	-91	-94	-99	-103	-107	-109	-111	-111
	10''	-64	-59	-60	-61	-63	-66	-69	-71	-73	-74	-75

Table A-7: Cross Sectional Values of Bending stress S_X (Psi) for Beam-BXL2W at load P=42,500 lbs (Middle Centre)

		Beam width $\rightarrow$										
		0''	1''	2''	3''	4''	5''	6''	7''	8''	9''	10''
Beam depth-h (from bottom) $\downarrow$	0''	0	-5	21	65	9	128	-7	15	3	-28	-42
	1''	6	38	119	31	95	59	12	83	92	138	347
	2''	10	-5	162	47	-15	36	106	67	-54	76	84
	3''	2	34	75	67	138	74	164	56	119	8	53
	4''	1	-1	3	46	16	-57	21	85	47	61	66
	5''	32	25	-56	-62	10	20	31	-77	161	116	11
	6''	-202	-187	-208	-236	-245	-239	-242	-278	-410	-412	-374
	7''	-1583	-1539	-1499	-1479	-1466	-1459	-1456	-1469	-1531	-1476	-1369
	8''	-2687	-2654	-2644	-2607	-2619	-2621	-2621	-2614	-2590	-2542	-2520
	9''	-3430	-3407	-3424	-3459	-3460	-3470	-3476	-3479	-3465	-3448	-3444
	10''	-3789	-3852	-3832	-3878	-3898	-3923	-3936	-3940	-3942	-3943	-3943

Table A8: Cross Sectional Values of Shear stress S_{XY} (psi) for Beam-BXL2W at Load P=42,500 lbs (15'' from Support)

		Beam width $\rightarrow$										
		0''	1''	2''	3''	4''	5''	6''	7''	8''	9''	10''
Beam depth-h (from bottom) $\rightarrow$	0''	-31	3	-5	-87	26	-13	-11	63	-41	6	-3
	1''	-30	-13	50	-86	-38	-13	49	-40	-40	-13	38
	2''	-155	-139	-192	-218	-169	-170	-276	-154	-27	-140	-327
	3''	-94	-271	-438	-352	-259	-348	-393	-281	-132	-345	-336
	4''	-293	-283	-371	-332	-290	-314	-339	-287	-263	-313	-366
	5''	-354	-318	-224	-285	-309	-273	-341	-342	-307	-233	-312
	6''	-379	-280	-321	-269	-285	-185	-284	-247	-232	-224	-227
	7''	-444	-396	-358	-334	-239	-286	-129	-212	-291	-318	-352
	8''	-417	-340	-380	-239	-231	-236	-186	-208	-238	-241	-252
	9''	-271	-209	-215	-131	-138	-140	-133	-122	-121	-117	-115
	10''	-160	-121	-95	-64	-69	-72	-68	-62	-57	-53	-49

Table A9: Cross Sectional Values of Bending Stress Sx (psi) for Beam-BZL1 at Load P=26,000 lbs (Middle Centre)

		Beam width →																			
		0''	1''	2''	3''	4''	5''	6''	7''	8''	9''	10''	11''	12''	13''	14''	15''	16''	17''	18''	19''	20''
Beam depth-h (from bottom) →	0''	0	0	0	0	0	0	0	0	0	-6	0	0	0	0	-1	-1	135	-138	-101	0	0
	1''	0	0	0	0	0	0	0	0	0	0	0	0	0	18	119	85	135	5	162	-9	-16
	2''	0	0	0	0	0	0	2	1	0	0	0	-5	67	74	43	26	136	61	-14	6	274
	3''	1	1	0	0	-1	1	2	9	23	-12	1	70	47	24	70	185	78	128	21	55	121
	4''	0	0	-1	2	3	-22	42	21	-14	-5	81	85	168	-5	6	29	-11	58	122	-62	-55
	5''	-5	-2	-1	181	119	138	196	124	88	147	115	106	105	130	108	49	5	43	111	26	-10
	6''	0	0	74	15	-68	-64	-63	0	37	-18	-14	122	111	40	167	146	182	196	234	152	154
	7''	121	181	71	87	78	101	94	90	64	85	67	66	61	88	30	-32	-64	-74	-66	16	48
	8''	-386	-361	-333	-332	-334	-351	-363	-374	-383	-396	-390	-383	-394	-401	-406	-410	-413	-420	-427	-433	-435
	9''	-1351	-1344	-1343	-1351	-1363	-1373	-1380	-1384	-1388	-1391	-1394	-1397	-1398	-1397	-1395	-1394	-1393	-1396	-1400	-1404	-1406
	10''	-2078	-2086	-2106	-2127	-2140	-2149	-2152	-2153	-2152	-2149	-2146	-2141	-2136	-2130	-2124	-2119	-2116	-2117	-2120	-2124	-2125

Table A10: Cross Sectional Values of Shear Stress S_{XY} (psi) for Beam-BZL1 at Load P=26,000 lbs (15'' from Support)

		Beam width →																			
		0''	1''	2''	3''	4''	5''	6''	7''	8''	9''	10''	11''	12''	13''	14''	15''	16''	17''	18''	19''	20''
Beam depth-h (from bottom) ↓	0''	15	8	8	77	12	28	36	-27	20	33	-27	27	8	-27	65	11	-37	-16	25	34	5
	1''	33	13	55	21	-1	62	47	30	12	21	29	24	11	46	36	1	0	30	33	37	-30
	2''	25	-79	-92	-38	-27	-81	-85	-79	-14	-76	-99	-49	42	-44	-89	-54	-44	-22	-102	-64	31
	3''	-64	-73	-242	-78	-5	-105	-235	-95	-26	-59	-233	-82	5	-52	-224	-69	-50	-84	-206	-91	-55
	4''	-22	-86	-89	-61	-4	-57	-86	-58	5	-50	-80	-73	-12	-44	-70	-50	-24	-46	-86	-42	-18
	5''	0	-40	-26	-28	-33	-28	-49	-45	-50	-35	-49	-51	-40	-40	-55	-61	-48	-43	-38	-49	-52
	6''	-12	-36	-54	-67	-66	-64	-68	-70	-71	-74	-70	-63	-69	-79	-82	-76	-74	-84	-89	-84	-77
	7''	-60	-71	-84	-95	-101	-105	-109	-113	-112	-108	-105	-106	-109	-114	-115	-113	-111	-112	-111	-109	-107
	8''	-106	-107	-113	-119	-122	-122	-123	-126	-129	-130	-131	-131	-131	-130	-129	-127	-125	-123	-121	-120	-119
	9''	-90	-86	-88	-90	-90	-90	-89	-91	-93	-97	-99	-98	-97	-95	-93	-91	-90	-89	-87	-87	-87
	10''	-61	-56	-57	-58	-58	-58	-57	-58	-59	-62	-63	-63	-62	-60	-59	-58	-57	-56	-56	-55	-55

Table A11: Cross Sectional Values of Bending Stress Sx (psi) for Beam-BZL2 at Load P=26,000 lbs (Middle Centre)

		Beam width →																			
		0''	1''	2''	3''	4''	5''	6''	7''	8''	9''	10''	11''	12''	13''	14''	15''	16''	17''	18''	19''	20''
Beam depth-h (from bottom) ↓	0''	-53	0	0	0	0	-30	-87	146	219	-54	-32	-31	-13	0	0	0	0	0	0	0	0
	1''	92	101	240	237	98	-37	94	119	307	18	195	92	-9	62	0	-256	-189	3	-4	0	1
	2''	243	53	-18	62	-3	168	-16	88	385	142	-8	250	-9	45	-11	-172	-242	-1	7	-3	1
	3''	155	156	65	126	215	176	113	-15	276	26	218	103	21	15	-9	-2	-2	4	-1	15	3
	4''	108	190	230	149	147	156	189	140	182	142	-21	45	-62	103	-66	102	6	-2	2	2	1
	5''	61	70	50	48	48	86	118	105	91	183	207	68	150	102	-2	28	185	162	-1	-10	-8
	6''	-223	-229	-217	-215	-211	-203	-194	-183	-173	-169	-130	-42	-7	2	30	72	-56	-31	95	40	65
	7''	-782	-779	-766	-757	-751	-746	-742	-739	-739	-740	-743	-748	-750	-748	-742	-732	-725	-720	-713	-702	-695
	8''	-1498	-1492	-1484	-1479	-1477	-1478	-1479	-1481	-1484	-1489	-1494	-1499	-1503	-1504	-1503	-1503	-1504	-1507	-1509	-1509	-1510
	9''	-2184	-2181	-2183	-2188	-2194	-2201	-2207	-2212	-2217	-2222	-2227	-2231	-2235	-2238	-2241	-2244	-2247	-2250	-2252	-2254	-2254
	10''	-2663	-2665	-2678	-2695	-2711	-2724	-2735	-2743	-2750	-2756	-2761	-2766	-2770	-2774	-2778	-2781	-2784	-2787	-2789	-2790	-2791

Table A12: Cross Sectional Values of Shear Stress S_{XY} (psi) for Beam-BZL2 at Load P=26,000 lbs (Middle Centre)

		Beam width →																			
		0''	1''	2''	3''	4''	5''	6''	7''	8''	9''	10''	11''	12''	13''	14''	15''	16''	17''	18''	19''	20''
Beam depth-h (from bottom) ↓	0''	2	26	-25	1	-8	32	15	2	-11	25	34	-1	-38	-18	40	-40	22	-30	-8	-31	34
	1''	15	-5	16	-35	-26	23	13	-17	-4	19	35	17	-46	-3	3	-3	1	-12	-10	14	-31
	2''	-60	-106	-119	-89	-51	-93	-132	-78	-102	-78	-122	-99	-85	-93	-134	-84	-51	-81	-147	-47	-56
	3''	-69	-174	-318	-177	-126	-178	-294	-204	-91	-143	-251	-147	-120	-186	-229	-157	-134	-212	-220	-175	-155
	4''	-207	-223	-209	-217	-186	-234	-241	-235	-183	-209	-200	-232	-181	-195	-197	-196	-194	-218	-192	-189	-194
	5''	-294	-204	-180	-155	-156	-169	-172	-163	-190	-186	-183	-183	-208	-196	-196	-191	-188	-180	-170	-171	-159
	6''	-237	-204	-173	-151	-138	-155	-141	-149	-150	-151	-183	-152	-167	-151	-159	-169	-146	-159	-162	-149	-141
	7''	-222	-200	-178	-163	-152	-151	-148	-152	-154	-165	-183	-186	-187	-180	-174	-175	-169	-169	-173	-173	-175
	8''	-217	-193	-175	-163	-156	-152	-151	-151	-155	-163	-172	-178	-178	-176	-175	-173	-171	-170	-171	-171	-170
	9''	-137	-118	-106	-101	-97	-95	-95	-95	-98	-102	-106	-109	-109	-109	-108	-107	-106	-105	-105	-105	-105
	10''	-81	-66	-59	-57	-55	-54	-54	-54	-56	-58	-60	-61	-62	-62	-61	-61	-60	-60	-59	-59	-59

Table A13: Cross Sectional Values of Sending Stress S$_X$ (psi) for Beam-BZL1W at Load P=28,000 lbs (Middle Centre)

		0''	1''	2''	3''	4''	5''	6''	7''	8''	9''	10''	11''	12''	13''	14''	15''	16''	17''	18''	19''	20''
												Beam width →										
	0''	0	0	0	0	0	0	0	0	0	0	0	0	0	0	2	13	1	0	0	0	0
	1''	0	0	0	-5	-1	0	1	0	-229	-237	1	0	6	89	24	26	36	38	32	0	0
	2''	2	1	1	0	0	0	7	37	13	8	-2	-2	-6	35	9	125	90	120	-7	82	0
	3''	4	1	0	-1	10	29	40	17	1	-18	-4	79	40	42	115	139	44	42	-5	2	0
Beam depth-h (from bottom) →	4''	0	0	0	0	3	2	15	15	162	138	60	15	1	33	96	104	58	110	15	-13	-13
	5''	0	1	1	1	0	-4	-8	-15	30	7	30	97	73	41	30	7	99	90	-208	-254	1
	6''	-2	-2	-1	2	2	1	59	73	81	99	-5	-35	19	-24	-25	64	59	119	132	123	137
	7''	0	0	0	0	247	150	77	59	53	58	70	89	118	84	70	67	54	64	88	95	108
	8''	-365	-352	-340	-330	-402	-395	-393	-389	-384	-385	-387	-387	-391	-391	-397	-405	-398	-405	-432	-439	-437
	9''	-1447	-1441	-1446	-1451	-1457	-1463	-1466	-1468	-1470	-1472	-1475	-1477	-1478	-1480	-1483	-1485	-1485	-1484	-1484	-1485	-1485
	10''	-2218	-2234	-2248	-2265	-2277	-2285	-2290	-2293	-2296	-2300	-2303	-2306	-2309	-2310	-2311	-2311	-2309	-2307	-2303	-2300	-2299

Table A14: Cross Sectional Values of Shear Stress S_{xy} (psi) for Beam-BZL1W at Load P=28,000 lbs (15'' from Support)

	Beam width →																				
	0''	1''	2''	3''	4''	5''	6''	7''	8''	9''	10''	11''	12''	13''	14''	15''	16''	17''	18''	19''	20''
0''	-9	-16	-129	41	38	61	2	-4	19	39	-76	38	14	43	-54	14	-11	-8	-23	-3	-33
1''	74	19	-41	42	21	36	1	-6	-51	49	-76	3	32	45	-79	50	-20	8	0	34	-2
2''	9	-46	-64	-60	27	-52	-116	-32	9	-50	-85	-75	32	-87	-133	-52	35	-87	-105	-8	-45
3''	-84	-83	-72	-90	-79	-141	-164	-158	-128	-124	-179	-136	-102	-137	-137	-122	-57	-122	-165	-153	-85
4''	-130	-156	-74	-78	-80	-87	-121	-45	-89	-109	-132	-77	-130	-95	-126	-90	-106	-140	-108	-79	-122
5''	-155	-25	-20	-31	-27	-23	-26	-8	-41	-73	-39	-43	-52	-17	-32	-68	-44	-70	-23	-32	-117
6''	-11	-43	-29	-19	-28	-16	-12	-28	-17	-16	-13	-4	11	-35	-29	-18	-4	-16	1	-9	-22
7''	-45	-73	-82	-51	-63	-71	-70	-71	-86	-90	-85	-77	-76	-108	-83	-78	-96	-85	-83	-86	-84
8''	-130	-135	-151	-126	-120	-121	-131	-140	-149	-154	-144	-136	-134	-133	-136	-143	-155	-157	-161	-164	-165
9''	-118	-116	-126	-115	-109	-109	-112	-112	-110	-108	-106	-103	-101	-101	-102	-105	-110	-115	-118	-119	-119
10''	-79	-78	-82	-78	-74	-73	-72	-71	-69	-68	-67	-67	-66	-66	-67	-68	-70	-71	-71	-72	-72

Beam depth-h (from bottom) ↓

Table A15: Cross Sectional Values of Bending Stress S$_X$ (psi) for Beam-BZL2W at Load P=85,000 lbs (Middle Center)

		Beam width →																			
		0''	1''	2''	3''	4''	5''	6''	7''	8''	9''	10''	11''	12''	13''	14''	15''	16''	17''	18''	19''	20''
Beam depth-h (from bottom) →	0''	0	0	0	0	0	0	0	-83	0	0	0	243	-1	0	0	0	6	-1	0	0	0
	1''	-1	0	41	101	31	83	50	120	258	82	-6	60	-6	-3	-11	0	3	4	-7	-4	-3
	2''	135	39	84	92	67	26	54	-12	180	45	74	71	16	-12	-30	-12	-3	-15	-27	-17	-6
	3''	9	42	154	43	90	246	39	43	1	119	111	-34	-4	10	1	13	1	21	-7	24	4
	4''	3	1	176	-9	51	40	156	120	-80	42	135	156	-20	6	12	0	-1	-1	-1	-2	-5
	5''	0	-17	155	64	148	88	147	117	68	92	106	-26	-37	-5	-8	-8	-4	-9	-5	-9	-56
	6''	-301	-284	-262	-281	-268	-247	-220	-211	-215	-235	-238	-270	-186	-124	-90	-62	-51	-50	-73	-91	-79
	7''	-1519	-1481	-1447	-1434	-1428	-1429	-1432	-1435	-1437	-1440	-1452	-1481	-1483	-1454	-1419	-1398	-1389	-1394	-1422	-1425	-1412
	8''	-2662	-2630	-2624	-2592	-2610	-2620	-2628	-2635	-2641	-2646	-2639	-2610	-2607	-2658	-2670	-2668	-2662	-2644	-2598	-2602	-2629
	9''	-3440	-3419	-3440	-3477	-3482	-3495	-3504	-3508	-3511	-3513	-3513	-3495	-3495	-3525	-3531	-3531	-3533	-3532	-3518	-3521	-3532
	10''	-3812	-3878	-3859	-3911	-3936	-3965	-3977	-3981	-3979	-3983	-3998	-4002	-4007	-4010	-4000	-3997	-4007	-4015	-4020	-4026	-4028

Table A16: Cross sectional Values of shear stress S_{XY} (psi) for Beam-BZL2W at load P=85,000 lbs (15'' from support)

| | | Beam width → | | | | | | | | | | | | | | | | | | | |
		0''	1''	2''	3''	4''	5''	6''	7''	8''	9''	10''	11''	12''	13''	14''	15''	16''	17''	18''	19''	20''
	0''	78	-75	-8	-53	55	-33	-10	12	22	33	23	-47	-3	42	-11	44	24	57	-55	33	60
	1''	-48	-17	25	32	-10	26	53	-10	33	24	70	-41	66	-20	16	-28	-23	3	-11	59	-43
	2''	-8	-128	-119	-162	-89	-186	-210	-102	-47	-159	-182	-142	-50	-121	-265	-99	-87	-194	-147	-59	-115
	3''	-158	-234	-422	-145	-117	-241	-396	-181	-151	-236	-485	-304	-128	-316	-441	-259	-221	-217	-514	-248	-170
Beam depth-h (from bottom) →	4''	-173	-227	-298	-278	-257	-297	-274	-264	-251	-251	-334	-265	-246	-279	-276	-328	-318	-346	-310	-350	-267
	5''	-397	-286	-323	-313	-320	-351	-283	-319	-336	-368	-292	-295	-305	-310	-332	-301	-294	-283	-272	-289	-316
	6''	-384	-347	-413	-380	-334	-347	-298	-269	-276	-275	-341	-340	-290	-276	-325	-343	-307	-314	-297	-305	-303
	7''	-421	-407	-435	-349	-338	-339	-228	-306	-298	-366	-344	-343	-338	-336	-354	-338	-305	-264	-414	-276	-253
	8''	-393	-374	-505	-313	-258	-232	-245	-237	-271	-260	-267	-276	-270	-293	-261	-238	-249	-279	-269	-252	-248
	9''	-268	-199	-347	-133	-147	-140	-150	-143	-143	-138	-130	-131	-128	-141	-146	-161	-152	-167	-142	-148	-154
	10''	-156	-124	-105	-87	-78	-87	-87	-83	-74	-65	-65	-64	-69	-67	-73	-78	-85	-86	-85	-80	-82

122

References:

Angelakos, D., Bentz, E. C., and Collins, M. P. (2001). "Effect of concrete strength and minimum stirrups on shear strength of large members." *ACI Structural Journal*, 98(3).

ANSYS-Multiphysics (2011). "14.0 User's Guide." *Ansys Inc*ANSYS, Inc. and ANSYS Europe, Ltd.

Bazant, Z. P., and Kazemi, M. T. (1991). "Size effect on diagonal shear failure of beams without stirrups." *ACI Structural Journal*, 88(3).

Bentz, E. C. (2005). "Empirical modeling of reinforced concrete shear strength size effect for members without stirrups." *ACI structural journal*, 102(2).

Clough, R. W., and Tocher, J. L. "Finite element stiffness matrices for analysis of plates in bending." *Proc., Proceedings of conference on matrix methods in structural analysis*, 515-545.

Collins, M. P., and Kuchma, D. (1999). "How safe are our large, lightly reinforced concrete beams, slabs, and footings?" *ACI Structural Journal*, 96(4).

Ghadhban, H. N. (2007). "Effect of beam size on shear strength of reinforced concrete normal beams." *Journal of Engineering and Development*, Vol. 11.

Hasegawa, T., Shioya, T., and Okada, T. "Size effect on splitting tensile strength of concrete." *Proc., Proceedings Japan Concrete Institute 7th Conference*, 309-312.

Hrennikoff, A. (1941). "Solution of problems of elasticity by the framework method." *Journal of applied mechanics*, 8(4), 169-175.

James K. Wight, and Macgregor, J. G. (2012). *Reinforced Concrete Mechanics And Design*, Pearson Education, Inc., Upper Saddle River, New Jersey 07458.

Kani, G. "Basic facts concerning shear failure." *Proc., ACI Journal Proceedings*, ACI.

Kani, G. (1979). *Kani on shear in reinforced concrete*, Deptartment of Civil Engineering, University of Toronto.

Kani, G. N. J. "How safe are our large reinforced concrete beams?" *Proc., ACI Journal Proceedings*, ACI.

Lai, J., Libby, J., and Stamenkovic, H. (1978). "Suggested revisions to shear provisions for building codes." American Concrete Institute 38800 International Way, Country Club Drive, PO Box 9094, Farmington Hills, MI 48333-9094, USA, 563-569.

Lubell, A., Sherwood, T., Bentz, E., and Collins, M. (2004). "Safe shear design of large, wide beams." *Concrete International*, 26(1), 66-78.

Nayak, G., and Zienkiewicz, O. (1972). "Elasto-plastic stress analysis. A generalization for various contitutive relations including strain softening." *International Journal for Numerical Methods in Engineering*, 5(1), 113-135.

Ngo, D., and Scordelis, A. "Finite element analysis of reinforced concrete beams." *Proc., ACI Journal Proceedings*, ACI.

Nilson, A. H. "Internal measurement of bond slip." *Proc., ACI Journal Proceedings*, ACI.

Scordelis, A., Ngo, D., and Franklin, H. (1974). "Finite element study of reinforced concrete beams with diagonal tension cracks." *ACI Special Publication*, 42.

Shehzad, M. K. (2014). "Shear behaviour of ordinary strength RC slender beams." M.Sc, NUST, NUST.

Shioya, T. (1989). "Shear Properties of Large Reinforced Concrete Members." *Special Report, Institute of Technology, Shimizu Corp., Japan.*

Shioya, T., Iguro, M., Nojiri, Y., Akiyama, H., and Okada, T. (1990). "Shear strength of large reinforced concrete beams." *ACI Special Publication*, 118.

Suidan, M., and Schnobrich, W. C. (1973). "Finite element analysis of reinforced concrete." *Journal of the Structural Division*, 99(10), 2109-2122.

Tompos, E. J., and Frosch, R. J. (2002). "Influence of beam size, longitudinal reinforcement, and stirrup effectiveness on concrete shear strength." *ACI Structural Journal*, 99(5).

Whitney, C. S. "Design of reinforced concrete members under flexure or combined flexure and direct compression." *Proc., ACI Journal Proceedings*, ACI.

Zararis, P. D. (2003). "Shear strength and minimum shear reinforcement of reinforced concrete slender beams." *ACI Structural Journal*, 100(2).